EPA/600/R-12/003
January 2012

Quantifying Methane Abatement Efficiency at Three Municipal Solid Waste Landfills

Final Report

Prepared for:
Susan A. Thorneloe
U.S. Environmental Protection Agency
Office of Research and Development
National Risk Management Research Laboratory
Air Pollution Prevention and Control Division
Research Triangle Park, NC 27711

Prepared by:
ARCADIS U.S., Inc.
4915 Prospectus Drive, Suite F
Durham, North Carolina 27713
Tel 919 544 4535
Fax 919 544 5690

Contract No.: EP-C-09-027

Project No.: RN990271.0007

January 2012

Table of Contents

List of Tables

List of Figures

Executive Summary

Biodegradable waste that is buried in municipal solid waste landfills will decompose over many decades forming methane, carbon dioxide, and trace constituents that include hazardous air pollutants (such as mercury), volatile organic compounds, and hydrogen sulfide. Usually larger landfills collect landfill gas to either flare or use in energy projects to produce electricity, heat, or steam. Depending upon the timing of gas collection and well placement in buried waste, addition of interim and final covers, and design and operation of the landfill, fugitive emissions can vary as found through the measurement conducted for this study. Even weather events can be a factor. Droughts can make surface and slope side cracks more difficult to maintain providing a path of least resistance for gas to pass through. High precipitation events such as tornados or hurricanes can make gas collection systems more difficult to maintain due to liquid build-up in collection wells. Landfills typically accept waste for 50 years or more. Even once the landfill closes, emissions can occur for decades requiring routine maintenance of the interim or final cover in addition to managing the well field and gas collection and control technology.

Landfills are considered an "area" source (versus point source) where emissions vary spatially and over time. The U.S. Environmental Protection Agency (EPA) has been working to develop technology and test methods to quantify emissions from area sources such as oil and gas pipelines, animal waste lagoons, and landfills. Of the area source emissions, landfills are considered the most challenging because of their size, and ever changing nature due to changes in waste composition, design and operation. Breakthroughs in technology, data analysis in allocating emissions to the entire footprint, and method development to standardize operating procedures have resulted in the ability to more accurately quantify fugitive landfill gas emissions using optical remote sensing technology.

Using the latest area source measurement techniques, a multi-week field campaign was conducted at three municipal landfills to quantify the methane abatement efficiency. Participation in the study was voluntary. Each site met requirements under the Resource Conservation and Recovery Act and the Clean Air Act. Each site has a gas collection and control system in place as required by the Clean Air Act New Source Performance Standards and Emission Guidelines for municipal solid waste landfills. The measurements were conducted using a scanning GasFinder 2.0 methane Open-Path Tunable Diode Laser (OP-TDL) instrument (Boreal, Inc).

The schedule in the quality assurance project plan was to conduct two rounds of measurements at each site beginning in the late fall of 2009 and in the late spring and early summer of 2010. Due to unseasonable wet and cold weather, measurements were conducted at only two of the three sites during the initial field campaign in the fall of 2009 and repeated in the spring of 2010. At the third site, measurements were conducted during the summer of 2010. The cells at sites A and C have not had waste added for several years. However, officials indicated that waste additions ceased at site B prior to the field measurement campaign (to go to a new call in the summer of 2010. Site B officials stated that the gas collection and control system was upgraded in the fall of 2010 (after the field measurement campaign).

In addition to the optical remote sensing measurements, the header pipe gas was analyzed for flow rate, composition, and the concentration of trace constituents including mercury and other hazardous air pollutants (HAPs), volatile organic compounds (VOC), and nonmethane organic compounds (NMOC). The header pipe gas analysis occurred in the fall of 2009 and the spring of 2010. The results of the

header pipe gas analysis combined with the OTM-10 measurements are used to estimate methane abatement efficiency which is calculated as:

$$CH_4 \text{ Abatement Efficiency} = CH_4 \text{ Collected} / (CH_4 \text{ Collected} + CH_4 \text{ Emissions}) \quad \text{Equation 1}$$

This calculation is different than what is in the U.S. EPA's guidance for emissions inventory in that it does not include soil oxidation in the denominator. (U.S. EPA, 2006, 2007) Inclusion of soil oxidation in the calculation above to allow for direct comparison with conventional collection efficiency[1] would result in lower values. The default gas collection efficiency recommended for EPA's guidance for emissions inventories is 75% (U.S. EPA, 2008). Two of the sites had interim covers and the third had a final cover in place.

The total cell fugitive methane flux rate from the five measurement campaigns varied from 2.3 to 52 million grams per day (Table E-1) and the methane abatement efficiency from 38 to 88% (Table E-2). For two of the sites the landfill methane abatement efficiency ranged from 70 to 88%. Assuming 10% soil oxidation, the inventory-ready gas collection efficiencies for all sites evaluated ranged from 36% to 87%. Landfill gas collation systems were fully operational during each testing period with no reports of downtime or operational upsets.

Table E-1. Summary of Fugitive Methane Emissions from the Landfill Sites

Site	Campaign	Cell Cover Type	Average Methane Emission Factor (grams/day/m^2)	Total Cell Fugitive Methane Emission Rate (grams/day)
A	Fall 2009	Interim	44 ± 10	5.6×10^6
A	Spring 2010	Interim	18 ± 9.1	2.3×10^6
B	Summer 2010	Interim	150 ± 46	52×10^6
C	Fall 2009	Final	19 ± 19	5.8×10^6
C	Spring 2010	Final	9.2 ± 9.7	2.8×10^6

Table E-2. Summary of Gas Collection Efficiency from the Landfill Sites

Site	Campaign	Total Cell Fugitive Methane Emission Rate (grams/day)	Methane Flow Rate in Gas Collection System (grams/day)	Methane Abatement Efficiency* (% value with lower and upper error bounds shown in parenthesis)
A	Fall 2009	5.6×10^6	1.3×10^7	70 (64,74)
A	Spring 2010	2.3×10^6	7.6×10^6	77 (67,84)
B	Summer 2010	52×10^6	3.2×10^7	38 (31,46)
C	Fall 2009	5.8×10^6	1.6×10^7	73 (51,88)
C	Spring 2010	2.8×10^6	2.0×10^7	88 (72,95)

* Calculated as CH_4 Collected / (CH_4 Collected + CH_4 Emissions). This is different than conventional collection efficiency used in AP 42 and other documents which include soil oxidation in the denominator.

[1] CH_4 Collection Efficiency = CH_4 Collected / (CH_4 Collected + CH_4 Emissions + CH_4 Oxidized)

In addition to optical remote sensing measurements, serpentine methane gas sampling was performed along the surface of each landfill using a Thermo TVA-1000 FID portable analyzer according to specifications by the State of California for conducting surface scans. The data were collected to compare to the US EPA Other Test Method-10 (OTM-10) measurements. For one of the three landfills, a forward-looking infrared (FLIR) camera was used to identify potential VOC leaks from the landfill surface and wellheads. Pictures of leaks are provided from the use of the FLIR.

Trace constituent gas analysis data will be used in any future updates to EPA's AP-42 which provides guidance for emission inventories. Although the data are provided in this report, the focus is on the methane abatement efficiency to compare to existing values being used. For mercury, both total and elemental mercury measurements were conducted at each landfill. For one of the sites, speciated mercury samples were collected and analyzed in the fall of 2009.

Table E-3 presents a summary of the results of the total mercury measurements at the three landfill sites. The table presents the average and range of total mercury concentrations from gas header pipes at each site. For the mercury measurements, there was little variation in the concentration between the fall and spring measurements. The concentration of total mercury varied between the three sites from 2.9 to 9.0 $\mu g/m^3$. Speciated measurements for mercury made at site B during the fall 2009 campaign had an average of 1.2% oxidized mercury and 98.8% elemental mercury.

Table E-3. Summary of Total Mercury Measurements from the Landfill Sites

Site	Campaign	Range of Total Mercury Concentration ($\mu g/m^3$)	Average Total Mercury Concentration ($\mu g/m^3$)
A	Fall 2009	3.4 to 3.7	3.5
A	Spring 2010	2.9 to 3.4	3.1
B	Fall 2009	8.4 to 8.9	8.7
B	Spring 2010	8.0 to 8.4	8.2
C	Fall 2010	8.8 to 9.0	8.9
C	Spring 2010	8.4 to 9.0	8.8

Chapter 1
Project Description

1.1 Background

Landfill gas is created from the anaerobic decomposition of biodegradable waste in a landfill. Most large municipal solid waste landfills (i.e., containing more than 2.5 million tons of waste) in the U.S. are required to install and operate gas collection systems that include header pipes, extraction wells, and blowers to minimize emissions that can escape to the atmosphere. The collected gas is piped under a slight negative pressure to a flare or energy recovery device. The collected gas is typically metered and reported as part of regulatory compliance or for energy contracts.

When landfill gas is combusted, methane emissions are traded off for increased carbon dioxide emissions. However, given that methane is 25 times more potent than carbon dioxide (based on assuming a 100-year time horizon) combustion of methane is a benefit even with increased emissions of carbon dioxide. A major issue in quantifying carbon emissions from municipal solid waste landfills is more accurate accounting of fugitive loss. The air regulatory requirements for municipal solid waste landfills allow active sites to take up to five years to collect and control landfill gas from initial waste placement. Even with gas controls in place, not all of the gas is collected due to failure of the cover to contain the gas resulting from leaks in the cover material, header piping and wells, leachate collection sumps, and cracks or penetrations in the landfill surface or side slopes. In addition, the Clean Air Act requirements allow gas systems to be discontinued once the emissions are below the regulatory threshold of 50 Mg nonmethane organic compounds (NMOC) / year. The fugitive emissions vary both temporally and spatially and can be difficult to measure as opposed to measuring emissions from a point source (e.g., landfill gas header pipe or combustion exhaust stack).

Most of the existing data that is available to evaluate fugitive emissions from landfills is based on flux box data. These measurements do not account for the majority of losses found at landfills and therefore can potentially understate the emissions that escape to the atmosphere. With the increased interest in improving greenhouse gas emission inventories and strategies for emission reductions, there is a need to better quantify landfill gas collection efficiency.

The U.S. EPA's Office of Research and Development in collaboration with the Office of Air Quality Planning and Standards has conducted research to advance measurements for quantifying area source emissions (i.e., Other Test Method-10, U.S. EPA 2006). Landfills are considered one of the more challenging area source emissions due to the ever changing design and operation, changes in waste composition over time, and the temporal and spatial variability of area source emissions (i.e., uncollected gas). Recent results from the use of tracer gas data and optical remote sensing measurements have resulted in the development of algorithms for the OTM-10 method to account for fugitive emissions from surface and side slopes at a landfill (Thoma et al., 2010).

Using updated guidance for evaluating landfill area source emissions, measurements were conducted at three municipal solid waste landfills to compare fugitive methane emissions to the collected gas (i.e., methane abatement efficiency). The measurements were conducted over a multi-week sampling campaign using EPA Other Test Method-10 (OTM-10) with a scanning GasFinder 2.0 methane Open-Path Tunable Diode Laser (OP-TDL) instrument (Boreal, Inc). At two of the sites, measurements were performed in the fall of 2009 and repeated in the spring of 2010. At the third site, measurements were conducted during the summer of 2010. Figures 1-1 through 1-3 provide an overhead view of each site along with the location of the cells where testing of area sources emissions was conducted.

In addition to optical remote sensing measurements, serpentine methane gas sampling was performed along the surface of each landfill using a Thermo TVA-1000 FID portable analyzer according to specifications by the State of California for conducting surface scans. The data were collected to compare to the OTM-10 measurements. For one of the three landfills, a FLIR infrared camera was used to identify potential VOC leaks from the landfill surface and wellheads.

At each of the three sites, the measurements conducted at the gas header system measured landfill gas flow rates, velocity, composition, and the concentration of trace constituents including hazardous air pollutants (HAPs), volatile organic compounds (VOC), and nonmethane organic compounds (NMOC). For each of the three sites, samples were taken in the fall of 2009 and repeated in the spring of 2010. The results of the header pipe gas analysis combined with the OTM-10 measurements provide data needed to quantify fugitive emissions of individual HAPs (including mercury), VOC, and NMOC. For mercury, both total and elemental mercury measurements were evaluated at each landfill. For one of the sites, speciated mercury samples were collected and analyzed during the fall 2009 sampling campaign.

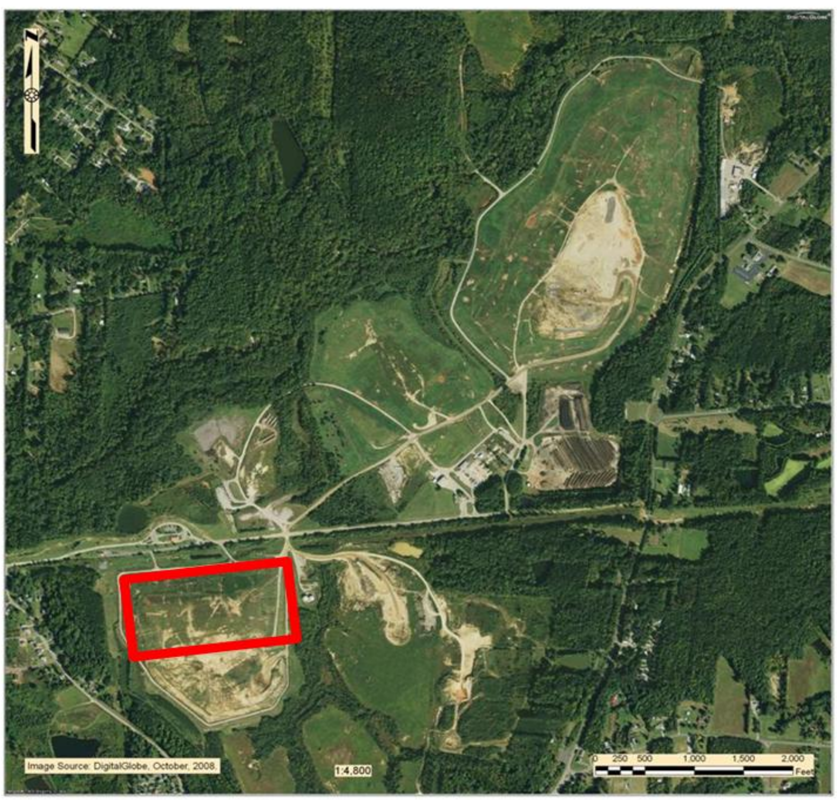

Figure 1-1. Overhead Map of Site A Detailing the Location of the Survey Cell

Figure 1-2. Overhead Map of Site B Detailing the Location of the Survey Cells

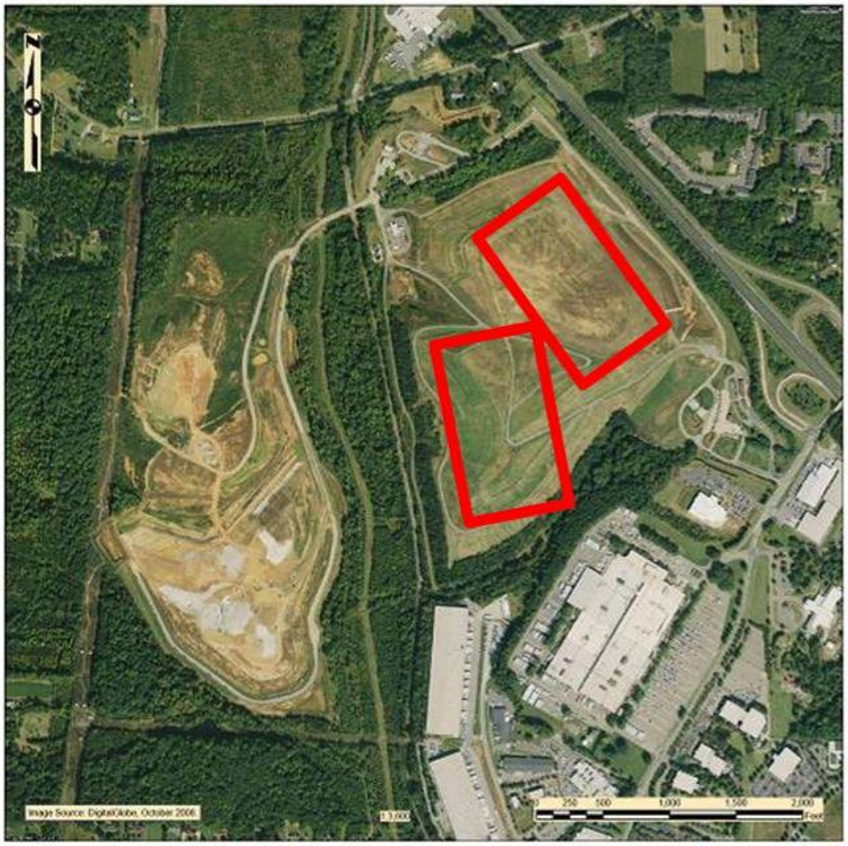

Figure 1-3. Overhead Map of Site C Detailing the Location of the Survey Cells

1.2 OP-TDL and the OTM-10 Method

Path-integrated methane concentrations were collected at the sites using a scanning OP-TDL and US EPA Other Test Method-10 (OTM-10). The method has been successfully employed to characterize emissions from a variety of sources, including landfills, wastewater treatment plants, waste lagoons from hog farms, and a variety of industrial sites (Thoma et al., 2005, U.S. EPA, 2004, U.S. EPA 2005, U.S. EPA 2007).

1.2.1 Vertical Radial Plume Mapping Methodology

The Vertical Radial Plume Mapping (VRPM) methodology of OTM-10 was applied to quantify fugitive methane emissions from the landfill cells. The VRPM method is described in EPA OTM-10 *Optical remote sensing for emission characterization from non-point sources,* which provides guidance on conducting measurements of pollutant mass emission flux from area sources using scanning optical remote sensing (ORS) instrumentation. The technique utilizes open-path optical remote sensing instrumentation (such as OP-TDL) to obtain path-integrated concentration information along multiple optical beam measurement paths. The measurement paths are defined by the distance between a scanning optical remote sensing instrument and a retro-reflecting mirror which is deployed at some distance from the scanning instrument. The multi-path concentration data along with meteorological data, collected concurrently, are processed to yield a mass emission flux from the source. Figure 1-4 shows an example 5-beam VRPM measurement configuration. For the current project, a 5-beam configuration was used with

2 beams deployed on the surface between the instrument and a vertical structure (scissor lift), and 3 beams extending along the ground, middle, and top of a scissor lift. The OP-TDL instrument beam collected data along each beam path for 30 seconds, before scanning to the next beam path in the configuration.

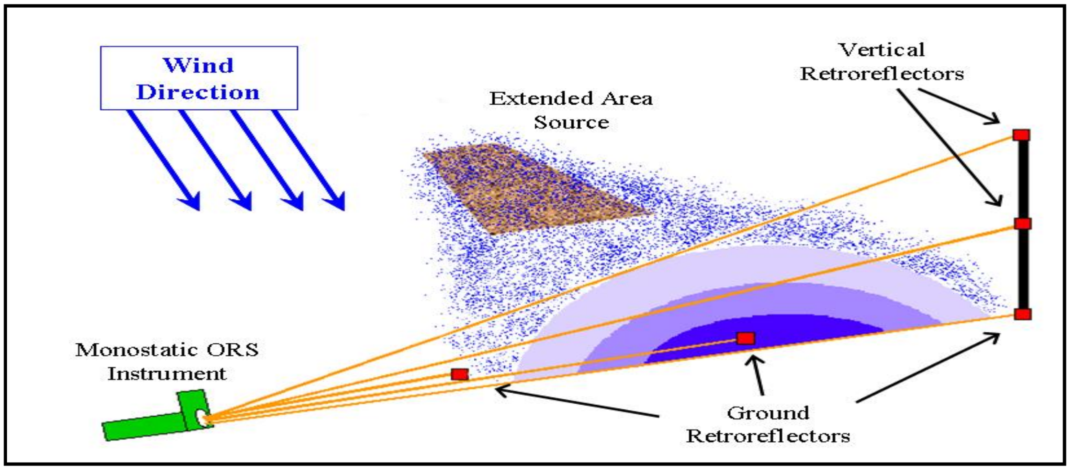

Figure 1-4. Example OTM 10 VRPM Measurement Configuration

Further information on the VRPM method can be found in Appendix A of this document.

1.2.2 Open-Path Tunable Diode Laser

The current study used one *GasFinder* 2.0 methane Open-Path Tunable Diode Laser (Boreal Laser, Spruce Grove, AB Canada) to collect path-integrated concentration data at the sites. The instrument was mounted on a scanner, and collected data along five measurement paths in each configuration.

The scanning Boreal *GasFinder* 2.0 OP-TDL instrument is designed for area and fugitive source emission characterization. The infrared laser emits radiation at a particular wavelength in the infrared region when an electrical current is passed through it. The light wavelength depends on the current and therefore allows scanning over an absorption feature and analyzing for the target gas concentration, using Beer's law. The laser signal is transmitted from a single telescope to a retro-reflecting mirror target, which is usually set up at a range of 100 to 1500 m. The returned light signal is received by the single telescope and directed to a detector. The instrument provides instantaneous, path-integrated methane concentration data. Figure 1-5 presents a picture of the *GasFinder* 2.0 OP-TDL that was used for the current study.

1.2.3 Meteorological Measurements

Wind speed and wind direction data were continuously collected during the measurement campaign with two R.M. Young model 05103 meteorological heads. The instrument is automated, and collects real-time data from its sensors and records time-stamped data, which is transmitted to a desktop computer via a radio frequency modem. During the measurements, one head was deployed at the base of the scissor lift at a height of approximately 2 meters, and the other head was deployed on top of the scissor lift platform at a height of approximately 10 meters.

1.3 FLIR Infrared Camera

Previous studies by EPA Region 6, EPA's Office of Research and Development (ORD) and ARCADIS have demonstrated that measurements can be improved by plume location using an infrared (IR) imaging camera to detect major leaks (U.S. EPA, 2009). A FLIR GasFindIR infrared camera was leased for a portion of the study, and deployed at Site A. The camera was used to gather further information on the spatial distribution of potential fugitive leaks from the cell.

The camera has a nominal spectra range of 1- 5.4 µm. Using a 30 x 30 µm InSb detector with a 320 x 240 pixel array, the camera has capabilities of varying the integration times from 5 µs to 16.5 ms. The detector is operated at near liquid nitrogen temperatures using an integral Sterling cooler which provides the system with an NEdT of no more than 18 mK providing excellent sensitivity.

The spectral range is further limited with the use of a notch filter specifically designed for the detection of hydrocarbon infrared adsorptions in the 3 micron region. The narrow bandpass range of the filter is less than the infrared spectral absorption of gas phase hexane. The filter notch is positioned such that alkane gases, such as methane, have a significant response within the bandpass range.

The camera was deployed during the Fall 2009 campaign at Site A to monitor multiple gas wells that in the landfill cell where ORS measurements were being conducted.

Figure 1-5. Scanning Boreal Laser GasFinder 2.0 System

1.4 Total VOC and NMOC Measurements

Concentrations of NMOC were determined from samples of landfill gas collected from the gas header pipe at each site. The samples were collected using an adapted version of EPA Method 0040 – *Sampling of Principal Organic Hazardous Constituents from Combustion Sources Using Tedlar Bags*. Analysis of VOC concentrations was done by Research Triangle Park Laboratories, Inc. using EPA Method TO-15, *Determination of Volatile Organic Compounds (VOCs) in Air Collected in Specially-Prepared Canisters and Analyzed by Gas Chromatography/Mass Spectrometry (GC/MS)* as seen in the *Compendium of Methods for the Determination of Toxic Organic Compounds in Ambient Air, Second Edition (EPA 625/R-96/010b),* and EPA Method 25-C, *Determination of Nonmethane Organic Compounds in Landfill GasTotal Gaseous Non-Methane Organics (TGNMO) as Hexane Analysis.* Landfill gases were also measured using a landfill gas monitor for the measurement of methane, carbon dioxide, oxygen, nitrogen, and hydrogen sulfide.

1.5 Elemental Mercury Measurements

Elemental mercury measurements were collected from the gas header pipe at all three sites using a Lumex RA915+ instrument. The Lumex instrument is considered to be ideally suited to quantify and screen landfill gas samples for elemental mercury. This instrument has been used by US EPA, industry, and academic groups to quantify elemental mercury in indoor air and to estimate elemental mercury emissions in industrial process flue gases.

The Lumex RA915+ mercury analyzer produces real-time mercury concentration measurements by performing atomic absorption spectrometry (at 253.7 nm wavelength) on elemental mercury atoms in a continuously extracted gas stream. It achieves the low detection limit of 2 ng/m^3 by using a multi-path absorption cell, which has an effective optical path of approximately 10 meters. Selectivity is achieved primarily by using the Zeeman Effect using high frequency modulation of light polarization (ZAAS-HFM).

1.6 Calculation of NMOC Fluxes

As described previously, concentrations of NMOC were determined from samples of landfill gas collected at the gas header pipe at each site. Upon completion of the sample analysis, the concentration of the detected target compounds (obtained from the EPA Method TO-15 data) was ratioed to the concentration of the methane in the landfill gas samples (obtained from the EPA Method 25-C data). This ratio was used with the methane emissions data collected with the OTM-10 method to calculate an estimated emissions flux value, from the top of the landfill cell for each of the target VOC compounds, using the following formula:

$$F_t = [(C_t * F_o)/C_o]\ [M_t/M_o] \tag{3}$$

Where

- F_t *is the flux of the target compound (VOC)*
- C_t *is the measured concentration of the target compound*
- F_o *is the calculated methane flux*
- C_o *is the measured methane concentration with background methane subtracted*
- M_t *is the molecular weight of the target compound*
- M_o *is the molecular weight of methane*

1.7 Determination of Methane Emission Factors and Total Cell Fugitive Methane Emissions

The methane flux values measured with the OTM 10 method can be used to calculate methane emission factor values and total cell fugitive methane emissions. Quantifying the emissions from landfill sites is generally complex due to many factors such as the size and non-homogenous nature of the emission sources, location of multiple cell sources adjacent to one another, and topography at the sites. In order to develop standard procedures for characterizing methane emissions at landfill sites using the OTM 10 method, a long-term tracer release study was conducted by US EPA and Waste Management, Inc (Thoma et al., 2010). The results of the study were used to develop guidance that is applied in the current study to calculate total site methane emissions using OTM 10 data.

The methane emission factor, in units of grams per day per square meter, is calculated by first determining the area contributing to the flux (ACF) measured by the OTM 10 configuration. The ACF is dependent upon the length of the OTM 10 configuration plane, the wind speed during the time of the measurements, and whether or not the OTM 10 plane is configured to capture emissions from the slope or flat surface area of the landfill cell. The ACF (in m^2) is dependent upon the angle of the wind direction relative to the measurement place and is calculated using the following formula when the OTM 10 plane is configured to capture emissions from the flat surface area of the landfill cell:

$$ACF\ (m^2) = \frac{1}{2}\ [(\text{Length to 0\% mass capture})*(\text{length of the OTM 10 plane}] \quad (4)$$

The Length to 0% mass capture is calculated using the following equation when the OTM 10 plane is configured to capture emissions from a flat surface area:

$$\text{Length to 0\% mass capture (m)} = [(0.102)*(WS) + 0.712]/\ 0.0031 \quad (5)$$

Where:

WS = the average prevailing wind speed (in m/s) during the measurement period.

When the OTM 10 plane is configured to capture emissions from the slope of the cell, the Length to 0% mass capture is calculated using Equation 6 below:

$$\text{Length to 0\% mass capture (m)} = [(0.0941)*(WS) + 0.732]/\ 0.00334 \quad (6)$$

Once the ACF value has been calculated, the measured methane flux (g/s) is converted to units of grams per day and divided by the ACF value to yield a methane emission factor (g/day/m^2). The methane emission factor is then used to calculate total cell methane emissions by incorporating the total surface area of the cell being monitored. Uncertainty values for the emission factors may be calculated using standard error coefficients presented in Thoma et al., 2010.

The methane flux measurements and total site emission calculations from each of the three sites are presented in Section 3 of this document.

1.8 Field Schedule

Measurement of fugitive methane emissions and analysis of the header pipe gas were to be conducted in the fall of 2009 and then 6 months later. However, for Site B, the weather was too cold and wet to deploy so only one round of optical remote sensing measurements were conducted. Table 1-1 presents the dates that measurements were conducted at each of the three sites.

Table 1-1. Schedule of Work Performed at the Sites

Day	Site	Detail of Work Performed
Tuesday, November 17, 2009	Site A	OTM-10 measurements collected with two configurations
Wednesday, November 18, 2009	Site A	OTM-10 measurements collected with one configuration
Wednesday, November 18, 2009	Sites A & C	TO-15, Method 25C, total mercury, and landfill gas samples collected
Friday, November 20, 2009	Site A	OTM-10 measurements collected with one configuration
Monday, November 23, 2009	Site B	TO-15, Method 25C, total mercury, and landfill gas samples collected
Tuesday, November 24, 2009	Site A	OTM-10 measurements collected with one configuration
Tuesday, December 1, 2009	Site A	OTM-10 measurements collected with two configurations
Tuesday, December 1, 2009	Site B	Additional mercury sampling
Monday, December 7, 2009	Site C	OTM-10 measurements collected with one configuration
Tuesday, December 8, 2009	Site C	OTM-10 measurements collected with one configuration
Thursday, April 22, 2010	Site C	OTM-10 measurements collected with one configuration
Friday, April 23, 2010	Site C	OTM-10 measurements collected with one configuration
Wednesday, April 28, 2010	Site C	OTM-10 measurements collected with one configuration
Friday, April 30, 2010	Site C	OTM-10 measurements collected with one configuration
Tuesday, May 4, 2010	Site C	Serpentine pattern sampling
Wednesday, May 5, 2010	Site C	OTM-10 measurements collected with one configuration
Thursday, May 6, 2010	Site C	Serpentine pattern sampling
Thursday, May 6, 2010	Site C	OTM-10 measurements collected with one configuration
Friday, May 7, 2010	Site C	OTM-10 measurements collected with one configuration
Friday, May 14, 2010	Site A	OTM-10 measurements collected with one configuration
Thursday, May 20, 2010	Site A	OTM-10 measurements collected with one configuration
Friday, May 21, 2010	Site A	OTM-10 measurements collected with one configuration
Wednesday, May 26, 2010	Site A	OTM-10 measurements collected with one configuration
Thursday, May 27, 2010	Site A	OTM-10 measurements collected with one configuration
Thursday, June 3, 2010	Site A	OTM-10 measurements collected with one configuration
Friday, June 4, 2010	Site A	OTM-10 measurements collected with one configuration

Day	Site	Detail of Work Performed
Thursday, June 17, 2010	Site A	TO-15, Method 25C, total mercury, and landfill gas samples collected
Wednesday, June 23, 2010	Site B	TO-15, Method 25C, total mercury, and landfill gas samples collected
Thursday, June 24, 2010	Site C	TO-15, Method 25C, total mercury, and landfill gas samples collected
Monday, June 28, 2010	Site B	OTM-10 measurements collected with one configuration
Wednesday, June 30, 2010	Site B	OTM-10 measurements collected with one configuration
Thursday, July 1, 2010	Site B	OTM-10 measurements collected with one configuration
Thursday, July 8, 2010	Site A	Serpentine pattern sampling
Friday, July 9, 2010	Site C	Serpentine pattern sampling
Tuesday, July 13, 2010	Site B	Serpentine pattern sampling
Monday, August 2, 2010	Site B	OTM-10 measurements collected with one configuration
Tuesday, August 3, 2010	Site B	OTM-10 measurements collected with one configuration
Wednesday, August 4, 2010	Site B	OTM-10 measurements collected with one configuration
Thursday, August 5, 2010	Site B	OTM-10 measurements collected with one configuration
Monday, August 9, 2010	Site B	Background measurements downwind of hog farm near site
Tuesday, August 10, 2010	Site B	OTM-10 measurements collected with one configuration
Wednesday, August 11, 2010	Site B	OTM-10 measurements collected with one configuration

Chapter 2
Test Procedures

The following subsections describe the test procedures used during the OTM-10 measurements at each of the three sites. Refer to Figures 1-1 through 1-3 for the geographical orientation of each cell measured at Site A, B, and C, respectively. Emissions measurements were collected in each cell using a 5-mirror OTM-10 configuration and a scanning OP-TDL instrument. The coordinates of the mirrors used in each configuration are presented in Appendix B of this report. Additionally, the test procedures used to collect the mercury samples, gas header pipe samples and gas flow measurements, are described.

2.1 OTM-10 Measurements

2.1.1 Landfill Site A

The measurement site at Landfill A is a 32-acre area consisting of 3 landfill sub-cells and an interim cover. Waste was filled in three phases with the third phase beginning in 1997 (when waste began to be added) and ended in 2006 (when waste additions stopped). The measurement area was located in the southwestern corner of the facility. Small quantities of well-digested municipal wastewater sludge and ash were disposed over the MSW during 2007-2010. The cell had an intermediate cover of mixed soil and an active LFG collection system. The LFG collection system became operative in 2007, but at low efficiency due to distant location of the wells (only 20 extraction wells). In 2009, 29 extraction wells were added to the gas collection system and horizontal trenches were also installed and operative in 2010. OTM-10 emissions data were collected at the site on November 17-18, November 20, November 24, and December 1of 2009; and May 14, May 20-21, May 26-27, and June 3-4 of 2010.

Figures 2-1 and 2-2 present a close-up view of the measurement cell showing the locations of the OTM-10 measurements during the fall 2009 and spring 2010 campaigns, respectively. The dashed black lines depict the boundaries of the flat surface area and the bottom of the slopes of the cell. The multi-colored boxes depict the approximate area contributing to the measured emission flux (ACF) for each configuration, or the representative surface cell area sampled during with each configuration, as described previously in Section 1.7. The orientation of the ACF boundaries shown were based on the orientation of the average prevailing wind direction during each survey, with respect to the plane of the OTM 10 configuration. The actual ACF values are dependent upon the length of the OTM-10 configuration as well as the prevailing wind speed during the time of the measurements (higher wind speeds result in larger ACF values). The ACF values were calculated for each emission flux calculation, and are presented in Appendix C of this report. In selecting the locations to deploy the OTM-10 configurations at each site, the goal was to cover as much cell surface area as possible considering prevailing wind conditions, as this leads to greater confidence that the methane emissions data collected were representative of actual emissions from the cell. More information on how the ACF value is used to calculate methane emission factors is presented in Section 3 of this document.

Figure 2-3 shows one of the OTM-10 measurement configurations deployed at the site.

The cell at Site A contained a series of elevated gas wells (as seen in Figure 2-3). The locations of the wells were measured with a Global Positioning System (GPS), and are presented in Figure 2-4. The wells and surrounding cell surface were monitored for fugitive leaks during the campaign using a FLIR

Portable Gas Imaging Camera. The results from the FLIR Camera surveys are presented in Section 3 of this document.

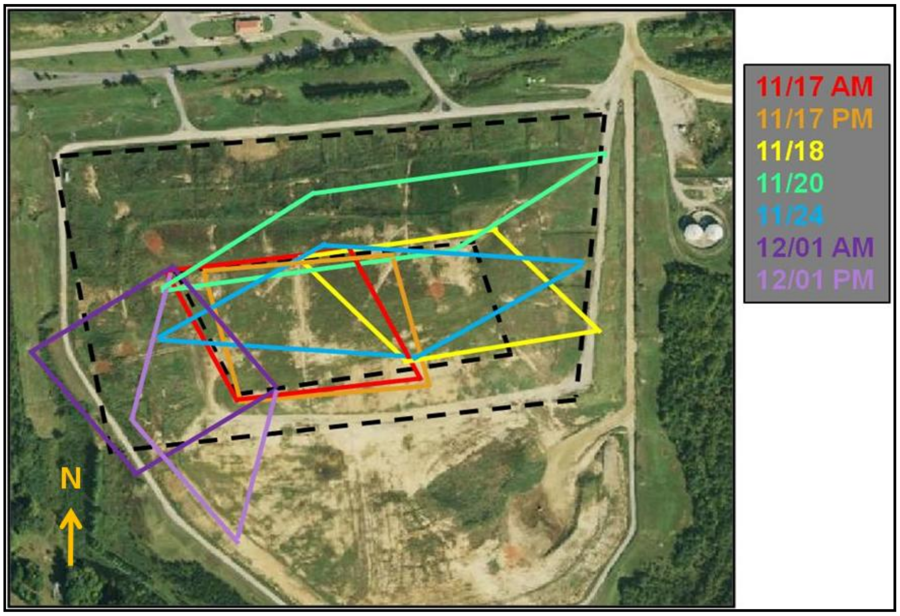

Figure 2-1. Overhead view of Measurement Cell at Site A Showing Areas Covered by OTM-10 Measurements During Fall 2009 Campaign.

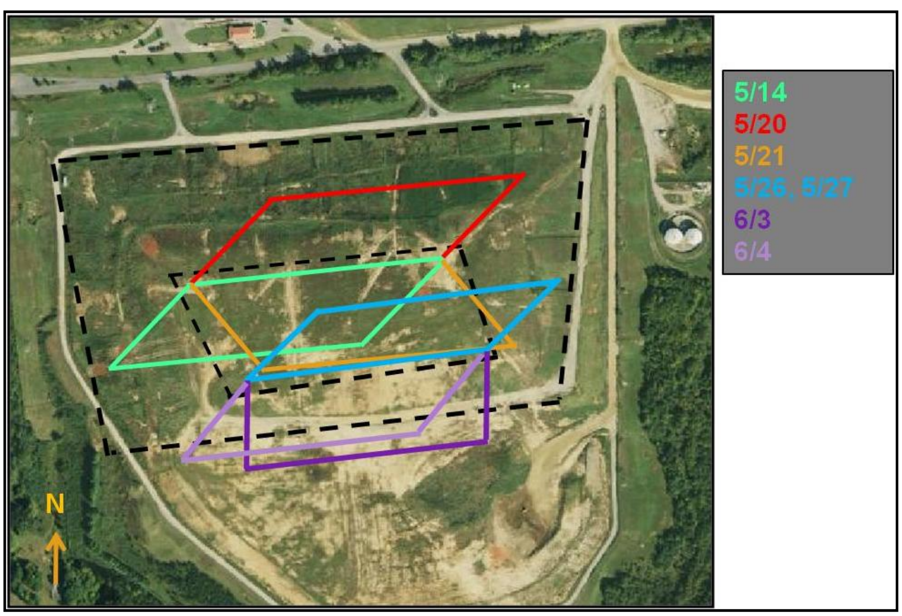

Figure 2-2. Overhead view of Measurement Cell at Site A Showing Areas Covered by OTM-10 Measurements During Spring 2010 Campaign.

Figure 2-3. OTM-10 Configuration at Site A

Figure 2-4. Location of Elevated Well Heads in Measurement Cell at Site A

2.1.2 Landfill Site B

OTM-10 monitoring was performed within two cells at Site B. The measurement cells were located on the northern side of the facility. The first cell is an 86-acre area with a gas collection system installed, and the gas extraction flow rate for the area can be obtained. Site operators estimated that 7.5 million tonnes of waste were disposed in this cell. This cell began accepting waste in 2000 and stopped accepting waste just prior to the beginning of the measurement campaign (in 2010). The cell was operated as a traditional landfill (i.e., no leachate recirculation). In 2003, the site began leachate recirculation. Landfill B had an active LFG collection system and the collected gas was flared at the time of this study. The gas collection system became operative in 2006 with the installation of 11 vertical wells in the lower elevations of the cell. Additional extraction wells were installed in 2008 and 2010 in the upper elevations; however, the west side-slope and the flat-top area did not have any gas collection wells at the time of this study. The cell has a mixed-soil intermediate cover, except on the east side-slope which had a geomembrane cover.

The second cell at Landfill Site B where measurements were conducted is a new cell that had only been accepting waste for approximately 3 months prior to the sampling. The approximate area of the new cell where waste was being accepted at the time of measurements was 6 acres. Because the cell is new, the gas collection system had not yet been installed.

OTM-10 emissions data were collected at the 86-acre cell on June 28, June 30, July 1, and August 2-5 of 2010. Data were collected at the new cell on August 10-11, 2010.

Figures 2-5 and 2-6 present a close-up view of the 86-acre and new cells respectively. The figures identify the locations of the OTM-10 measurements during the summer 2010 campaign. The dashed black lines depict the boundaries of the flat surface area and the bottom of the slopes of the cell. The multi-colored boxes depict the area of the cell contributing to the measured emission flux (ACF) for each configuration, or the representative surface cell area sampled with each configuration.

2.1.3 Additional Measurements at Site B

Upon arrival at Site B, the project team noted a hog farm located approximately 300 meters to the south of the cells being surveyed (see Figure 2-7). Although the farm was upwind to where the measurements were conducted and did not appear to be of potential concern, measurements were conducted to determine if there was any potential issues with methane emissions from the hog farm being detected at the landfill measurement locations. Methane emissions were not found to be above typical background concentrations for methane. Additional discussion is presented in Section 3.

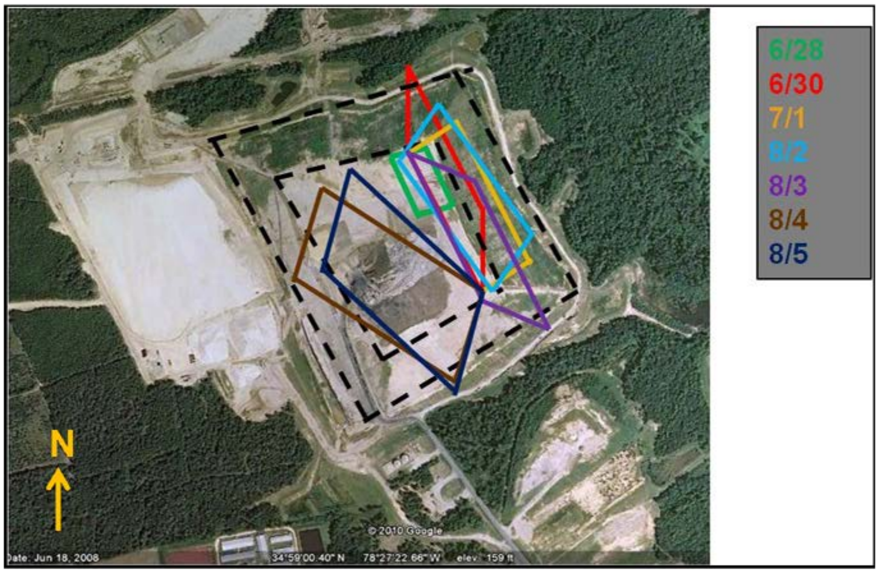

Figure 2-5. Overhead view of 86-acre Cell at Site B Showing Areas Covered by OTM-10 Measurements During Summer 2010 Campaign.

Figure 2-6. Overhead view of New Cell at Site B Showing Areas Covered by OTM-10 Measurements During Summer 2010 Campaign.

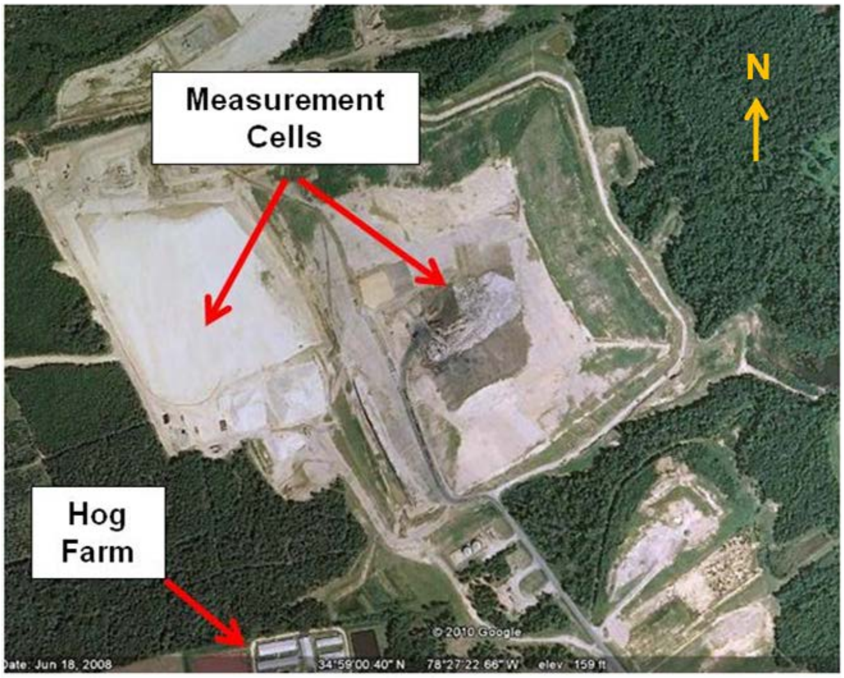

Figure 2-7. Overhead view of Site B Showing Location of the Hog Farm and the Measurement Cells (Hog farm was upwind from measurements)

2.1.4 Landfill Site C

The measurement cell at Site C is a closed area (closed in 2005) with active gas controls in place. The area is approximately 76 acres in size and contains a final cover. The measurement area, which is located near the center of the site, consists of two sub cells, each with steep side slopes. OTM-10 emissions data were collected at the site on December 7-8, 2009; and April 22-23, April 28, April 30, and May 5-7 of 2010.

Figures 2-8 and 2-9 present a close-up view of the measurement cell showing the locations of the OTM-10 measurements during the fall 2009 and spring 2010 campaigns, respectively. The dashed black lines depict the boundaries of the flat surface area and the bottom of the slopes of the cell. The multi-colored boxes depict the area of the cell contributing to the measured emission flux (ACF) for each configuration, or the representative surface cell area sampled with each configuration.

Figure 2-10 shows one of the OTM-10 measurement configurations deployed at the site.

Landfill C received MSW since 1972 and consisted of an unlined older cell and a newer piggyback cell. MSW disposal in the old cell stopped in 1997 and the cell was covered with a mixed-soil cover. An impermeable bottom linear was installed on one slope of the old cell and MSW was disposed in the adjacent piggyback and over the old cell. Waste disposal continued in the piggyback cell until 2005 and the new cell was covered with geosynthetics clay linear. An active LFG collection system with vertical wells was installed in the old cell in 1997 and in the piggyback cell in 2006. Landfill gas records starting from 1997 were available, with cumulative quantities from both cells since 2006. Approximately 7.7 million tonnes of MSW was disposed in the two cells.

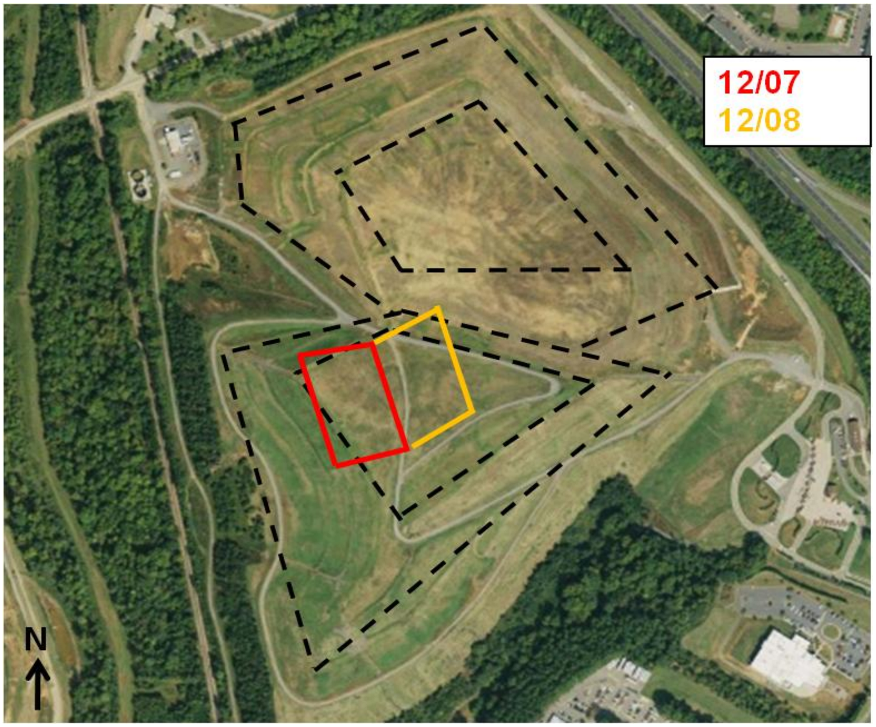

Figure 2-8. **Overhead view of Measurement Cell at Site C Showing Areas Covered by OTM-10 Measurements During Fall 2009 Campaign**

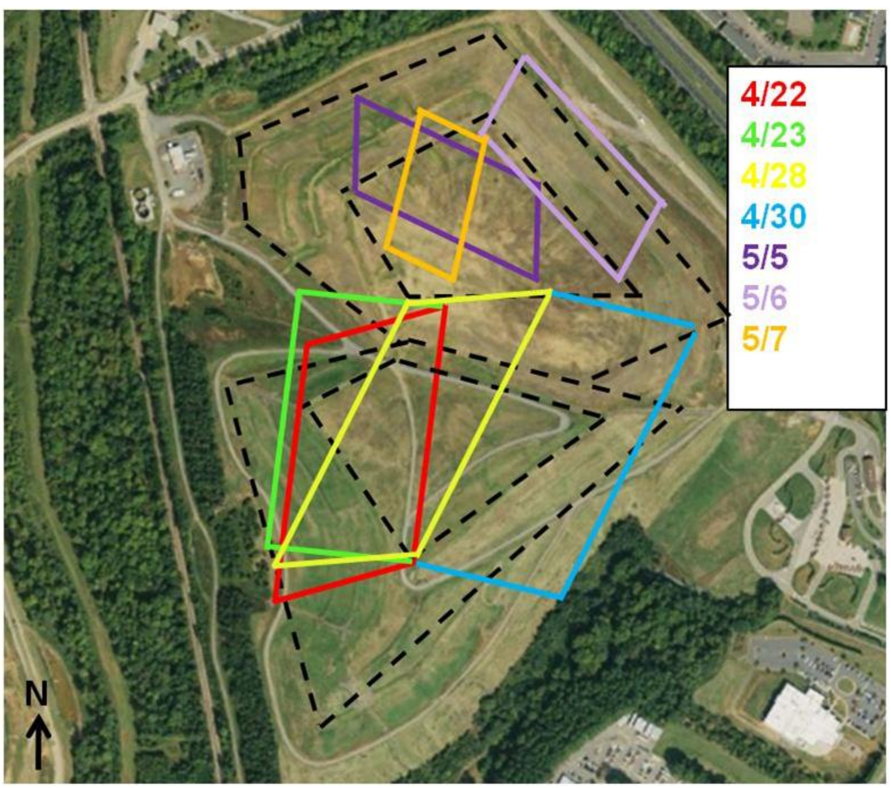

Figure 2-9. **Overhead view of Measurement Cell at Site C Showing Areas Covered by OTM-10 Measurements During Spring 2010 Campaign**

Figure 2-10. OTM-10 Configuration at Site C

2.2 Summa Canister Sampling

Summa canister samples were collected using a pre-cleaned critical orifice set for 300 mL/min connected to a 6 liter Summa canister sample container. The vacuum from the canister was used to pull the purge flow from the landfill gas header pipe through the critical orifice. TO-15 samples were collected for 3 minutes for a total volume of approximately 900 mL to reduce matrix effects and control moisture. Method 25-C samples were collected for 6 minutes for an approximate volume of 1,800 mL. Summa canister samples were analyzed using EPA Method TO-15 and EPA Method 25-C. These samples were collected for each site.

2.3 Total and Speciated Mercury Sampling

For the total mercury measurements, carbon tube samples taken from each site were analyzed by a modified SW-846 Method 7473, “Mercury in Solids and Solutions by Thermal Decomposition, Mercury Amalgamation, and Atomic Adsorption Spectroscopy” and CFR Part 60 Method 30B, “Determination of Total Vapor Phase Mercury Emissions from Coal-Fired Combustion Sources Using Carbon Sorbent Tubes.” Samples were analyzed using a Lumex RA-915+ Zeeman spectrometer with a RP-M324 decomposition furnace attachment cell. No mercury amalgamation was necessary due to the sensitivity of the instrument. The iodated carbon samples were loaded into a quartz combustion boat and inserted into a decomposition furnace at 775 °C. The mercury species were converted to elemental mercury and detected by the Zeeman atomic adsorption spectrometer. The analyzer was calibrated using NIST certified $HgCl_2$ standards from SCP Sciences. Elemental mercury spiking of the carbon tubes was performed using an impinger containing a stannous chloride solution. The mercury standard was dispensed into the impinger and the elemental mercury was pulled through the glassware system onto the iodated carbon. The elemental mercury spike was used to assess the recovery of the mercury from the carbon tubes.

Speciated measurements were made at Site B during the fall 2009 sampling campaign using specially designed mercury sampling traps to differentiate between oxidized and elemental mercury in the landfill header pipe gas samples. These traps have two sections of potassium chloride (KCl) for oxidized mercury capture and two sections of the iodated carbon for elemental mercury capture. By analyzing each section separately, the split between the species can be assessed.

2.4 Lumex Elemental Mercury Field Sampling

The Lumex mercury analyzer was used to sample elemental mercury concentration of the landfill gas at each site. The Lumex mercury analyzer was connected to a standard 500 ml 45/50 impinger using 28/15 connections to knock out excessive moisture. The impinger was cooled using a standard Apex Instruments cold box with water and ice. Gas was forced by positive pressure through the impinger to the Lumex analyzer using an atmospheric vent to eliminate over pressurization of the Lumex sample cell.

2.5 Serpentine Monitoring

A Thermo TVA-1000 flame ionization detector (FID) and a Micro FID portable analyzer were used to detect methane emissions from the landfill surface at each site during the spring 2010 field campaign. These measurements were collected 5 to 10 cm above the landfill surface. A 500 ppmv methane in air calibration gas was used to adjust the span of the instrument and a certified clean nitrogen cylinder was used to adjust the instrument zero. Measurements were collected at 25 foot intervals across the landfill surface. Methane emissions exceeding the background were recorded in conjunction with GPS readings.

This page intentionally left blank.

Chapter 3
Results and Discussion

The results from the measurement campaign are presented in the following subsections, including the calculated methane emission values from the OTM-10 measurements, FLIR camera data from Site A, data on VOC, and HAP and mercury analysis of the header pipe gas. This section also includes total cell fugitive methane emission calculations, and calculation of the landfill gas abatement efficiency at each site.

3.1 OTM-10 Measurements

The following subsections present a summary of the OTM-10 measurements at each of the three sites. The subsections contain summary tables reporting the average measured daily methane flux, the average daily calculated emission factor, and the average methane flux and emission factor from each campaign. Uncertainty in the average methane emission factor from each campaign was calculated using standard propagation-of-error calculations with a 95% confidence interval. The uncertainty values associated with the calculation of average methane emission factors are presented in Table 4-1 of this report. Daily summary tables showing all measured emission fluxes, wind conditions, and the calculated ACF are presented in Appendix C of this document. The methane emission flux values are calculated using methane concentration data collected along the 5-beam paths in each configuration, and wind data collected concurrently. An emission flux value is calculated for each measurement cycle, where a cycle is defined as one complete sequential data collection along all beam paths in the OTM-10 configuration. The methane emission flux values presented in Appendix C, and used to calculate daily average methane emission flux values presented in this report, were calculated using a moving average of 3 sequential measurement cycles.

Appendix D presents sample calculations of methane emission factors and measurement uncertainty using data collected during the fall 2009 campaign at Site A. In reporting the fugitive methane emissions from each site, the following assumptions are made regarding the representativeness of the measurements collected:

1) The areas within each landfill cell where measurements were collected are statistically representative of the entire cell, and an approximately equal number of measurements were collected from each sample area within the landfill cell.

2) The cover material (either interim or final) is homogeneous for all areas within a particular measurement cell.

As presented in Section 1.7, the equations used to calculated the Length to 0% Mass Capture differ when the OTM 10 plane is configured to capture emissions from the flat surface area or slope of the cell (see Equations 5 and 6). The Length to 0% Mass Capture value is used to calculate the ACF value, which is used in calculating the methane emission factor from the cell. As shown in Figures 2-1, 2-2, 2-5, 2-6, 2-8, and 2-9, there were many instances where the ACF of each OTM 10 measurement plane included both flat surface and slope areas of the measurement cell. In these cases, the Length to 0% Mass Capture was calculated using the flat surface area equation (Equation 5) if the majority of the ACF was located over flat surface areas of the cell, and the slope equation (Equation 6) if the majority of the ACF was located over slope areas of the cell.

In order to assess any potential bias to the methane emission factor calculation by using this approach, an additional calculation of methane emission factors was performed for instances where the measurement plane ACF included both slope and flat surface areas. This additional calculation was done by applying both Equation 5 and 6, and performing a weighted average calculation based on the apportionment of flat surface area and slope area within the ACF. The results of this calculation showed negligible differences in average site methane emission factors when compared to the approach used to calculate methane emission factors reported in this document.

It should be noted that prior to performing the OTM-10 emission flux calculations, the accepted global methane background concentration value of 1.7 ppmv was subtracted from all methane concentration data.

3.1.1 Landfill Site A

OTM-10 emissions data were collected at Site A on November 17-18, November 20, November 24, December 1 of 2009, and May 14, May 20-21, May 26-27, and June 3-4 of 2010. Tables 3-1 and 3-2 present a summary of the methane emissions measurements from the fall and spring campaigns at Site A, respectively. The tables present the average daily measured methane flux, as well as the average daily methane emission factor, which was calculated using the method described in Section 1.7. Figures 3-1 and 3-2 present a plot of all methane emission factor values calculated from the fall and spring campaigns at Site A, respectively. The figures are presented to illustrate the amount of variability in methane emissions observed during the campaigns.

Table 3-1. Methane Emission Results from the Fall 2009 Survey at Site A

Day	Average Daily Methane Flux (g/s)	Number of Flux Measurements	Average Daily Methane Emission Factor (g/day/m^2)
November 17	11	85	51
November 18	11	142	43
November 20	16	146	36
November 24	15	45	37
December 1	12	83	54

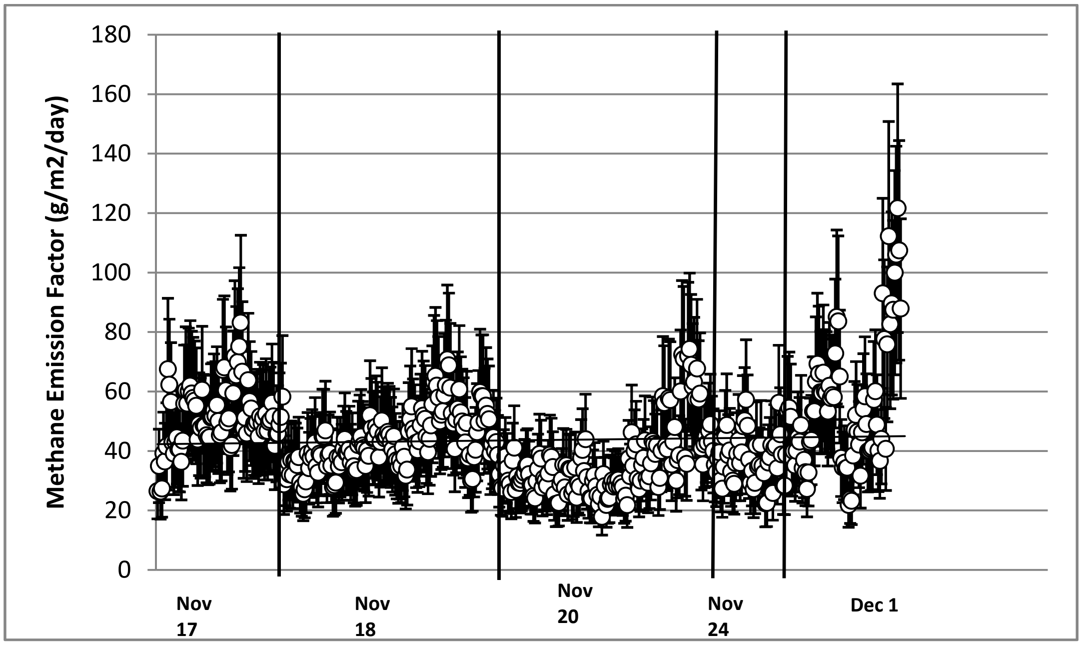

Figure 3-1. Plot of Methane Emission Factors from the Fall 2009 Survey at Site A

The average methane emission factor for the Fall 2009 measurement campaign at Site A was 44 ± 10 g/day/m^2. Figure 3-1 shows that the methane emission factor values were relatively consistent for most of the campaign, however higher emission factor values (greater than 70 g/day/m^2) were calculated from data collected during the last day of the study. The total cell methane emission rate is calculated by multiplying the methane emission factor by the total surface area of the cell. The surface area of the cell at Site A was estimated using **Google Earth** software. It should be noted that for each site, the **Google Earth** overhead depiction of the site was very similar to actual conditions encountered. The estimated cell surface area is 128,160 m^2. Multiplying this value by 44 g/day/m^2 yields a total cell methane emission rate of 5.6 x 10^6 grams/day.

Table 3-2. Methane Emission Results from the Spring 2010 Survey at Site A

Day	Average Daily Methane Flux (g/s)	Number of Flux Measurements	Average Daily Methane Emission Factor (g/day/m^2)
May 14	4.6	24	13
May 20	3.3	53	10
May 21	3.5	45	10
May 26	15	85	37
May 27	4.8	100	14
June 3	7.5	70	25
June 4	6.1	77	20

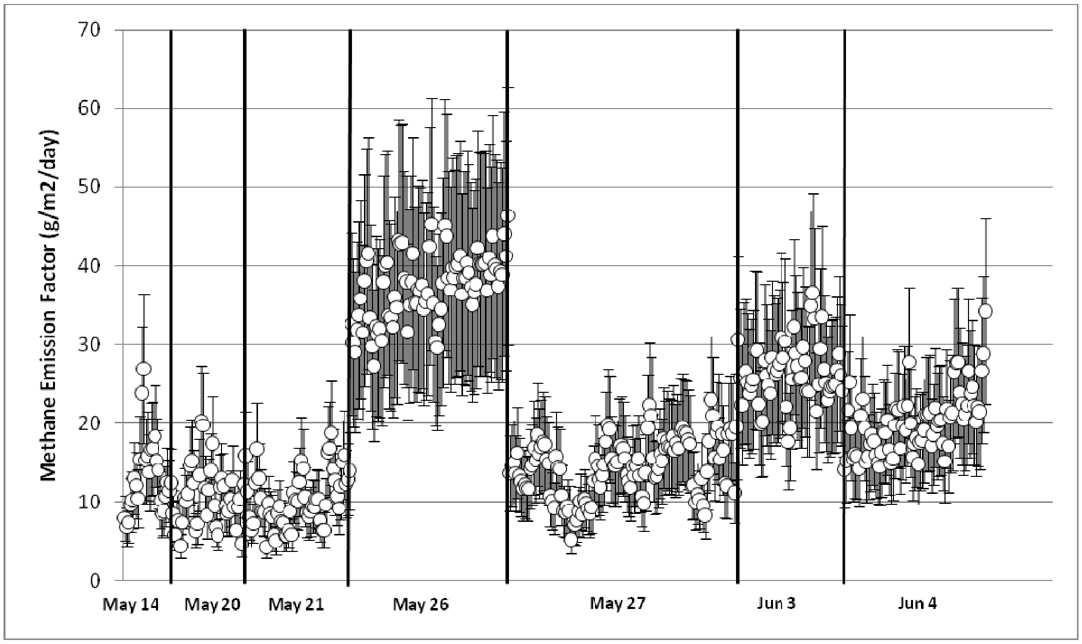

Figure 3-2. Plot of Methane Emission Factors from the Spring 2010 Survey at Site A

The average methane emission factor for the spring 2010 measurement campaign at Site A was 18 ± 9.1 g/day/m^2. Figure 3-2 shows that the methane emission factor values were relatively consistent for most of the campaign. However, higher emission factor values (greater than 30 g/day/m^2) were calculated from data collected on May 26. In fact, emission factor values calculated on May 26 were approximately twice as high as emission factor values calculated on May 27, although the landfill area sampled on the two days was similar (see Figure 2-2). The higher emission values observed on May 26 could be due to a number of factors, including differences in meteorological conditions on this day as compared to the other measurement days, differences in the landfill area being measured on May 26, or differences in landfill operations on this particular day.

In comparing meteorological conditions during the May 26 and May 27 surveys, there were differences in the average prevailing wind speed and wind direction during data collection. The average prevailing wind speed and wind direction were 4.2 m/s and 14 degrees, respectively during the May 26 survey, and 2.6 m/s and 22 degrees, respectively, during the May 27 survey. Differences in average prevailing wind speeds affect the calculation of ACF (see Section 1.7), as stronger wind speeds result in a larger representative cell area being sampled by the OTM-10 configuration. Since stronger wind speeds were observed on May 26 than on May 27, the representative cell area sampled on May 26 was larger than on May 27, meaning that emissions captured from cell areas on May 26 may not have been captured on May 27. Differences in prevailing wind direction also affect the location of the representative cell area sampled by the OTM-10 configuration. Although the difference in average wind direction during the May 26 and May 27 surveys is small (8 degrees), this difference shows that the area sampled during the two surveys was not identical. Because of the differences in the size and orientation of the representative cell area sampled during the May 26 and May 27 surveys, it is possible that localized methane emission hot spots captured during the May 26 survey were not captured by the May 27 survey. It is also possible that the relatively high methane emissions captured during the May 26 survey are the result of differences in landfill operations on this particular day.

The estimated cell surface area is 128,160 m^2. Multiplying this value by 18 g/day/m^2 yields a total cell methane emission rate of 2.3 x 10^6 grams/day.

3.1.2 Landfill Site B

OTM-10 emissions data were collected at Site B at the 86-acre cell on June 28, June 30, July 1, and August 2-5, 2010. Data were collected at the new cell August 10-11, 2010. Tables 3-3 and 3-4 present a summary of the methane emissions measurements from the 86-acre cell and new cell during the spring campaign, respectively. The tables present the average daily measured methane flux, as well as the average daily methane emission factor, which was calculated using the method described in Section 1.7. Figures 3-3 and 3-4 present a plot of all methane emission factor values calculated from the 86-acre, and new cells at Site B, respectively.

Table 3-3. Methane Emission Results from the Summer 2010 Survey of the 86-acre Cell at Site B

Day	Average Daily Methane Flux (g/s)	Number of Flux Measurements	Average Daily Methane Emission Factor (g/day/m^2)
June 28	25	9	87
June 30	62	103	123
July 1	104	141	207
August 2	45	63	105
August 3	74	85	169
August 4	101	82	148
August 5	147	161	217

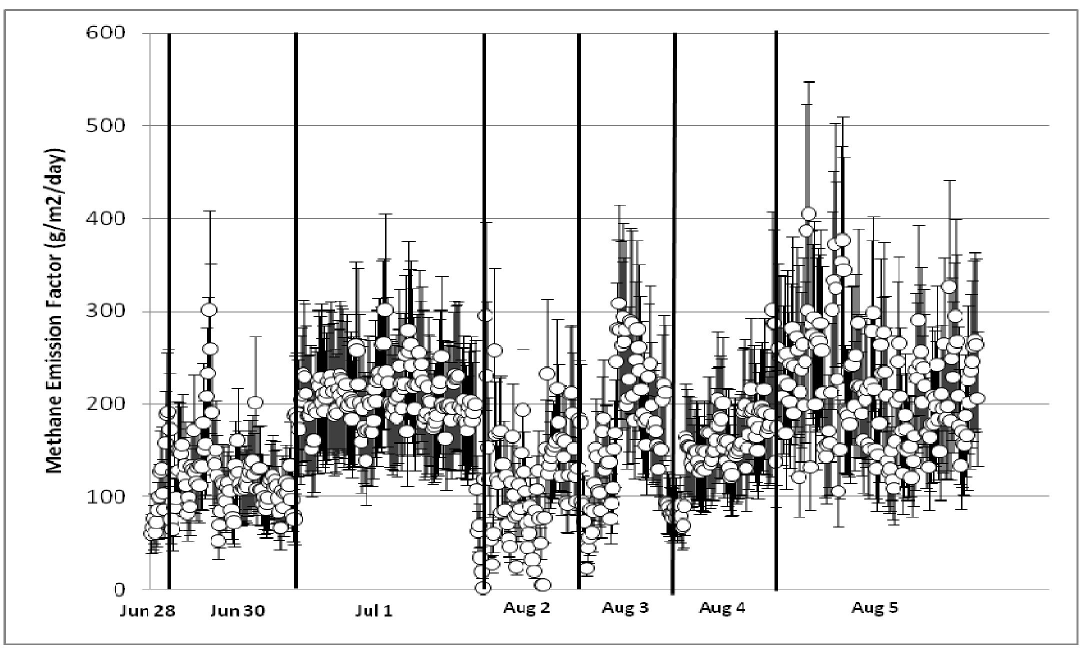

Figure 3-3. Plot of Methane Emission Factors from the Survey of the 86-Acre Cell at Site B

The average methane emission factor for the summer 2010 measurement campaign of the 86-acre cell at Site B was 150 ± 46 g/day/m^2. Figure 3-3 shows that there was a large amount of variability in the emission factors calculated from the site, with the highest values (greater than 250 g/day/m^2) calculated from data collected August 3-5.

Converting 86-acres to units of square meters yields a surface area of 348,030 m^2. Multiplying this value by 150 g/day/m^2 yields a total cell methane emission rate of 5.2 x 10^7 grams/day.

Table 3-4. Methane Emission Results from the Summer 2010 Survey of the New Cell at Site B

Day	Average Daily Methane Flux (g/s)	Number of Flux Measurements	Average Daily Methane Emission Factor (g/day/m^2)
August 10	5.9	106	26
August 11	5.3	145	23

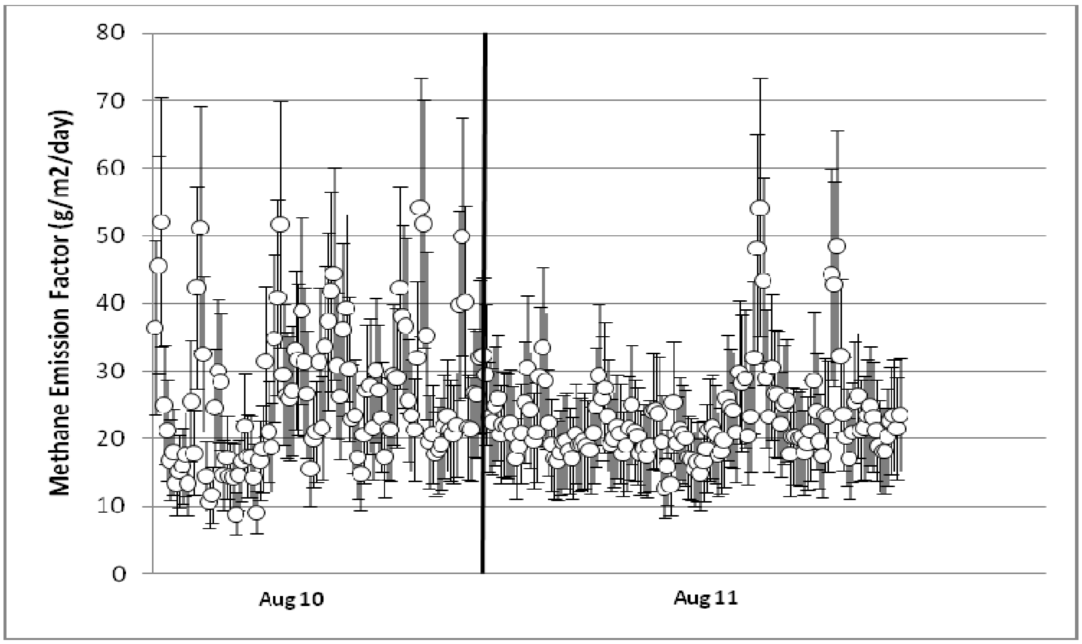

Figure 3-4. Plot of Methane Emission Factors from the Survey of the New Cell at Site B

The average methane emission factor for the summer 2010 measurement campaign of the new cell at Site B was 24 ± 8.6 g/day/m^2. As shown in Figure 3-4, the calculated methane emission factors from the survey did not show a large amount of variability over the two days that data were collected. The estimated surface area of the new cell is 25,650 m^2. Multiplying this value by 24 g/day/m^2 yields a total cell methane emission rate of 6.3 x 10^5 grams/day.

As discussed in Section 2.2.1, a hog farm was located approximately 300 meters to the south of the cells being surveyed at Site B (see Figure 2-7). In order to assess whether or not there were any fugitive methane emissions coming from the farm, methane concentration measurements were conducted directly downwind of the hog farm on August 9 using a single optical measurement path. Measurements were collected for a total of 45 minutes. The average measured methane concentration during the background measurement was 1.95 ± 0.1311 ppmv. This value is well below the average methane concentration measured along the 3 ground-level beam paths during the surveys conducted within the 86-acre cell at Site B (40.2 ppmv). The fact that the methane values measured downwind of the hog farm were well below values measured within the 86-acre cell, and the hog farm was located 300 meters south of the measurement cells suggest that any fugitive methane emissions from the hog farm had a negligible contribution to emission estimates from Site B. .

3.1.3 Landfill Site C

OTM-10 emissions data were collected at Site C on December 7-8, 2009, and April 22-23, April 28, April 30, and May 5-7, 2010. Tables 3-5 and 3-6 present a summary of the methane emissions measurements from the fall and spring campaigns at Site C, respectively. The tables present the average daily measured methane flux, as well as the average daily methane emission factor, which was calculated using the method described in Section 1.7. Figures 3-5 and 3-6 present a plot of all methane emission factor values calculated from the fall and spring campaigns at Site C, respectively.

Table 3-5. Methane Emission Results from the Fall 2009 Survey at Site C

Day	Average Daily Methane Flux (g/s)	Number of Flux Measurements	Average Daily Methane Emission Factor (g/day/m^2)
December 7	4.7	75	20
December 8	4.2	157	17

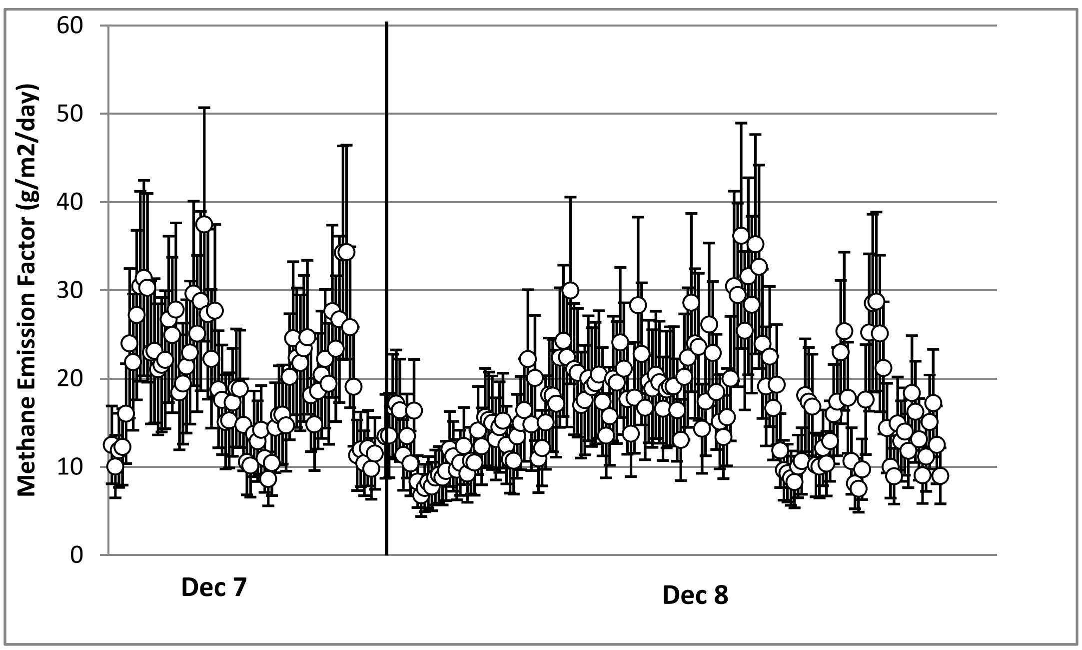

Figure 3-5. Plot of Methane Emission Factors from the Fall 2009 Survey at Site C

The average methane emission factor for the Fall 2009 measurement campaign at Site C was 19 ± 19 g/day/m^2.Although there was a large amount of variability in the methane emission factor values calculated during the survey (see Figure 3-5), the average daily methane emission factors were very similar for the two days of the survey.

The estimated cell surface area is 307,335 m^2. Multiplying this value by 19 g/day/m^2 yields a total cell methane emission rate of 5.8 x 10^6 grams/day.

Table 3-6. Methane Emission Results from the Spring 2010 Survey at Site C

Day	Average Daily Methane Flux (g/s)	Number of Flux Measurements	Average Daily Methane Emission Factor (g/day/m^2)
April 22	2.6	9	5.7
April 23	8.0	61	18
April 28	3.9	100	5.2
April 30	18	72	30
May 5	0.63	4	1.3
May 6	0.87	82	3.2
May 7	2.3	55	4.2

*Although the survey area at Site C was considered to be one cell, data was collected May 5-7 in the northern portion of the survey area. This area could considered a sub-cell within the survey area or a separate cell (see Figure 2-9)

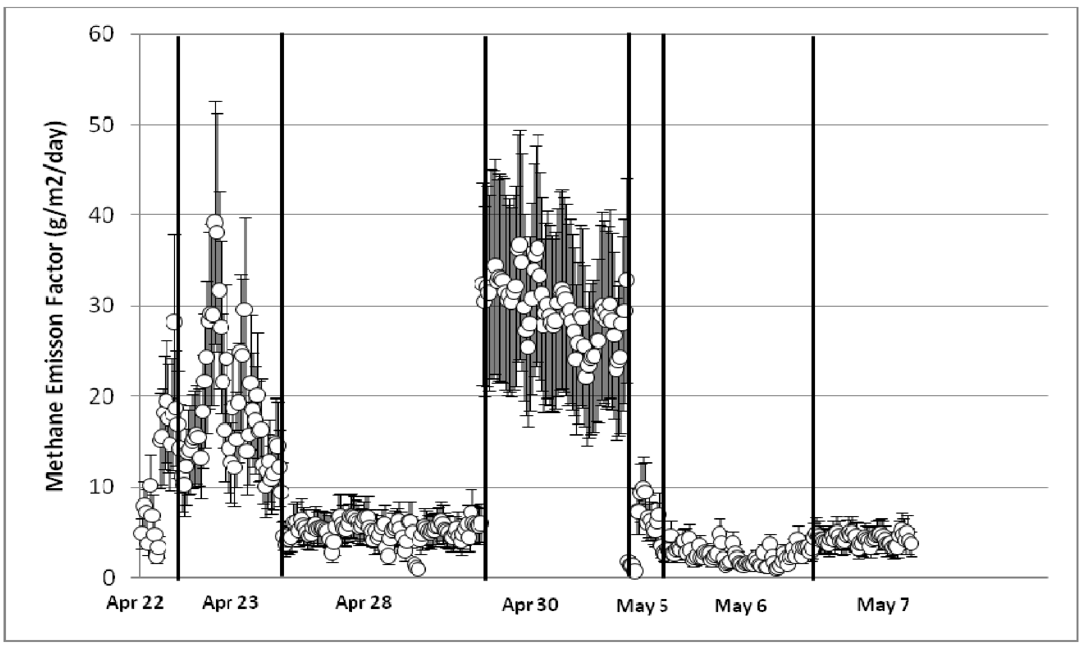

Figure 3-6. Plot of Methane Emission Factors from the Spring 2010 Survey at Site C

The average methane emission factor for the spring 2010 measurement campaign at Site C was 9.2 ± 9.7 g/day/m2. Figure 3-6 shows that there was a large amount of variability in the emission factors calculated from the site, with the highest values (greater than 15 g/day/m^2) calculated from data collected April 23 and April 30. As mentioned previously, differences in observed daily emission values could be due to a number of factors, including differences in meteorological conditions, differences in the landfill area being surveyed, or differences in landfill operations on a particular day. It is possible that the representative cell areas measured on April 23 and April 30 (as defined by the prevailing wind speed, wind direction, and length of the OTM-10 configuration) contained localized strong methane emission hot spots, which were not captured by the configurations on the other days of sampling.

It should also be noted that although the survey area at Site C was considered to be the same landfill cell, data was collected on May 5, 6, and 7 in the northern portion of the survey area, separate from data collected during the other days of the survey (see Figure 2-9). This area could be considered a sub-cell within the survey area or a separate cell, and may explain why methane emission factors from these days exhibited some of the lowest values found during the survey.

The estimated cell surface area is 307,335 m^2. Multiplying this value by 9.2 g/day/m^2 yields a total cell methane emission rate of 2.8×10^6 grams/day.

3.2 FLIR Infrared Camera Data

As mentioned in Section 2 and shown in Figure 2-4, the measurement cell at Site A contained a series of elevated gas wells. The wells and surrounding cell surface were monitored for fugitive emissions during the Fall 2009 campaign at Site A using the FLIR Portable Gas Imaging Camera.

The FLIR camera dataset contains multiple movies from several days of monitoring at Site A. Multiple leak events were confirmed from the dataset, with leaks detected from the base of several gas wells and various points along the surface of the landfill cell. Figures 3-7 and 3-8 present representative images from the detected events. The landfill surface observed during the FLIR camera surveys consisted of soil and grass. It should be noted that it is not possible to reproduce the details of a visible leak (as captured with video footage) using a single representative snap shot as presented in this report. The leaks, when viewed in moving video images, are much more pronounced and generally easier to identify.

Figure 3-7. Screenshots from FLIR Camera of Fugitive Leaks from Base of Gas Wells at Site A.

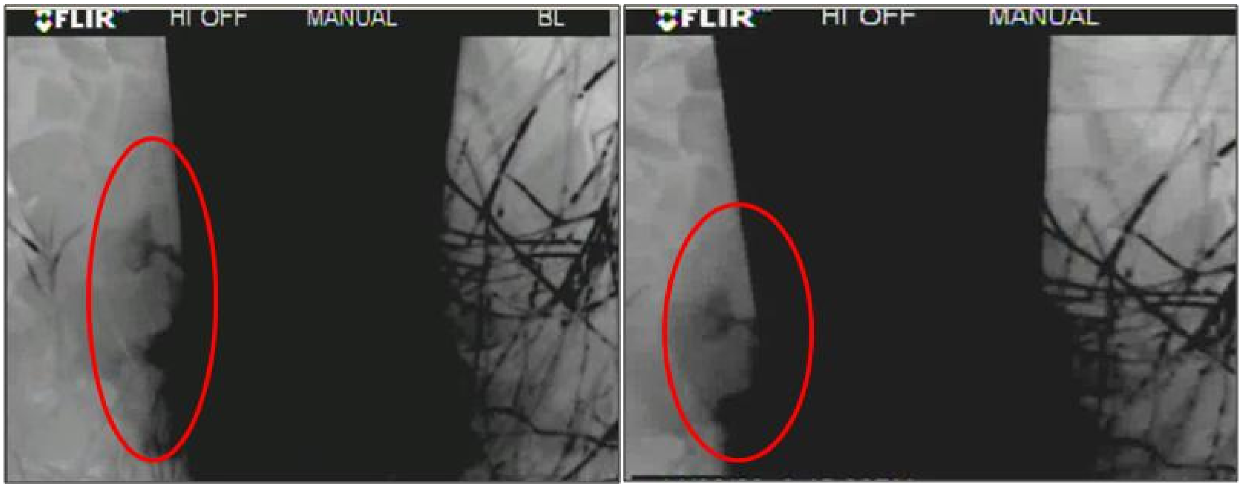

Figure 3-8. Additional Screenshots from FLIR Camera of Fugitive Leaks from Base of Gas Wells at Site A.

3.3 Summa Canister Sampling

3.3.1 Landfill Site A

Summa canister samples were collected from the gas collection header pipe in triplicate at Site A. These samples represent a composite of landfill gas (LFG) from the entire site. Samples were collected upstream of the vacuum pump to minimize losses and contamination. A blank was also collected using a nitrogen gas stream to purge the critical orifice. Samples were analyzed using Methods TO-15 and 25-C, and permanent gases (CH_4, O_2, N_2, CO_2, CO, and H_2S) using a landfill gas monitor. Results are presented in Tables 3-7 through 3-8. The results from the ambient sample show some detectable compounds. The results from the TO-15 nitrogen blank are shown and can be seen to be quite low, but above ambient levels. The TO-15 samples were analyzed by Eastern Research Group (ERG, Morrisville, NC). In computing averages, when all measurements are ND, the average is reported as ND. When one or more measurement is above detection, the ND measurement is treated as 50% of the stated MDL. Though not applicable here, the method further specifies that if the MDL is not reported, a ND measurement is treated as zero.

After data review, three of the samples collected during the Spring 2010 campaign were found to be invalid due to a leak either during sampling or transport to the laboratory. Results from this sample were excluded and a not reported (NR) flag was noted in Tables 3-8, 3-12, and 3-16.

The average TO-15 gas concentration values for the Fall 2009 and Spring 2010 samples shown in the VOC tables were corrected for air infiltration that can occur from landfill gas sample dilution and air intrusion into the landfill. The corrections were performed on the following formula provided in the U.S. Environmental Protection Agency document, *Compilation of Air Pollutant Emission Factors, AP-42*, Volume 1: Stationary Point and Area Sources, 5th ed., Chapter 2.4 (U.S. EPA, 1997).

$$C_P \ (\textit{corrected for air infiltration}) = \frac{C_P \ x \ (1 x 10^6)}{C_{CO_2} + C_{CH_4}} \qquad (7)$$

where:

C_P	=	*Concentration of pollutant P in LFG (i.e., NMOC as hexane), ppmv;*
C_{CO2}	=	*CO_2 concentration in LFG, ppmv;*
C_{CH4}	=	*CH_4 Concentration in LFG, ppmv; and*
1×10^6	=	*Constant used to correct concentration of P to units of ppmv.*

Table 3-7. Results of TO-15 Analysis from Site A / Fall 2009

	Sample Type:	Landfill Gas	Landfill Gas	Landfill Gas	Landfill Gas	Nitrogen Blank	Average Landfill Gas Concentration	Corrected Landfill Gas Concentration
	Can ID:	Can GS#1	Can GS#2	Can GS#3	Ambient (#4)	Blank (#5)		
CAS NO.	**COMPOUND**	**ppbv**	**ppbv**	**ppbv**	**ppbv**	**ppbv**	**ppbv**	**ppbv**
71-55-6	1,1,1-Trichloroethane	7.88	10.9	9.49	ND	ND	9.42	10.1
79-34-5	1,1,2,2-Tetrachloroethane	ND	ND	ND	ND	ND	ND	ND
79-00-5	1,1,2-Trichloroethane	ND	ND	ND	ND	ND	ND	ND
75-34-3	1,1-Dichloroethane	43.7	64.2	58.8	ND	ND	55.6	59.5
75-35-4	1,1-Dichloroethene	5.95	11.1	8.4	ND	ND	8.48	9.08
120-82-1	1,2,4-Trichlorobenzene	3.51	3.58	2.63	ND	ND	3.24	3.47
95-63-6	1,2,4-Trimethylbenzene	1060	1210	1090	0.231	1.47	1120	1200
106-93-4	1,2-Dibromoethane	ND	ND	ND	ND	ND	ND	ND
107-06-2	1,2-Dichloroethane	15.6	22.9	20.7	ND	ND	19.7	21.1
78-87-5	1,2-Dichloropropane	ND	ND	ND	ND	ND	ND	ND
108-67-8	1,3,5-Trimethylbenzene	387	440	417	0.114	0.770	415	444
106-99-0	1,3-Butadiene	17.7	26.1	23.9	ND	ND	22.6	24.2
75-05-8	Acetonitrile	240	370	333	ND	ND	314	337
74-86-2	Acetylene	71.8	98.8	84.5	1.83	8.45	85.0	91.0
107-02-8	Acrolein	ND	ND	ND	ND	ND	ND	ND
107-13-1	Acrylonitrile	21.6	ND	ND	ND	ND	8.11	8.68
71-43-2	Benzene	294	463	431	0.475	4.07	396	424
74-97-5	Bromochloromethane	ND	ND	ND	ND	ND	ND	ND
75-27-4	Bromodichloromethane	ND	ND	ND	ND	ND	ND	ND
75-25-2	Bromoform	ND	ND	ND	ND	ND	ND	ND
74-83-9	Bromomethane	ND	ND	ND	ND	ND	ND	ND
75-15-0	Carbon Disulfide	5.89	9.95	7.94	ND	ND	7.93	8.49
56-23-5	Carbon Tetrachloride	ND	ND	ND	ND	ND	ND	ND

	Sample Type:	Landfill Gas	Landfill Gas	Landfill Gas	Landfill Gas	Nitrogen Blank	Average Landfill Gas Concentration	Corrected Landfill Gas Concentration
	Can ID:	Can GS#1	Can GS#2	Can GS#3	Ambient (#4)	Blank (#5)		
CAS NO.	**COMPOUND**	**ppbv**	**ppbv**	**ppbv**	**ppbv**	**ppbv**	**ppbv**	**ppbv**
108-90-7	Chlorobenzene	ND	ND	ND	ND	ND	ND	ND
75-00-3	Chloroethane	31.9	51.3	42.9	ND	ND	42.0	45.0
67-66-3	Chloroform	ND	ND	ND	ND	ND	ND	ND
74-87-3	Chloromethane	17.0	21.1	19.1	0.390	ND	19.1	20.4
100-44-7	Chloromethylbenzene	ND	ND	ND	ND	ND	ND	ND
126-99-8	Chloroprene	ND	ND	ND	ND	ND	ND	ND
156-59-2	cis-1,2-Dichloroethylene	296	446	408	1.84	ND	383	410
10061-01-5	cis-1,3-Dichloropropene	ND	ND	ND	ND	ND	ND	ND
124-48-1	Dibromochloromethane	ND	ND	ND	ND	ND	ND	ND
75-71-8	Dichlorodifluoromethane	336	410	366	0.464	ND	371	397
75-09-2	Dichloromethane	185	269	228	0.358	ND	227	243
76-14-2	Dichlorotetrafluoroethane	32.8	39.7	35.0	ND	ND	35.8	38.4
140-88-5	Ethyl Acrylate	ND	ND	ND	ND	ND	ND	ND
637-92-3	Ethyl tert-Butyl Ether	ND	ND	ND	ND	ND	ND	ND
100-41-4	Ethylbenzene	3380	4030	4000	0.466	4.01	3800	4070
87-68-3	Hexachloro-1,3-butadiene	ND	ND	ND	ND	ND	ND	ND
100-01-6	m,p-Xylene	7590	8900	8650	0.858	6.83	8380	8970
541-73-1	m-Dichlorobenzene	ND	ND	ND	ND	ND	ND	ND
78-93-3	Methyl Ethyl Ketone	3710	5550	5300	0.591	6.32	4850	5200
108-10-1	Methyl Isobutyl Ketone	626	748	801	ND	ND	725	776
80-62-6	Methyl Methacrylate	ND	ND	ND	ND	ND	ND	ND
1634-04-4	Methyl tert-Butyl Ether	12.0	18.8	17.0	ND	ND	15.9	17.1
111-65-9	n-Octane	730	948	987	ND	0.816	888	951
95-50-1	o-Dichlorobenzene	ND	5.89	4.67	ND	ND	3.59	3.84
95-47-6	o-Xylene	2210	2560	2580	0.292	2.05	2450	2620

	Sample Type:	Landfill Gas	Landfill Gas	Landfill Gas	Landfill Gas	Nitrogen Blank	Average Landfill Gas Concentration	Corrected Landfill Gas Concentration
	Can ID:	Can GS#1	Can GS#2	Can GS#3	Ambient (#4)	Blank (#5)		
CAS NO.	**COMPOUND**	**ppbv**	**ppbv**	**ppbv**	**ppbv**	**ppbv**	**ppbv**	**ppbv**
106-46-7	p-Dichlorobenzene	463	522	448	0.174	1.83	478	511
115-07-1	Propylene	3400	4120	3830	2.57	14.8	3780	4050
100-42-5	Styrene	541	636	623	0.218	2.10	600	642
994-05-8	tert-Amyl Methyl Ether	ND	ND	ND	ND	ND	ND	ND
127-18-4	Tetrachloroethylene	423	549	527	ND	ND	500	535
108-88-3	Toluene	10100	13600	11700	1.42	13.2	11800	12600
156-60-5	trans-1,2-Dichloroethylene	11.9	18.3	15.4	ND	ND	15.2	16.3
10061-02-6	trans-1,3-Dichloropropene	ND	ND	ND	ND	ND	ND	ND
79-01-6	Trichloroethylene	196	274	253	ND	ND	241	258
75-69-4	Trichlorofluoromethane	10.4	15.6	11.9	0.223	ND	12.6	13.5
76-13-1	Trichlorotrifluoroethane	2.68	3.53	2.83	ND	ND	3.01	3.23
75-01-4	Vinyl chloride	310	427	384	ND	ND	374	400

ND = Not detected

Table 3-8. Results of TO-15 Analysis from Site A / Spring 2010

	Sample Type:	Landfill Gas	Landfill Gas	Landfill Gas	Nitrogen Blank	Average Landfill Gas Concentration	Corrected Landfill Gas Concentration
	Can ID:	00707030-01	00707030-02	00707030-03	00707030-11		
CAS NO.	**COMPOUND**	**ppbv**	**ppbv**	**ppbv**	**ppbv**	**ppbv**	**ppbv**
71-55-6	1,1,1-Trichloroethane	6.63	6.99	NR	ND	6.81	6.89
79-34-5	1,1,2,2-Tetrachloroethane	ND	ND	NR	ND	ND	ND
79-00-5	1,1,2-Trichloroethane	ND	ND	NR	ND	ND	ND
75-34-3	1,1-Dichloroethane	73.8	77.7	NR	ND	75.8	76.6
75-35-4	1,1-Dichloroethene	15.9	16.8	NR	ND	16.4	16.5
120-82-1	1,2,4-Trichlorobenzene	7.27	7.43	NR	ND	7.35	7.43
95-63-6	1,2,4-Trimethylbenzene	1780	1860	NR	0.132	1820	1840
106-93-4	1,2-Dibromoethane	ND	ND	NR	ND	ND	ND
107-06-2	1,2-Dichloroethane	19.9	20.7	NR	ND	20.30	20.5
78-87-5	1,2-Dichloropropane	12.6	ND	NR	ND	6.81	6.89
108-67-8	1,3,5-Trimethylbenzene	708	738	NR	0.054	723	731
106-99-0	1,3-Butadiene	30.9	33.8	NR	ND	32.4	32.7
75-05-8	Acetonitrile	389	453	NR	0.44	421	426
74-86-2	Acetylene	ND	ND	NR	0.422	ND	ND
107-02-8	Acrolein	ND	ND	NR	4.85	ND	ND
107-13-1	Acrylonitrile	ND	ND	NR	ND	ND	ND
71-43-2	Benzene	663	695	NR	0.211	679	687
74-97-5	Bromochloromethane	ND	ND	NR	ND	ND	ND
75-27-4	Bromodichloromethane	ND	ND	NR	ND	ND	ND
75-25-2	Bromoform	ND	ND	NR	ND	ND	ND
74-83-9	Bromomethane	ND	ND	NR	ND	ND	ND
75-15-0	Carbon Disulfide	9.29	10.6	NR	ND	9.95	10.1
56-23-5	Carbon Tetrachloride	ND	ND	NR	0.085	ND	ND

	Sample Type:	Landfill Gas	Landfill Gas	Landfill Gas	Nitrogen Blank	Average Landfill Gas Concentration	Corrected Landfill Gas Concentration
	Can ID:	00707030-01	00707030-02	00707030-03	00707030-11		
CAS NO.	COMPOUND	ppbv	ppbv	ppbv	ppbv	ppbv	ppbv
108-90-7	Chlorobenzene	64.5	78.4	NR	ND	71.5	72.2
75-00-3	Chloroethane	47.5	51.1	NR	ND	49.3	52.8
67-66-3	Chloroform	ND	ND	NR	ND	ND	ND
74-87-3	Chloromethane	19.2	21.5	NR	0.514	20.4	20.6
100-44-7	Chloromethylbenzene	ND	ND	NR	ND	ND	ND
126-99-8	Chloroprene	ND	ND	NR	ND	ND	ND
156-59-2	cis-1,2-Dichloroethylene	511	539	NR	ND	525	530
10061-01-5	cis-1,3-Dichloropropene	ND	ND	NR	ND	ND	ND
124-48-1	Dibromochloromethane	ND	ND	NR	ND	ND	ND
75-71-8	Dichlorodifluoromethane	5.61	1.94	NR	0.453	3.78	3.82
75-09-2	Dichloromethane	341	362	NR	0.083	352	355
76-14-2	Dichlorotetrafluoroethane	33.8	37.9	NR	ND	35.9	36.2
140-88-5	Ethyl Acrylate	ND	ND	NR	ND	ND	ND
637-92-3	Ethyl tert-Butyl Ether	ND	ND	NR	ND	ND	ND
100-41-4	Ethylbenzene	5660	5990	NR	0.321	5830	5890
87-68-3	Hexachloro-1,3-butadiene	ND	ND	NR	ND	ND	ND
100-01-6	m,p-Xylene	11400	12100	NR	0.661	11800	11900
541-73-1	m-Dichlorobenzene	ND	ND	NR	ND	ND	ND
78-93-3	Methyl Ethyl Ketone	9660	10600	NR	0.912	10100	10200
108-10-1	Methyl Isobutyl Ketone	1180	1370	NR	0.122	1280	1290
80-62-6	Methyl Methacrylate	ND	ND	NR	ND	ND	ND
1634-04-4	Methyl tert-Butyl Ether	26.5	28.9	NR	ND	27.7	28.0
111-65-9	n-Octane	1630	1700	NR	0.107	1670	1680
95-50-1	o-Dichlorobenzene	6.34	6.5	NR	ND	6	6.49

	Sample Type:	**Landfill Gas**	**Landfill Gas**	**Landfill Gas**	**Nitrogen Blank**	**Average Landfill Gas Concentration**	**Corrected Landfill Gas Concentration**
	Can ID:	**00707030-01**	**00707030-02**	**00707030-03**	**00707030-11**		
CAS NO.	**COMPOUND**	**ppbv**	**ppbv**	**ppbv**	**ppbv**	**ppbv**	**ppbv**
95-47-6	o-Xylene	3500	3680	NR	0.212	3590	3630
106-46-7	p-Dichlorobenzene	683	706	NR	0.05	695	702
115-07-1	Propylene	10.5	9.87	NR	0.4	10	10.3
100-42-5	Styrene	1150	1200	NR	0.075	1180	1190
994-05-8	tert-Amyl Methyl Ether	ND	ND	NR	ND	ND	ND
127-18-4	Tetrachloroethylene	662	688	NR	0.045	675	683
108-88-3	Toluene	14000	15500	NR	1.26	14800	14900
156-60-5	trans-1,2-Dichloroethylene	28.6	30.1	NR	ND	29.4	29.7
10061-02-6	trans-1,3-Dichloropropene	84.3	92.5	NR	ND	88.4	89.4
79-01-6	Trichloroethylene	341	354	NR	ND	348	351
75-69-4	Trichlorofluoromethane	17.2	18.6	NR	0.224	17.9	18.1
76-13-1	Trichlorotrifluoroethane	3.83	4.15	NR	0.082	3.99	4.03
75-01-4	Vinyl chloride	442	488	NR	ND	465	470

NR = Not Reported / Can had leak

ND = Not detected

Table 3-9 shows the results for non-methane organic compounds (NMOC) as hexane by Method 25-C at Site A for the fall 2009 and Table 3-10 for the spring 2010 sampling. After data review, one of the samples collected during the spring 2010 campaign (P1002396-003) was found to be invalid due to a leak either during sampling or transport to the laboratory. Results from this sample were excluded and a not reported (NR) flag was noted in Table 3-10.

Table 3-9. Results for NMOC as Hexane by Method 25-C from Site A / Fall 2009

Sample Type	Analyte: Sample ID	NMOC (ppmv)
Landfill Gas	P0904145-001	460
Landfill Gas	P0904145-002	460
Landfill Gas	P0904145-003	450
Nitrogen Blank	P0904145-010	ND

Table 3-10. Results for NMOC as Hexane by Method 25-C from Site A / Spring 2009

Sample Type	Analyte: Sample ID	NMOC (ppmv)
Landfill Gas	P1002396-001	460
Landfill Gas	P1002396-002	460
Landfill Gas	P1002396-003	NR
Nitrogen Blank	P1002396-011	0.81

NR = Not reported / leak during sampling

3.3.2 Landfill Site B

Summa canister samples were collected from the gas collection header pipe in triplicate at Site B. These samples represent a composite of LFG from the entire site. Samples were collected upstream of the vacuum pump to minimize losses and contamination. A blank was also collected using a nitrogen gas stream to purge the sample loop through a slip-stream while the canister was sampled. Samples were analyzed using Methods TO-15 (VOC) and 25-C (NMOC). Results for the TO-15 samples are presented in Tables 3-11 and 3-12 for the Fall 2009 and Spring 2010 campaigns. After data review, one VOC sample from the Spring 2010 sampling campaign (Can ID 00707030-05) had results an order of magnitude lower than the other two replicates suggesting a leak from the can or a dilution error at the laboratory and was not reported.

Table 3-11. Results of TO-15 Analysis from Site B / Fall 2009

	Sample Type:	**Landfill Gas**	**Landfill Gas**	**Landfill Gas**	**Landfill Gas**	**Nitrogen Blank**	**Average Landfill Gas Concentration**	**Corrected Landfill Gas Concentration**
	Can ID:	**Can SC#1**	**Can SC#2**	**Can SC#3**	**Can SC#4**	**Blank (#5)**		
CAS NO.	**COMPOUND**	**ppbv**	**ppbv**	**ppbv**	**ppbv**	**ppbv**	**ppbv**	**ppbv**
71-55-6	1,1,1-Trichloroethane	6.88	9.09	9.05	6.31	ND	7.83	7.86
79-34-5	1,1,2,2-Tetrachloroethane	ND	ND	ND	ND	ND	ND	ND
79-00-5	1,1,2-Trichloroethane	ND	ND	ND	ND	ND	ND	ND
75-34-3	1,1-Dichloroethane	35.6	51.0	56.6	38.4	ND	45.4	45.6
75-35-4	1,1-Dichloroethene	11.5	16.3	17.5	12.8	ND	14.5	14.6
120-82-1	1,2,4-Trichlorobenzene	1.54	2.42	1.95	1.59	ND	1.88	1.88
95-63-6	1,2,4-Trimethylbenzene	1220	1420	1380	1110	1.47	1280	1290
106-93-4	1,2-Dibromoethane	ND	ND	ND	ND	ND	ND	ND
107-06-2	1,2-Dichloroethane	238	282	362	234	ND	279	280
78-87-5	1,2-Dichloropropane	ND	ND	50.4	ND	ND	12.7	12.8
108-67-8	1,3,5-Trimethylbenzene	476	550	547	436	0.770	502	504
106-99-0	1,3-Butadiene	71.8	93.1	98.7	74.0	ND	84.4	84.7
75-05-8	Acetonitrile	ND	ND	ND	ND	ND	ND	ND
74-86-2	Acetylene	144	177	174	140	8.45	159	159
107-02-8	Acrolein	ND	ND	ND	ND	ND	ND	ND
107-13-1	Acrylonitrile	ND	ND	ND	ND	ND	ND	ND
71-43-2	Benzene	984	1130	1490	898	4.07	1130	1140
74-97-5	Bromochloromethane	ND	ND	ND	ND	ND	ND	ND
75-27-4	Bromodichloromethane	ND	ND	ND	ND	ND	ND	ND
75-25-2	Bromoform	ND	ND	ND	ND	ND	ND	ND
74-83-9	Bromomethane	ND	ND	ND	ND	ND	ND	ND
75-15-0	Carbon Disulfide	24.0	31.0	35.4	24.9	ND	28.8	28.9
56-23-5	Carbon Tetrachloride	ND	ND	ND	ND	ND	ND	ND
108-90-7	Chlorobenzene	ND	ND	76.6	ND	ND	19.2	19.3

	Sample Type:	Landfill Gas	Landfill Gas	Landfill Gas	Landfill Gas	Nitrogen Blank	Average Landfill Gas Concentration	Corrected Landfill Gas Concentration
	Can ID:	Can SC#1	Can SC#2	Can SC#3	Can SC#4	Blank (#5)		
CAS NO.	COMPOUND	ppbv	ppbv	ppbv	ppbv	ppbv	ppbv	ppbv
75-00-3	Chloroethane	41.9	58.7	59.7	44.3	ND	51.2	51.4
67-66-3	Chloroform	ND	ND	ND	ND	ND	ND	ND
74-87-3	Chloromethane	32.5	39.4	39.7	31.4	ND	35.8	35.9
100-44-7	Chloromethylbenzene	ND	ND	ND	ND	ND	ND	ND
126-99-8	Chloroprene	ND	ND	ND	ND	ND	ND	ND
156-59-2	cis-1,2-Dichloroethylene	442	520	630	418	ND	503	505
10061-01-5	cis-1,3-Dichloropropene	ND	ND	ND	ND	ND	ND	ND
124-48-1	Dibromochloromethane	ND	ND	ND	ND	ND	ND	ND
75-71-8	Dichlorodifluoromethane	587	736	719	596	ND	660	662
75-09-2	Dichloromethane	98.0	136	153	108	ND	124	124
76-14-2	Dichlorotetrafluoroethane	47.7	59.7	59.5	49.0	ND	54.0	54.2
140-88-5	Ethyl Acrylate	ND	ND	ND	ND	ND	ND	ND
637-92-3	Ethyl tert-Butyl Ether	ND	ND	ND	ND	ND	ND	ND
100-41-4	Ethylbenzene	4430	4700	5030	3890	4.01	4510	4530
87-68-3	Hexachloro-1,3-butadiene	ND	ND	ND	ND	ND	ND	ND
100-01-6	m,p-Xylene	8560	9100	9540	7460	6.83	8670	8710
541-73-1	m-Dichlorobenzene	ND	ND	ND	ND	ND	ND	ND
78-93-3	Methyl Ethyl Ketone	7950	8540	12200	7680	6.32	9090	9130
108-10-1	Methyl Isobutyl Ketone	1360	1430	1580	1170	ND	1390	1400
80-62-6	Methyl Methacrylate	ND	ND	ND	ND	ND	ND	ND
1634-04-4	Methyl tert-Butyl Ether	12.8	20.2	20.8	16.3	ND	17.5	17.6
111-65-9	n-Octane	1030	1110	1330	950	0.816	1110	1110
95-50-1	o-Dichlorobenzene	7.15	8.66	8.25	6.61	ND	7.67	7.70
95-47-6	o-Xylene	2230	2450	2560	2000	2.05	2310	2320
106-46-7	p-Dichlorobenzene	653	752	732	586	1.83	681	683

	Sample Type:	Landfill Gas	Landfill Gas	Landfill Gas	Landfill Gas	Nitrogen Blank	Average Landfill Gas Concentration	Corrected Landfill Gas Concentration
	Can ID:	Can SC#1	Can SC#2	Can SC#3	Can SC#4	Blank (#5)		
CAS NO.	**COMPOUND**	**ppbv**	**ppbv**	**ppbv**	**ppbv**	**ppbv**	**ppbv**	**ppbv**
115-07-1	Propylene	8800	10500	10200	8430	14.8	9480	9520
100-42-5	Styrene	1340	1470	1570	1200	2.10	1400	1410
994-05-8	tert-Amyl Methyl Ether	ND	ND	ND	ND	ND	ND	ND
127-18-4	Tetrachloroethylene	765	804	954	692	ND	804	807
108-88-3	Toluene	12200	12200	12100	10200	13.2	11700	11700
156-60-5	trans-1,2-Dichloroethylene	14.1	17.9	21.1	13.7	ND	16.7	16.8
10061-02-6	trans-1,3-Dichloropropene	ND	ND	ND	ND	ND	ND	ND
79-01-6	Trichloroethylene	279	275	376	244	ND	294	295
75-69-4	Trichlorofluoromethane	20.0	28.2	26.2	22.3	ND	24.2	24.3
76-13-1	Trichlorotrifluoroethane	2.24	3.18	2.81	2.59	ND	2.71	2.72
75-01-4	Vinyl chloride	574	753	759	591	ND	669	672

ND = Not detected

Table 3-12. Results of TO-15 Analysis from Site B / Spring 2010

	Sample Type:	**Landfill Gas**	**Landfill Gas**	**Landfill Gas**	**Nitrogen Blank**	**Average Landfill Gas Concentration**	**Corrected Landfill Gas Concentration**
	Can ID:	**00707030-04**	**00707030-05**	**00707030-06**	**00707030-11**		
CAS NO.	**COMPOUND**	**ppbv**	**ppbv**	**ppbv**	**ppbv**	**ppbv**	**ppbv**
71-55-6	1,1,1-Trichloroethane	3.10	NR	3.76	ND	3.43	3.53
79-34-5	1,1,2,2-Tetrachloroethane	ND	NR	ND	ND	ND	ND
79-00-5	1,1,2-Trichloroethane	ND	NR	ND	ND	ND	ND
75-34-3	1,1-Dichloroethane	26.9	NR	30.8	ND	28.9	29.7
75-35-4	1,1-Dichloroethene	22.1	NR	28.1	ND	25.1	25.8
120-82-1	1,2,4-Trichlorobenzene	3.73	NR	4.01	ND	3.87	3.99
95-63-6	1,2,4-Trimethylbenzene	1820	NR	2110	0.132	1970	2020
106-93-4	1,2-Dibromoethane	ND	NR	ND	ND	ND	ND
107-06-2	1,2-Dichloroethane	191	NR	233	ND	212	218
78-87-5	1,2-Dichloropropane	50.8	NR	62.3	ND	56.6	58.2
108-67-8	1,3,5-Trimethylbenzene	757	NR	885	0.054	821	846
106-99-0	1,3-Butadiene	88.1	NR	105	ND	96.6	99.4
75-05-8	Acetonitrile	643	NR	785	0.44	714	735
74-86-2	Acetylene	ND	NR	ND	0.422	ND	ND
107-02-8	Acrolein	ND	NR	ND	4.85	ND	ND
107-13-1	Acrylonitrile	ND	NR	ND	ND	ND	ND
71-43-2	Benzene	1860	NR	2250	0.211	2060	2120
74-97-5	Bromochloromethane	ND	NR	ND	ND	ND	ND
75-27-4	Bromodichloromethane	ND	NR	ND	ND	ND	ND
75-25-2	Bromoform	ND	NR	ND	ND	ND	ND
74-83-9	Bromomethane	1.00	NR	1.32	ND	1.16	1.19
75-15-0	Carbon Disulfide	24.7	NR	31.2	ND	28.0	28.8
56-23-5	Carbon Tetrachloride	ND	NR	ND	0.085	ND	ND

	Sample Type:	Landfill Gas	Landfill Gas	Landfill Gas	Nitrogen Blank	Average Landfill Gas Concentration	Corrected Landfill Gas Concentration
	Can ID:	00707030-04	00707030-05	00707030-06	00707030-11		
CAS NO.	COMPOUND	ppbv	ppbv	ppbv	ppbv	ppbv	ppbv
108-90-7	Chlorobenzene	129	NR	139	ND	134	138
75-00-3	Chloroethane	52.7	NR	63.8	ND	58.3	60.0
67-66-3	Chloroform	ND	NR	ND	ND	ND	ND
74-87-3	Chloromethane	1.32	NR	7.18	0.514	4.25	4.38
100-44-7	Chloromethylbenzene	ND	NR	ND	ND	ND	ND
126-99-8	Chloroprene	ND	NR	ND	ND	ND	ND
156-59-2	cis-1,2-Dichloroethylene	526	NR	641	ND	584	601
10061-01-5	cis-1,3-Dichloropropene	ND	NR	ND	ND	ND	ND
124-48-1	Dibromochloromethane	ND	NR	ND	ND	ND	ND
75-71-8	Dichlorodifluoromethane	6.99	NR	76.8	0.453	41.9	43.1
75-09-2	Dichloromethane	142	NR	174	0.083	158	163
76-14-2	Dichlorotetrafluoroethane	38.3	NR	46.5	ND	42.4	43.7
140-88-5	Ethyl Acrylate	ND	NR	ND	ND	ND	ND
637-92-3	Ethyl tert-Butyl Ether	ND	NR	ND	ND	ND	ND
100-41-4	Ethylbenzene	6050	NR	7160	0.321	6610	6800
87-68-3	Hexachloro-1,3-butadiene	ND	NR	ND	ND	ND	ND
100-01-6	m,p-Xylene	10700	NR	12700	0.661	11700	12000
541-73-1	m-Dichlorobenzene	ND	NR	ND	ND	ND	ND
78-93-3	Methyl Ethyl Ketone	16000	NR	19500	0.912	17600	18300
108-10-1	Methyl Isobutyl Ketone	1870	NR	2300	0.122	2090	2150
80-62-6	Methyl Methacrylate	ND	NR	ND	ND	ND	ND
1634-04-4	Methyl tert-Butyl Ether	23.2	NR	28.6	ND	25.9	26.7
111-65-9	n-Octane	1580	NR	1910	0.107	1750	1800
95-50-1	o-Dichlorobenzene	10.3	NR	12	ND	11.2	11.5

	Sample Type:	Landfill Gas	Landfill Gas	Landfill Gas	Nitrogen Blank	Average Landfill Gas Concentration	Corrected Landfill Gas Concentration
	Can ID:	00707030-04	00707030-05	00707030-06	00707030-11		
CAS NO.	**COMPOUND**	**ppbv**	**ppbv**	**ppbv**	**ppbv**	**ppbv**	**ppbv**
95-47-6	o-Xylene	3000	NR	3550	0.212	3280	3370
106-46-7	p-Dichlorobenzene	944	NR	1120	0.05	1030	1060
115-07-1	Propylene	48.2	NR	550	0.4	299	308
100-42-5	Styrene	1990	NR	2370	0.075	2180	2250
994-05-8	tert-Amyl Methyl Ether	ND	NR	ND	ND	ND	ND
127-18-4	Tetrachloroethylene	767	NR	917	0.045	842	867
108-88-3	Toluene	13500	NR	16000	1.26	14800	15200
156-60-5	trans-1,2-Dichloroethylene	27.7	NR	34.2	ND	31.0	31.9
10061-02-6	trans-1,3-Dichloropropene	143	NR	181	ND	162	167
79-01-6	Trichloroethylene	311	NR	376	ND	344	354
75-69-4	Trichlorofluoromethane	26.4	NR	31.8	0.224	29.1	30.0
76-13-1	Trichlorotrifluoroethane	3.2	NR	3.88	0.082	3.54	3.60
75-01-4	Vinyl chloride	21.4	NR	45	ND	33.2	34.0

NR = Not Reported / Can had leak

ND = Not detected

Tables 3-13 and 3-14 show the results for NMOC as hexane by Method 25-C at Site B.

Table 3-13. Results for NMOC as Hexane by Method 25-C from Site B / Fall 2009

Sample Type	Analyte: Sample ID	TGNMO (ppmv)
Landfill Gas	P0904145-007	240
Landfill Gas	P0904145-008	1100
Landfill Gas	P0904145-009	790
Nitrogen Blank	P0904145-010	ND

Table 3-14. Results for NMOC as Hexane by Method 25-C from Site B / Spring 2009

Sample Type	Analyte: Sample ID	TGNMO (ppmv)
Landfill Gas	P1002396-004	1,000
Landfill Gas	P1002396-005	1,100
Landfill Gas	P1002396-006	380
Nitrogen Blank	P1002396-011	0.81

3.3.3 Landfill Site C

Summa canister samples were collected from the gas collection header pipe in triplicate at Site C. These samples represent a composite of LFG from the entire site. Samples were collected upstream of the vacuum pump to minimize losses and contamination.

After data review, one of the samples collected at Site C during the spring 2010 campaign (00707030-08) was found to be invalid due to a leak either during sampling or transport to the laboratory. Results from this sample were excluded and a not reported (NR) flag was noted in Table 3-16.

Samples for Site C were analyzed using Methods TO-15 and 25-C. Results are presented in Tables 3-15 and 3-16.

Table 3-15. Results of TO-15 Analysis from Site C / Fall 2009

	Sample Type:	Landfill Gas	Landfill Gas	Landfill Gas	Landfill Gas	Nitrogen Blank	Average Landfill Gas Concentration	Corrected Landfill Gas Concentration
	Can ID:	Can WS#1	Can WS#2	Can WS#3	Can WS#4	Blank (#5)		
CAS NO.	**COMPOUND**	**ppbv**	**Ppbv**	**ppbv**	**ppbv**	**ppbv**	**ppbv**	**ppbv**
71-55-6	1,1,1-Trichloroethane	2.90	3.14	2.76	2.68	ND	2.87	2.91
79-34-5	1,1,2,2-Tetrachloroethane	17.8	ND	ND	ND	ND	4.56	4.62
79-00-5	1,1,2-Trichloroethane	ND	ND	ND	ND	ND	ND	ND
75-34-3	1,1-Dichloroethane	40.9	49.8	41.6	39.5	ND	43.0	43.5
75-35-4	1,1-Dichloroethene	9.92	12.2	10.1	9.89	ND	10.5	10.7
120-82-1	1,2,4-Trichlorobenzene	3.32	2.94	2.99	2.83	ND	3.02	3.06
95-63-6	1,2,4-Trimethylbenzene	1380	1340	1310	1280	1.47	1330	1350
106-93-4	1,2-Dibromoethane	ND	ND	ND	ND	ND	ND	ND
107-06-2	1,2-Dichloroethane	27.5	33.4	28.6	27.7	ND	29.3	29.7
78-87-5	1,2-Dichloropropane	ND	ND	ND	ND	ND	ND	ND
108-67-8	1,3,5-Trimethylbenzene	538	531	513	502	0.770	521	528
106-99-0	1,3-Butadiene	31.3	37.2	31.7	31.6	ND	33.0	33.4
75-05-8	Acetonitrile	504	636	530	472	ND	536	543
74-86-2	Acetylene	112	121	105	103	8.45	110	112
107-02-8	Acrolein	ND	ND	ND	ND	ND	ND	ND
107-13-1	Acrylonitrile	ND	ND	ND	ND	ND	ND	ND
71-43-2	Benzene	374	459	383	360	4.07	394	399
74-97-5	Bromochloromethane	ND	ND	ND	ND	ND	ND	ND
75-27-4	Bromodichloromethane	ND	ND	ND	ND	ND	ND	ND
75-25-2	Bromoform	ND	ND	ND	ND	ND	ND	ND
74-83-9	Bromomethane	ND	ND	ND	ND	ND	ND	ND
75-15-0	Carbon Disulfide	4.98	5.87	5.07	4.87	ND	5.20	5.27
56-23-5	Carbon Tetrachloride	ND	ND	ND	ND	ND	ND	ND
108-90-7	Chlorobenzene	ND	ND	ND	ND	ND	ND	ND

	Sample Type:	Landfill Gas	Landfill Gas	Landfill Gas	Landfill Gas	Nitrogen Blank	Average Landfill Gas Concentration	Corrected Landfill Gas Concentration
	Can ID:	Can WS#1	Can WS#2	Can WS#3	Can WS#4	Blank (#5)		
CAS NO.	**COMPOUND**	**ppbv**	**Ppbv**	**ppbv**	**ppbv**	**ppbv**	**ppbv**	**ppbv**
75-00-3	Chloroethane	27.6	32.4	28.0	27.6	ND	28.9	29.3
67-66-3	Chloroform	ND	ND	ND	ND	ND	ND	ND
74-87-3	Chloromethane	12.1	13.5	11.6	11.0	ND	12.1	12.2
100-44-7	Chloromethylbenzene	ND	ND	ND	ND	ND	ND	ND
126-99-8	Chloroprene	ND	ND	ND	ND	ND	ND	ND
156-59-2	cis-1,2-Dichloroethylene	451	548	465	443	ND	477	483
10061-01-5	cis-1,3-Dichloropropene	ND	ND	ND	ND	ND	ND	ND
124-48-1	Dibromochloromethane	ND	ND	ND	ND	ND	ND	ND
75-71-8	Dichlorodifluoromethane	375	415	358	352	ND	375	380
75-09-2	Dichloromethane	44.7	50.5	43.7	41.7	ND	45.2	45.7
76-14-2	Dichlorotetrafluoroethane	35.8	39.5	34.2	33.1	ND	35.7	36.1
140-88-5	Ethyl Acrylate	ND	ND	ND	ND	ND	ND	ND
637-92-3	Ethyl tert-Butyl Ether	ND	ND	ND	ND	ND	ND	ND
100-41-4	Ethylbenzene	3460	3680	3300	3250	4.01	3420	3470
87-68-3	Hexachloro-1,3-butadiene	ND	ND	ND	ND	ND	ND	ND
100-01-6	m,p-Xylene	7140	7560	6820	6750	6.83	7070	7160
541-73-1	m-Dichlorobenzene	ND	ND	ND	ND	ND	ND	ND
78-93-3	Methyl Ethyl Ketone	4900	6030	5010	4630	6.32	5140	5210
108-10-1	Methyl Isobutyl Ketone	983	1160	890	795	ND	957	970
80-62-6	Methyl Methacrylate	ND	ND	83.7	ND	ND	22.0	22.3
1634-04-4	Methyl tert-Butyl Ether	14.1	16.8	14.6	13.2	ND	14.7	14.9
111-65-9	n-Octane	931	1010	904	878	0.816	931	943
95-50-1	o-Dichlorobenzene	7.54	7.22	7.28	7.01	ND	7.26	7.36
95-47-6	o-Xylene	2010	2110	1920	1900	2.05	1990	2020
106-46-7	p-Dichlorobenzene	628	605	605	581	1.83	605	613

	Sample Type:	**Landfill Gas**	**Landfill Gas**	**Landfill Gas**	**Landfill Gas**	**Nitrogen Blank**	**Average Landfill Gas Concentration**	**Corrected Landfill Gas Concentration**
	Can ID:	**Can WS#1**	**Can WS#2**	**Can WS#3**	**Can WS#4**	**Blank (#5)**		
CAS NO.	**COMPOUND**	**ppbv**	**Ppbv**	**ppbv**	**ppbv**	**ppbv**	**ppbv**	**ppbv**
115-07-1	Propylene	2760	3000	2600	2530	14.8	2720	2760
100-42-5	Styrene	605	643	577	561	2.10	597	604
994-05-8	tert-Amyl Methyl Ether	ND	ND	ND	ND	ND	ND	ND
127-18-4	Tetrachloroethylene	528	580	519	502	ND	532	539
108-88-3	Toluene	10700	11400	10300	10300	13.2	10700	10800
156-60-5	trans-1,2-Dichloroethylene	12.8	16.3	13.7	12.8	ND	13.9	14.1
10061-02-6	trans-1,3-Dichloropropene	ND	ND	ND	ND	ND	ND	ND
79-01-6	Trichloroethylene	243	284	244	230	ND	250	254
75-69-4	Trichlorofluoromethane	6.25	7.38	6.25	6.40	ND	6.57	6.66
76-13-1	Trichlorotrifluoroethane	ND	1.96	ND	ND	ND	1.96	1.99
75-01-4	Vinyl chloride	371	427	366	357	ND	380	385

ND = Not detected

Table 3-16. Results of TO-15 Analysis from Site C / Spring 2010

	Sample Type:	Landfill Gas	Landfill Gas	Landfill Gas	Nitrogen Blank	Average Landfill Gas Concentration	Corrected Landfill Gas Concentration
	Can ID:	00707030-07	00707030-08	00707030-09	00707030-11		
CAS NO.	COMPOUND	ppbv	ppbv	ppbv	ppbv	ppbv	ppbv
71-55-6	1,1,1-Trichloroethane	ND	NR	15.3	ND	7.86	7.96
79-34-5	1,1,2,2-Tetrachloroethane	ND	NR	ND	ND	ND	ND
79-00-5	1,1,2-Trichloroethane	ND	NR	ND	ND	ND	ND
75-34-3	1,1-Dichloroethane	23.4	NR	128	ND	75.7	76.7
75-35-4	1,1-Dichloroethene	6.19	NR	36.1	ND	21.1	21.4
120-82-1	1,2,4-Trichlorobenzene	5.32	NR	12.5	ND	8.91	9.03
95-63-6	1,2,4-Trimethylbenzene	943	NR	3510	0.132	2230	2260
106-93-4	1,2-Dibromoethane	ND	NR	ND	ND	ND	ND
107-06-2	1,2-Dichloroethane	8.77	NR	49.9	ND	29.3	29.7
78-87-5	1,2-Dichloropropane	ND	NR	28.2	ND	14.4	ND
108-67-8	1,3,5-Trimethylbenzene	415	NR	1480	0.054	948	960
106-99-0	1,3-Butadiene	12.6	NR	57.3	ND	35.0	35.4
75-05-8	Acetonitrile	421	NR	1270	0.44	846	857
74-86-2	Acetylene	ND	NR	ND	0.422	ND	ND
107-02-8	Acrolein	ND	NR	ND	4.85	ND	ND
107-13-1	Acrylonitrile	ND	NR	ND	ND	ND	ND
71-43-2	Benzene	222	NR	1370	0.211	796	806
74-97-5	Bromochloromethane	ND	NR	ND	ND	ND	ND
75-27-4	Bromodichloromethane	ND	NR	ND	ND	ND	ND
75-25-2	Bromoform	ND	NR	ND	ND	ND	ND
74-83-9	Bromomethane	ND	NR	ND	ND	ND	ND
75-15-0	Carbon Disulfide	3.29	NR	19.2	ND	11.2	11.4
56-23-5	Carbon Tetrachloride	ND	NR	ND	0.085	ND	ND

	Sample Type:	Landfill Gas	Landfill Gas	Landfill Gas	Nitrogen Blank	Average Landfill Gas Concentration	Corrected Landfill Gas Concentration
	Can ID:	00707030-07	00707030-08	00707030-09	00707030-11		
CAS NO.	**COMPOUND**	**ppbv**	**ppbv**	**ppbv**	**ppbv**	**ppbv**	**ppbv**
108-90-7	Chlorobenzene	37.3	NR	172	ND	105	ND
75-00-3	Chloroethane	14	NR	122	ND	68.0	68.9
67-66-3	Chloroform	ND	NR	ND	ND	ND	ND
74-87-3	Chloromethane	ND	NR	46.3	0.514	23.3	23.6
100-44-7	Chloromethylbenzene	ND	NR	ND	ND	ND	ND
126-99-8	Chloroprene	ND	NR	ND	ND	ND	ND
156-59-2	cis-1,2-Dichloroethylene	164	NR	1230	ND	697	706
10061-01-5	cis-1,3-Dichloropropene	ND	NR	ND	ND	ND	ND
124-48-1	Dibromochloromethane	ND	NR	ND	ND	ND	ND
75-71-8	Dichlorodifluoromethane	ND	NR	153	0.453	76.6	78
75-09-2	Dichloromethane	20.5	NR	885	0.083	453	458
76-14-2	Dichlorotetrafluoroethane	16.2	NR	89.8	ND	89.8	91.0
140-88-5	Ethyl Acrylate	ND	NR	ND	ND	ND	ND
637-92-3	Ethyl tert-Butyl Ether	ND	NR	ND	ND	ND	ND
100-41-4	Ethylbenzene	2050	NR	8560	0.321	5310	3470
87-68-3	Hexachloro-1,3-butadiene	ND	NR	ND	ND	ND	ND
100-01-6	m,p-Xylene	4090	NR	15800	0.661	9950	7160
541-73-1	m-Dichlorobenzene	ND	NR	ND	ND	ND	ND
78-93-3	Methyl Ethyl Ketone	2990	NR	18200	0.912	10600	5210
108-10-1	Methyl Isobutyl Ketone	485	NR	2870	0.122	1680	1700
80-62-6	Methyl Methacrylate	ND	NR	ND	ND	ND	ND
1634-04-4	Methyl tert-Butyl Ether	ND	NR	61.1	ND	30.6	31.1
111-65-9	n-Octane	519	NR	3590	0.107	2060	2080
95-50-1	o-Dichlorobenzene	8.35	NR	13.4	ND	13.4	13.6

	Sample Type:	Landfill Gas	Landfill Gas	Landfill Gas	Nitrogen Blank	Average Landfill Gas Concentration	Corrected Landfill Gas Concentration
	Can ID:	00707030-07	00707030-08	00707030-09	00707030-11		
CAS NO.	COMPOUND	ppbv	ppbv	ppbv	ppbv	ppbv	ppbv
95-47-6	o-Xylene	1250	NR	6260	0.212	3760	2020
106-46-7	p-Dichlorobenzene	362	NR	1440	0.05	901	913
115-07-1	Propylene	ND	NR	ND	0.4	ND	ND
100-42-5	Styrene	249	NR	2450	0.075	1350	1370
994-05-8	tert-Amyl Methyl Ether	ND	NR	ND	ND	ND	ND
127-18-4	Tetrachloroethylene	136	NR	1420	0.045	778	788
108-88-3	Toluene	5310	NR	15500	1.26	10405	10800
156-60-5	trans-1,2-Dichloroethylene	ND	NR	66.7	ND	33.5	33.9
10061-02-6	trans-1,3-Dichloropropene	18.6	NR	187	ND	103	ND
79-01-6	Trichloroethylene	75.9	NR	745	ND	410	416
75-69-4	Trichlorofluoromethane	4.33	NR	43.6	0.224	43.6	44.2
76-13-1	Trichlorotrifluoroethane	2.08	NR	9.49	0.082	9.49	9.61
75-01-4	Vinyl chloride	181	NR	1000	ND	591	598

NR= Not Reported / Can had leak
ND = Not detected

Table 3-17 and 3-18 show the results for nonmethane organic compounds (NMOC) as hexane by Method 25-C at Site C.

Table 3-17. Results for NMOC as Hexane by Method 25-C from Site C / Fall 2009

Sample Type	Analyte: Sample ID	TGNMO (ppmv)
Landfill Gas	P0904145-001	650
Landfill Gas	P0904145-002	610
Landfill Gas	P0904145-003	600
Nitrogen Blank	P0904145-010	ND

Table 3-18. Results for NMOC as Hexane by Method 25-C from Site C / Spring 2010

Sample Type	Analyte: Sample ID	TGNMO (ppmv)
Landfill Gas	P1002396-007	170
Landfill Gas	P1002396-008	270
Landfill Gas	P1002396-009	280
Nitrogen Blank	P1002396-011	0.81

3.4 Total and Speciated Mercury Measurements

3.4.1 Landfill Site A

During the Fall 2009 sampling, the total mercury concentrations in the landfill gas from Site A ranged from 3.4 to 3.7 µg/m^3, with an average of 3.5 µg/m^3 and a relative standard deviation (RSD) of 5 percent. Table 3-19 presents the total mercury concentration data from Site A. The sample data have been corrected to 20 °C, 760 mm Hg, and dry volumes.

Table 3-19. Total Mercury Sample Concentrations from Site A / Fall 2009

Sample #	Total Mercury Gas Concentration (µg/m^3)
Gas Sample 1	3.7
Gas Sample 2	3.4
Gas Sample 3	3.4
RSD	5%

During the Spring 2010 sampling, the total mercury concentrations in the landfill gas from Site A ranged from 2.9 to 3.4 µg/m^3, with an average of 3.1 µg/m^3 and a relative standard deviation (RSD) of 10 percent. Table 3-20 presents the total mercury concentration data from Site A. The sample data have been corrected to 20 °C, 760 mm Hg, and dry volumes.

Table 3-20. Total Mercury Sample Concentrations from Site A / Spring 2010

Sample #	Total Mercury Gas Concentration (µg/m^3)
Gas Sample 1	3.4
Gas Sample 2	3.0
Gas Sample 3	2.9
RSD	10%

3.4.2 Landfill Site B

During the fall 2009 sampling, the total mercury concentrations in the landfill gas from Site B ranged from 8.4 to 8.9 µg/m^3, with an average of 8.7 µg/m^3 and an RSD of 3 percent. The elemental spike recovery for the total mercury sample was 60 percent. Table 3-21 presents the total mercury concentration data from Site B collected on November 23, 2009.

Table 3-21. Total Mercury Sample Concentrations from Site B / Fall 2009

Sample / Well Location	Total Mercury Gas Concentration (µg/m^3)	Spike Recovery (%)
Gas Sample 1	8.9	
Gas Sample 2	8.9	60
Gas Sample 3	8.4	
RSD	3%	

During the fall 2009 sampling, the total mercury concentrations in the landfill gas from Site B ranged from 8.4 to 8.9 µg/m^3, with an average of 8.7 µg/m^3 and an RSD of 3 percent. The elemental mercury spike recovery for the total mercury sample was 60%. This low elemental mercury spike recovery was due to a much lower spike level (10 ng) compared to the Hg mass loading from the landfill gas sampling (184 ng). Method 30B requires the spike level to be with 50 to 150% of the estimated sample mass loading to be considered a valid measurement to eliminate the difficulty of subtracting orders of magnitude when determining spike recoveries. The spike level determination does require some information on the expected concentrations in the gas which was unknown prior to sampling. This lower elemental spike recovery would have little effect on the accuracy of the mercury concentration result presented and would only effect spike recovery. Table 3-21 presents the total mercury concentration data from Site B collected on November 23, 2009.

Following the initial round of sampling at all three sites, additional sampling was performed at Site B on December 1, 2009 to collect some additional samples, spikes, and some speciated tube measurements to determine the split between oxidized and elemental mercury. Table 3-22 summarizes the spike results. Ten additional samples were collected with an average concentration of 5.9 ± 0.3 µg/m^3 and an RSD of 5 percent. Elemental spike recoveries for A and B were 94 and 98 percent, respectively and showed good capture of the mercury without interferences from the landfill gas. The sample data have been corrected to 20 °C, 760 mm Hg, and dry volumes.

Speciated measurements were made at this site during the fall 2009 sampling campaign using a combination trap that uses two sections of potassium chloride (KCl) for oxidized and two iodated carbon sections for elemental mercury. Results for the speciated samples collected are presented in Table 3-23. The speciated samples had an average of 1.2% oxidized and 98.8% elemental mercury.

Table 3-22. Additional Mercury Sampling Conducted at Site B / Fall 2009

	Total Mercury Gas Sampling
Average Concentration	5.9 μg/m3
N =	10
Standard Deviation	0.3 μg/m3
RSD	4.6%
Elemental Spike Recovery A	94%
Elemental Spike Recovery B	98%
Speciated Elemental A	99%
Speciated Elemental B	99%
Speciated Elemental C	98%

Table 3-23. Total Mercury Sample Concentrations from Site B / Fall 2009

Sample / Well Location	**Oxidized Mercury (%)**	**Elemental Mercury (%)**
Speciated Sample 1	0.7	99.3
Speciated Sample 2	0.4	98.6
Speciated Sample 3	1.6	98.4
RSD	38%	0.47%

During the spring 2010 sampling, the total mercury concentrations in the landfill gas from Site B ranged from 8.0 to 8.4 μg/m^3, with an average of 8.2 μg/m^3 and a relative standard deviation (RSD) of 3 percent. Table 3-24 presents the total mercury concentration data from Site B. The sample data have been corrected to 20 °C, 760 mm Hg, and dry volumes.

Table 3-24. Total Mercury Sample Concentrations from Site B / Spring 2010

Sample #	**Total Mercury Gas Concentration (μg/m^3)**
Gas Sample 1	8.4
Gas Sample 2	8.0
Gas Sample 3	8.1
RSD	3%

3.4.3 Landfill Site C

Total mercury concentrations in the landfill gas from Site C ranged from 8.8 to 9.0 µg/m^3, with an average of 8.9 µg/m^3 and an RSD of 1 percent. Table 3-25 presents the total mercury concentration data from Site C. The sample data have been corrected to 20 °C, 760 mm Hg, and dry volumes.

Table 3-25. Total Mercury Sample Concentrations from Site C / Fall 2009

Sample / Well Location	Total Mercury Gas Concentration (µg/m^3)
Gas Sample 1	9.0
Gas Sample 2	8.9
Gas Sample 3	8.8
RSD	1%

During the Spring 2010 sampling, the total mercury concentrations in the landfill gas from Site C ranged from 8.4 to 9.0 µg/m^3, with an average of 8.8 µg/m^3 and a relative standard deviation (RSD) of 4 percent. Table 3-26 presents the total mercury concentration data from Site C. The sample data have been corrected to 20 °C, 760 mm Hg, and dry volumes.

Table 3-26. Total Mercury Sample Concentrations from Site C / Spring 2010

Sample #	Total Mercury Gas Concentration (µg/m^3)
Gas Sample 1	9.0
Gas Sample 2	8.4
Gas Sample 3	9.0
RSD	4%

3.5 Lumex Elemental Mercury Measurements

3.5.1 Landfill Site A

Lumex elemental mercury continuous measurements at Site A were not performed during the Fall 2009 testing due to high negative vacuum at the sampling location. The Lumex elemental mercury measurements require a sample under positive pressure to operate. A sampling location downstream of the fan was installed during the Spring 2010 sampling trip. The Lumex elemental mercury continuous sampling concentrations from Site A ranged from 980 to 2355 ng/m^3 with an average of 1733 ng/m^3. These samples were collected during a 1 hour period on June 17, 2010. The sampling with the Lumex was also performed in conjunction with the total mercury samples at this site.

3.5.2 Landfill Site B

During the Fall 2009 sampling trip, the Lumex elemental mercury continuous sampling concentrations from Site #B ranged from 6226 to 6267 ng/m^3 with an average of 6243 ng/m^3. These samples were collected during a 2 hour period on November 23, 2009. During the spring 2010 sampling trip, the Lumex elemental mercury continuous sampling concentrations from Site B ranged from 1586 to 2897 ng/m^3 with an average of 2494 ng/m^3. These samples were collected during a 2 hour period on June 23, 2010. The sampling with the Lumex was also performed in conjunction with the total mercury samples at this site.

3.5.3 Landfill Site C

During the fall 2009 sampling trip, the Lumex elemental mercury continuous sampling concentrations from Site C ranged from 940 to 1010 ng/m^3 with an average of 975 ng/m^3. These samples were collected during a 1 hour period on November 18, 2009. During the spring 2010 sampling trip, the Lumex elemental mercury continuous sampling concentrations from Site C ranged from 697 to 826 ng/m^3 with an average of 747 ng/m^3. These samples were collected during a 2 hour period on June 24, 2010. The sampling with the Lumex was also performed in conjunction with the total mercury samples at this site.

3.6 Total Cell Gas Determination of Methane, O_2, CO_2, N_2, CO, and H_2S

Analysis for gas header pipe methane, O_2, CO_2, N_2, CO, and H_2S concentrations was performed using a Lantec GEM 2000+ landfill gas monitor rented from Ashtead Rentals. This monitor has an internal pump to draw sample from the header pipe and various chemical sensors to determine constituent concentrations. Calibration of the analyzer was performed using a certified mixture of these compounds to be obtained from the rental vendor. Tables 3-27 and 3-28 present the data collected at the landfills. During the monitoring for carbon monoxide for the fall 2009 sampling campaign, the landfill gas monitor displayed and error for this constituent.

Table 3-27. Gas Concentrations for the Landfills / Fall 2009

Site	CH_4 (%)	O_2 (%)	CO_2 (%)	N_2 (%)	CO (ppmv)	H_2S (ppmv)
A	53.8	2.1	39.6	4.5	NA	3
B	57.4	0.2	42.2	0.2	NA	0
C	56.3	1.2	42.4	0.1	NA	7

NA = Not Available

Table 3-28. Gas Concentrations for the Landfills / Spring 2010

Site	CH_4 (%)	O_2 (%)	CO_2 (%)	N_2 (%)	CO (ppmv)	H_2S (ppmv)
A	60.4	0	38.5	0	56	7
B	61.2	0	35.9	0	385	0
C	55.5	0	44.5	0	30	36

3.7 Serpentine Monitoring

3.7.1 Landfill Site A

On July 8, 2010 serpentine gas sampling was performed along the cap of the landfill using a Thermo TVA-1000 FID portable analyzer. All measurements were collected within 5 to 10 centimeters of the landfill surface. A DeLorme Earthmate PN-60 GPS was used to mark to location of the hits that were measured at the site. The results from the serpentine sampling at Site A are presented in Table 3-29. These results show a total of 18 points exceeding background levels (65 to 5000 ppmv) out of a total of

692 sampled points. The integrated concentration of methane measured at Landfill A was 44.6 ppmv. The location of the monitoring instruments, within the landfill cell, are shown in Figure 3-9.

Table 3-29. Locations and Methane Concentrations for Site A from Serpentine Sampling

Waypoint I.D.	Concentration (ppmv methane)	Latitude (N)	Longitude (W)
GI-1	65	36.10601	79.7318
GI-2	415	36.10607	79.7318
GI-3	578	36.10639	79.7316
GI-4	4200	36.10621	79.7314
GI-5	1500	36.10557	79.7313
GI-6	3000	36.10632	79.7314
GI-7	2600	36.10572	79.7308
GI-8	3800	36.10606	79.7308
GI-9	250	36.10544	79.7305
GI-10	1600	36.10544	79.7302
GI-12	4000	36.10597	79.7300
GI-13	740	36.10565	79.7301
GI-14	5000	36.10593	79.7297
GI-15	500	36.10569	79.7296
GI-16	700	36.10599	79.7288
GI-17	140	36.10592	79.7295
GI-166	1800	36.10629	79.7285

Figure 3-9. Map of Serpentine Sampling Locations at Site A

3.7.2 Landfill Site B

On July 13, 2010 serpentine gas sampling was performed along the cap of the landfill using a Thermo TVA-1000 FID portable analyzer. All measurements were collected within 5 to 10 centimeters of the landfill surface. A DeLorme Earthmate PN-60 GPS was used to mark to location of the hits that were measured at the site. Note that the wind speeds were between 5 to10 MPH. The wind direction was blowing directly off the open cells. The site was also spraying runoff water on top of this cell at the time of sampling. The site was still accepting trash in one section of the cap. The results from the serpentine sampling at Site B are presented in Table 3-30. These results show a total of 12 points exceeding background levels (350 to 4000 ppmv) out of a total of 903 sampled points. The integrated concentration of methane measured at Landfill A was 22.0 ppmv. The location of the monitoring locations, within the landfill cell, are shown in Figure 3-10.

Table 3-30. Locations and Methane Concentrations for Site B from Serpentine Sampling

Waypoint I.D.	Concentration (ppmv methane)	Latitude (N)	Longitude (W)
S-1	1400	34.98198	78.4571
S-2	800	34.98192	78.4565
S-3	350	34.98161	78.4570
S-4	1000	34.98157	78.4567
S-5	3500	34.98147	78.4565
S-6	1000	34.98076	78.4559
S-7	1400	34.98122	78.4558
S-8	1000	34.98103	78.4561
S-9	1000	34.98121	78.4561
S-10	600	34.98133	78.456
S-11	3800	34.98111	78.4567
S-12	4000	34.98134	78.4565

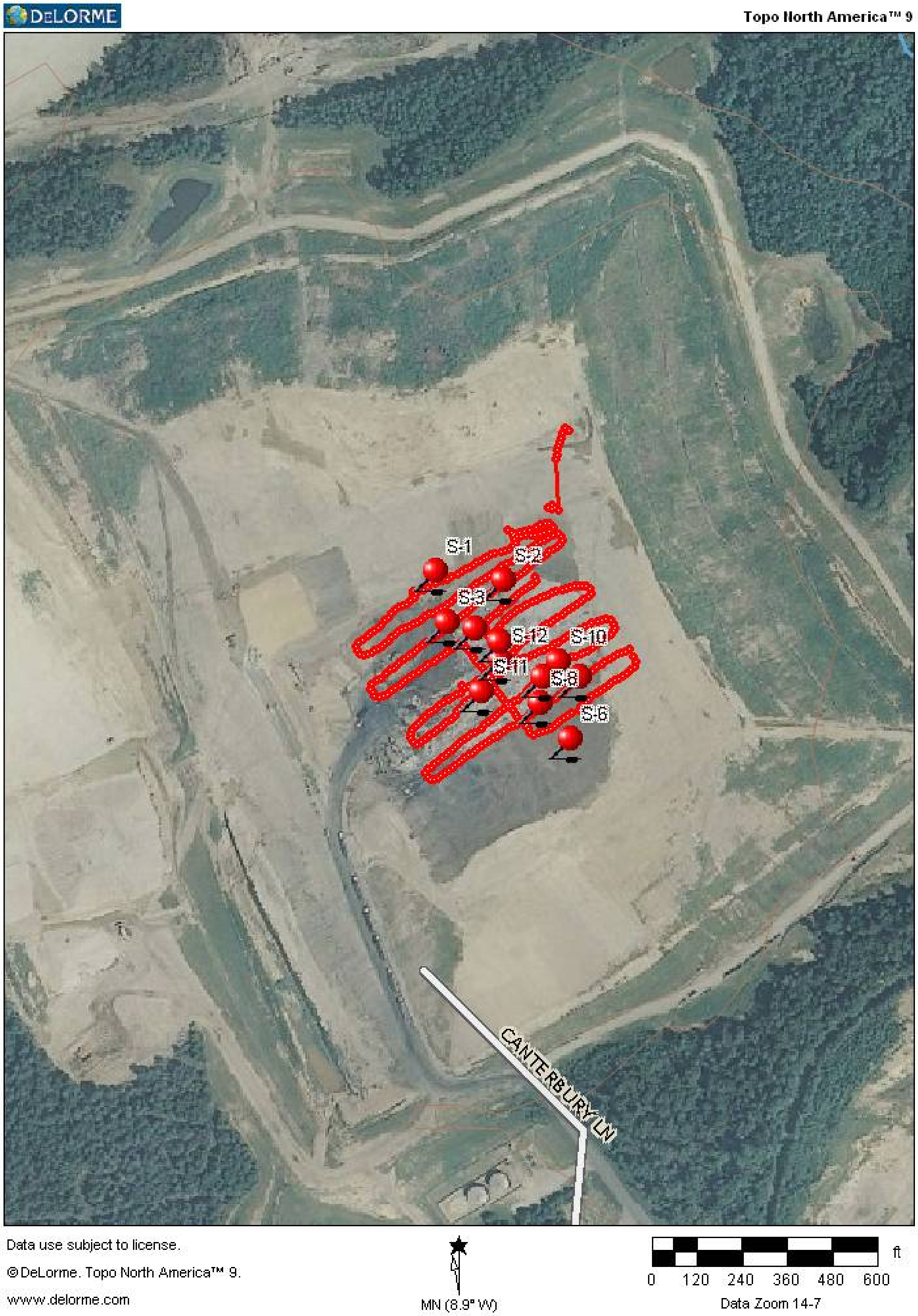

Figure 3-10. Map of Serpentine Sampling Locations at Site B

3.7.3 Landfill Site C

On May 4, 2010 serpentine gas sampling was started along the cap of the landfill using a Micro FID portable analyzer. All measurements were collected within 5 to 10 centimeters of the landfill surface. The batteries on the analyzers failed shortly after testing had started.

On May 6, 2010 Serpentine gas sampling was continued at site C. There were four hits recorded but there was no GPS information recorded. The locations are spotted on the map below.

On July 9, 2010 serpentine gas sampling was continued at site C using a Thermo TVA-1000 FID portable analyzer. A DeLorme Earthmate PN-60 GPS was used to mark to location of the serpentine pattern samples. The readings in Table 3-31 for Site C were collected before using the GPS. The approximate areas of these measurements were bounded by gas wells Vw-201, Vw-212, and Vw-222.

The results from the serpentine sampling at Site C are presented in Table 3-30. These results show a total of 4 points exceeding background levels (180 to 1430 ppmv) out of a total of 1798 sampled points. The integrated concentration of methane measured at Landfill A was 2.1 ppmv. The coordinates of the monitoring locations, within the landfill cell, are shown in Figure 3-11.

Table 3-31. Locations and Methane Concentrations for Site C from Serpentine Sampling

Waypoint I.D.	Concentration (ppmv methane)	Latitude (W)	Longitude (N)
W-1	1400	NA	NA
W-2	180	NA	NA
W-3	1430	NA	NA
W-4	750	NA	NA

NA = Not Available / No GPS used at Site C

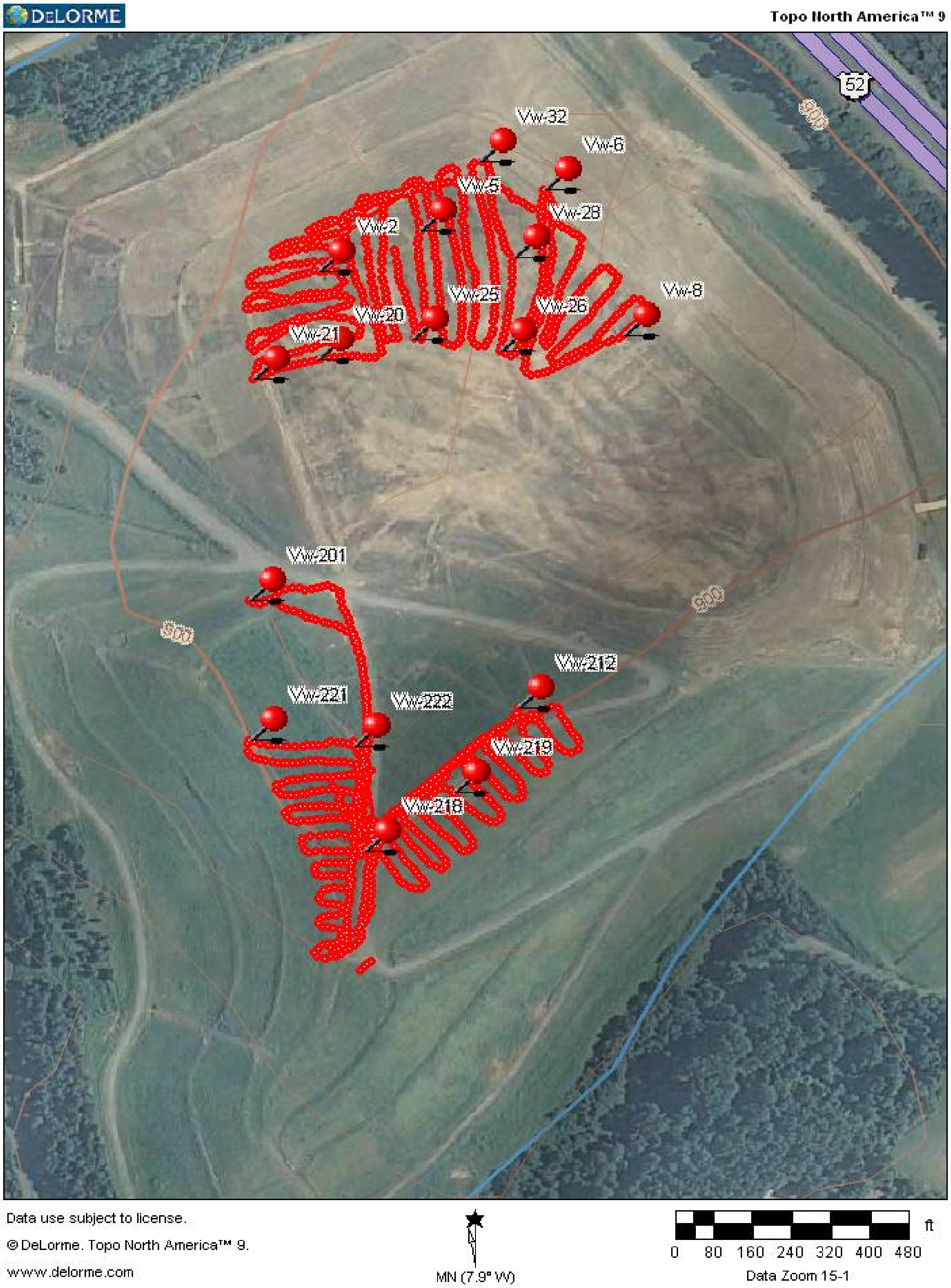

Figure 3-11. Map of Serpentine Sampling Locations at Site C

3.8 Calculation of VOC Fluxes

The emissions flux value of each speciated VOC was estimated using the rationing method described in Section 1.6 of this document. The average measured methane flux values from each landfill cell were used to estimate the emissions flux value of each VOC. Table 3-32 presents the average methane flux values used to estimate VOC flux values from each campaign.

Table 3-32. Summary of Average Methane Flux Values Used for Estimation of VOC Flux Values at each Site

Site	Campaign	Average Methane Flux Value (g/s)
A	Fall 2009	13
A	Spring 2010	6.9
B	Summer 2010	97
C	Fall 2009	4.3
C	Spring 2010	6.4

3.8.1 Site A

Table 3-33 presents the estimated flux of each speciated VOC from the fall 2009 and spring 2010 Site A Campaigns.

Table 3-33. Estimated VOC Flux Values from the Fall 2009 and Spring 2010 Site A Campaigns

Compound	Corrected Fall 2009 Landfill Gas Concentration (ppbv)	Fall 2009 Estimated Flux Value (grams per day)	Corrected Spring 2010 Landfill Gas Concentration (ppbv)	Spring 2010 Estimated Flux Value (grams per day)
1,1,1-Trichloroethane	10.1	0.17	6.89	0.057
1,1,2,2-Tetrachloroethane	ND	ND	ND	ND
1,1,2-Trichloroethane	ND	ND	ND	ND
1,1-Dichloroethane	59.5	0.75	76.6	0.47
1,1-Dichloroethene	9.08	0.11	16.5	0.10
1,2,4-Trichlorobenzene	3.47	0.080	7.43	0.084
1,2,4-Trimethylbenzene	1200	18	1840	14
1,2-Dibromoethane	ND	ND	ND	ND
1,2-Dichloroethane	21.1	0.27	20.5	0.13
1,2-Dichloropropane	ND	ND	6.89	0.048
1,3,5-Trimethylbenzene	444	6.8	731	5.4
1,3-Butadiene	24.2	0.17	32.7	0.11
Acetonitrile	337	1.8	426	1.1
Acetylene	91	0.30	ND	ND
Acrolein	ND	ND	ND	ND
Acrylonitrile	8.68	0.059	ND	ND
Benzene	424	4.2	687	3.3
Bromochloromethane	ND	ND	ND	ND
Bromodichloromethane	ND	ND	ND	ND
Bromoform	ND	ND	ND	ND
Bromomethane	ND	ND	ND	ND
Carbon Disulfide	8.49	0.082	10.1	0.047
Carbon Tetrachloride	ND	ND	ND	ND
Chlorobenzene	ND	ND	72.2	0.50
Chloroethane	45	0.37	52.8	0.21
Chloroform	ND	ND	ND	ND
Chloromethane	20.4	0.13	20.6	0.064
Chloromethylbenzene	ND	ND	ND	ND
Chloroprene	ND	ND	ND	ND
cis-1,2-Dichloroethylene	410	5.1	531	3.2
cis-1,3-Dichloropropene	ND	ND	ND	ND
Dibromochloromethane	ND	ND	ND	ND
Dichlorodifluoromethane	397	6.1	3.82	0.029
Dichloromethane	243	2.6	355	1.9

Compound	Corrected Fall 2009 Landfill Gas Concentration (ppbv)	Fall 2009 Estimated Flux Value (grams per day)	Corrected Spring 2010 Landfill Gas Concentration (ppbv)	Spring 2010 Estimated Flux Value (grams per day)
Dichlorotetrafluoroethane	38.4	0.83	36.2	0.38
Ethyl Acrylate	ND	ND	ND	ND
Ethyl tert-Butyl Ether	ND	ND	ND	ND
Ethylbenzene	4070	55	5890	39
Hexachloro-1,3-butadiene	ND	ND	ND	ND
m,p-Xylene	8970	120	11900	78
m-Dichlorobenzene	ND	ND	ND	ND
Methyl Ethyl Ketone	5200	48	10200	46
Methyl Isobutyl Ketone	776	9.9	1290	8.0
Methyl Methacrylate	ND	ND	ND	ND
Methyl tert-Butyl Ether	17.1	0.19	28.0	0.15
n-Octane	951	14	1680	12
o-Dichlorobenzene	3.84	0.072	6.49	0.059
o-Xylene	2620	35	3630	24
p-Dichlorobenzene	511	9.6	702	6.4
Propylene	4050	22	10.3	0.027
Styrene	642	8	1190	7.7
tert-Amyl Methyl Ether	ND	ND	ND	ND
Tetrachloroethylene	535	11	683	7.0
Toluene	12600	150	14900	85
trans-1,2-Dichloroethylene	16.3	0.20	29.7	0.18
trans-1,3-Dichloropropene	ND	ND	89.4	0.61
Trichloroethylene	258	4.3	351	2.9
Trichlorofluoromethane	13.5	0.24	18.1	0.15
Trichlorotrifluoroethane	3.23	0.077	4.03	0.047
Vinyl chloride	400	3.2	471	1.8

*ND indicates NMOC was not detected above instrument MDL

3.8.2 Site B

Table 3-34 presents the estimated flux of each VOC from the summer 2010 Site B Campaign.

Table 3-34. Estimated VOC Flux Values from the Summer 2010 Site B Campaign

Compound	Corrected Spring 2010 Landfill Gas Concentration (ppbv)	Spring 2010 Estimated Flux Value (grams per day)
1,1,1-Trichloroethane	3.53	0.40
1,1,2,2-Tetrachloroethane	ND	ND
1,1,2-Trichloroethane	ND	ND
1,1-Dichloroethane	29.7	2.5
1,1-Dichloroethene	25.8	2.1
1,2,4-Trichlorobenzene	4.00	0.62
1,2,4-Trimethylbenzene	2020	210
1,2-Dibromoethane	ND	ND
1,2-Dichloroethane	218	18
1,2-Dichloropropane	58.2	5.6
1,3,5-Trimethylbenzene	846	87
1,3-Butadiene	99.4	4.6
Acetonitrile	735	26
Acetylene	ND	ND
Acrolein	ND	ND
Acrylonitrile	ND	ND
Benzene	2120	140
Bromochloromethane	ND	ND
Bromodichloromethane	ND	ND
Bromoform	ND	ND
Bromomethane	1.19	0.10
Carbon Disulfide	28.8	1.9
Carbon Tetrachloride	ND	ND
Chlorobenzene	138	13
Chloroethane	60.0	3.3
Chloroform	ND	ND
Chloromethane	4.38	0.19
Chloromethylbenzene	ND	ND
Chloroprene	ND	ND
cis-1,2-Dichloroethylene	601	50
cis-1,3-Dichloropropene	ND	ND

Compound	Corrected Spring 2010 Landfill Gas Concentration (ppbv)	Spring 2010 Estimated Flux Value (grams per day)
Dibromochloromethane	ND	ND
Dichlorodifluoromethane	43.1	4.4
Dichloromethane	163	12
Dichlorotetrafluoroethane	43.7	6.4
Ethyl Acrylate	ND	ND
Ethyl tert-Butyl Ether	ND	ND
Ethylbenzene	6800	610
Hexachloro-1,3-butadiene	ND	ND
m,p-Xylene	12000	1100
m-Dichlorobenzene	ND	ND
Methyl Ethyl Ketone	18300	1100
Methyl Isobutyl Ketone	2150	180
Methyl Methacrylate	ND	ND
Methyl tert-Butyl Ether	26.7	2.0
n-Octane	1800	180
o-Dichlorobenzene	11.5	1.4
o-Xylene	3370	310
p-Dichlorobenzene	1060	130
Propylene	308	11
Styrene	2250	200
tert-Amyl Methyl Ether	ND	ND
Tetrachloroethylene	867	120
Toluene	15200	1200
trans-1,2-Dichloroethylene	31.9	2.6
trans-1,3-Dichloropropene	167	16
Trichloroethylene	354	39
Trichlorofluoromethane	30.0	3.5
Trichlorotrifluoroethane	3.60	0.58
Vinyl chloride	34	1.8

*ND indicates VOC was not detected above instrument MDL

3.8.3 Site C

Table 3-35 presents the estimated flux of each VOC from the Fall 2009 and Spring 2010 Site C Campaigns.

Table 3-35. Estimated VOC Flux Values from the Fall 2009 and Spring 2010 Site C Campaigns

Compound	Corrected Fall 2009 Landfill Gas Concentration (ppbv)	Fall 2009 Estimated Flux Value (grams per day)	Corrected Spring 2010 Landfill Gas Concentration (ppbv)	Spring 2010 Estimated Flux Value (grams per day)
1,1,1-Trichloroethane	2.91	0.016	7.96	0.066
1,1,2,2-Tetrachloroethane	4.62	0.032	ND	ND
1,1,2-Trichloroethane	ND	ND	ND	ND
1,1-Dichloroethane	43.5	0.18	76.7	0.47
1,1-Dichloroethene	10.7	0.043	21.4	0.13
1,2,4-Trichlorobenzene	3.06	0.023	9.03	0.10
1,2,4-Trimethylbenzene	1350	6.7	2260	17
1,2-Dibromoethane	ND	ND	ND	ND
1,2-Dichloroethane	29.7	0.12	29.7	0.18
1,2-Dichloropropane	ND	ND	ND	ND
1,3,5-Trimethylbenzene	528	2.6	960	7.1
1,3-Butadiene	33.4	0.075	35.4	0.12
Acetonitrile	543	0.93	857	2.2
Acetylene	112	0.12	ND	ND
Acrolein	ND	ND	ND	ND
Acrylonitrile	ND	ND	ND	ND
Benzene	399	1.3	806	3.9
Bromochloromethane	ND	ND	ND	ND
Bromodichloromethane	ND	ND	ND	ND
Bromoform	ND	ND	ND	ND
Bromomethane	ND	ND	ND	ND
Carbon Disulfide	5.27	0.017	11.4	0.053
Carbon Tetrachloride	ND	ND	ND	ND
Chlorobenzene	ND	ND	ND	ND
Chloroethane	29.3	0.079	68.9	0.27
Chloroform	ND	ND	ND	ND
Chloromethane	12.2	0.026	23.6	0.074
Chloromethylbenzene	ND	ND	ND	ND
Chloroprene	ND	ND	ND	ND
cis-1,2-Dichloroethylene	483	1.9	706	4.2

Compound	Corrected Fall 2009 Landfill Gas Concentration (ppbv)	Fall 2009 Estimated Flux Value (grams per day)	Corrected Spring 2010 Landfill Gas Concentration (ppbv)	Spring 2010 Estimated Flux Value (grams per day)
cis-1,3-Dichloropropene	ND	ND	ND	ND
Dibromochloromethane	ND	ND	ND	ND
Dichlorodifluoromethane	380	1.9	78	0.58
Dichloromethane	45.7	0.16	459	2.4
Dichlorotetrafluoroethane	36.1	0.26	91.0	0.96
Ethyl Acrylate	ND	ND	ND	ND
Ethyl tert-Butyl Ether	ND	ND	ND	ND
Ethylbenzene	3470	15	3470	23
Hexachloro-1,3-butadiene	ND	ND	ND	ND
m,p-Xylene	7160	32	7160	47
m-Dichlorobenzene	ND	ND	ND	ND
Methyl Ethyl Ketone	5210	16	5210	23
Methyl Isobutyl Ketone	970	4.0	1700	11
Methyl Methacrylate	22.3	0.093	ND	ND
Methyl tert-Butyl Ether	14.9	0.053	31.1	0.16
n-Octane	943	4.5	2080	15
o-Dichlorobenzene	7.36	0.045	13.6	0.12
o-Xylene	2020	8.9	2020	13
p-Dichlorobenzene	613	3.7	913	8.3
Propylene	2760	4.8	ND	ND
Styrene	604	2.6	1370	8.8
tert-Amyl Methyl Ether	ND	ND	ND	ND
Tetrachloroethylene	539	3.7	788	8.1
Toluene	10800	41	10800	61
trans-1,2-Dichloroethylene	14.1	0.057	33.9	0.20
trans-1,3-Dichloropropene	ND	ND	ND	ND
Trichloroethylene	254	1.4	416	3.4
Trichlorofluoromethane	6.66	0.038	44.2	0.37
Trichlorotrifluoroethane	1.99	0.015	9.61	0.11
Vinyl chloride	385	1.0	598	2.3

*ND indicates VOC was not detected above instrument MDL

3.9 Calculation of Landfill Gas Abatement Efficiency

The efficiency of the landfill gas collection system can be calculated by comparing the fugitive methane emission values (reported in Section 3.1) to the quantity of collected gas from the header pipe analysis. The following sections present data from the header pipe analysis, the calculated abatement efficiency at each site, and a sample calculation of the abatement efficiency from Site A using the Fall 2009 ORS data. The calculation of an inventory-ready collection efficiency which considers the potential impacts of soil oxidation, is also presented.

3.9.1 Landfill Site A

In order to calculate the efficiency of the gas collection system at Site A, data from the header pipe surveys were used to calculate the mass flow rate of landfill gas captured by the system. Table 3-36 presents a summary of data from the header pipe surveys at Landfill Site A.

Table 3-36. Summary of Data from the Header Pipe Surveys at Site A

Study	Header Pipe Flow Rate (cfm)	% Methane in Header Pipe	Methane Flow Rate in Header Pipe (cfm)	Temperature (°F)	Pressure (inches H_2O)
Fall 2009	897	53.8	483	60	-14
Spring 2010	496	60.4	300	94	-14

In order to calculate the mass flow rate of methane gas captured by the collection system during the Fall campaign, the methane flow rate in the header pipe (in cfm), is calculated by multiplying the total header pipe flow rate (897 cfm) by the percent methane in the header pipe (53.8%) to yield a methane flow rate of 482 cfm. This value is then converted from volumetric flow (cfm) to mass flow (g/s) by considering the temperature and pressure during the time of the measurements. The equivalent mass flow rate of methane captured by the gas collection system is 149 g/s, or 1.29×10^7 g/day. The flow rate from the gas collection system is then compared to the total cell fugitive methane emission measured during the Fall 2009 survey at Site A using the OTM-10 technique (5.6×10^6 g/day). The abatement efficiency of the gas collection system is calculated by dividing the methane flow rate in the gas collection system by the sum of the methane flow rate in the gas collection system and the total cell fugitive methane emission rate:

1.29×10^7 (g/day) / 1.85×10^7 (g/day) = 70% gas abatement efficiency during fall 2009, with lower and upper error bounds of 64% and 74%, respectively.

The lower and upper error bounds of the gas abatement efficiency values were calculated using standard propagation-of-error calculations with a 95% confidence interval. The calculations included uncertainty associated with the average methane emission factor calculated from each site, and the measurement of total header pipe flow rate and percent methane in the header pipe. It should be noted that there is uncertainty associated with the estimate of the total surface area of each landfill cell. However, applying different levels of uncertainty in the total surface area values did not change the final uncertainty estimates significantly, so this uncertainty was not included in the propagation-of-error calculations.

The same procedure was applied to calculate the abatement efficiency from all campaigns at each of the sites. Using the header pipe survey data from the Spring 2010 Site A campaign (shown in Table 3-35) and the total cell fugitive methane emission measured during the Spring 2010 survey at Site A (2.3×10^6 g/day), the calculated abatement efficiency during the Spring 2009 campaign was 77%, with lower and upper error bounds of 67% and 84%, respectively.

Soil oxidation was not assessed during this study; however, emissions inventories rely on default collection efficiencies calculated as CH_4 Collected / (CH_4 Collected + CH_4 Emissions + CH_4 Oxidized in cover soils). A default soil oxidation rate of 10% of uncollected gas is often used. Estimates of the amount of methane oxidized were calculated using assumed soil oxidation rates of 5 to 20%. An example calculation is provided below based on the default soil oxidation of 10%. 5.6×10^6 g/day x 10% / (1 – 10%) = 0.62×10^6 g/day estimated soil oxidation at 20% during Fall 2009

An inventory-ready collection efficiency is calculated using the equation outlined above:

1.29×10^7 g/day / 1.9×10^7 g/day = 68% inventory-ready gas collection efficiency during fall 2009

5% soil oxidation yields an inventory-ready collection efficiency of 69%, and a 20% soil oxidation yields a collection efficiency of 65%. During the spring campaign, calculated inventory collection efficiencies ranged from 73% - 76% for the soil oxidation rates of 5-20%.

3.9.2 Landfill Site B

In order to calculate the efficiency of the gas collection system at Site B, data from the header pipe survey were used to calculate the mass flow rate of gas captured by the system. Table 3-37 presents a summary of data from the header pipe survey at Landfill Site B. It should be noted that although a header pipe survey was conducted during the fall 2009 at Site B, the data is not presented in this section because OTM-10 measurements were not collected at Site B during the fall 2009.

Table 3-37. Summary of Data from the Header Pipe Surveys at Site B

Study	Header Pipe Flow Rate (cfm)	% Methane in Header Pipe	Methane Flow Rate in Header Pipe (cfm)	Temperature (°F)	Pressure (inches H_2O)
Spring 2010	2084	61.2	1275	112	-12

Using the header pipe survey data from the Spring 2010 Site B campaign (shown in Table 3-36) and the total cell fugitive methane emission measured in the 86-acre cell during the Spring 2010 survey (5.2×10^7 g/day), the calculated abatement efficiency during the Spring 2010 campaign was 38%, with lower and upper error bounds of 31% and 46%, respectively. During the Spring campaign, calculated inventory-ready collection efficiencies ranged from 33% - 37% for the soil oxidation rates of 20% and 5% respectively.It should also be noted that fugitive methane emission data from the new cell surveys at Site B were not included in this calculation because the new cell was not connected to the gas collection system at the time of the survey.

3.9.3 Landfill Site C

In order to calculate the efficiency of the gas collection system at Site C, data from the header pipe surveys were used to calculate the mass flow rate of gas captured by the system. Table 3-38 presents a summary of data from the header pipe surveys at Landfill Site C.

Table 3-38. Summary of Data from the Header Pipe Surveys at Site C

Study	Header Pipe Flow Rate (cfm)	% Methane in Header Pipe	Methane Flow Rate in Header Pipe (cfm)	Temperature (°F)	Pressure (inches H_2O)
Fall 2009	1101	56.3	620	79.1	-10
Spring 2010	1400	55.5	770	86.0	-45

Using the header pipe survey data from the Fall 2009 Site C campaign (shown in Table 3-38) and the total cell fugitive methane emission measured during the Fall 2009 survey at Site C (5.8 x 10^6 g/day), the calculated abatement efficiency during the Fall 2009 campaign was 73%, with lower and upper error bounds of 51% and 88%, respectively. Calculated inventory-ready collection efficiencies ranged from 69% - 72% for the soil oxidation rates of 20% and 5% respectively.

The calculated abatement efficiency during the Spring 2010 campaign (calculated using data in Table 3-38 and a total cell fugitive methane emission rate of 2.8 x 10^6 g/day) was 88%, with lower and upper error bounds of 72% and 95%, respectively. Calculated inventory-ready collection efficiencies ranged from 85% - 87% for the soil oxidation rates of 20% and 5% respectively.

Chapter 4
Conclusion

Field measurements were conducted at three municipal solid waste landfills to compare fugitive methane to collected methane (i.e., abatement efficiency). The measurements were conducted during several multi-week sampling campaign using a scanning GasFinder 2.0 methane Open-Path Tunable Diode Laser (OP-TDL) instrument (Boreal, Inc). At two of the sites, measurements were performed in the fall of 2009 and repeated in the spring of 2010. At the third site, measurements were conducted during the summer of 2010 and not during the first phase due to unseasonable wet and cold weather.

In addition to the optical remote sensing measurements, the header pipe gas was analyzed for flow rate, composition, and the concentration of trace constituents including mercury and other hazardous air pollutants (HAPs), volatile organic compounds (VOC), and nonmethane organic compounds (NMOC). The header pipe gas analysis occurred in the fall of 2009 and the spring of 2010. The results of the header pipe gas analysis combined with the OTM-10 measurements are used to estimate methane abatement efficiency which is calculated as:

$$CH_4 \text{ Abatement Efficiency} = CH_4 \text{ Collected} / (CH_4 \text{ Collected} + CH_4 \text{ Emissions}) \quad \text{Equation 1}$$

This calculation is different than what is in the U.S. EPA's guidance for emissions inventory in that it does not include soil oxidation in the denominator. (U.S. EPA, 2006, 2007) Inclusion of soil oxidation in the calculation above to allow for direct comparison with conventional collection efficiency would result in lower values. The default gas collection efficiency recommended for EPA's guidance for emissions inventories is 75% (U.S. EPA, 2008). Two of the sites had interim covers and the third had a final cover in place.

The total cell fugitive methane flux rate from the five measurement campaigns varied from 2.3 to 52 million grams per day (Table 4-1) and the methane abatement efficiency from 38 to 88% (Table 4-2). For two of the sites the landfill methane abatement efficiency ranged from 70 to 88%. Landfill gas collation systems were fully operational during each testing period with no reports of downtime or operational upsets.

Table 4-1. Summary of Fugitive Methane Emissions from the Landfill Sites

Site	Campaign	Cell Cover Type	Average Methane Emission Factor (grams/day/m^2)	Total Cell Fugitive Methane Emission Rate (grams/day)
A	Fall 2009	Interim	44 ± 10	5.6×10^6
A	Spring 2010	Interim	18 ± 9.1	2.3×10^6
B	Summer 2010	Interim	150 ± 46	5.2×10^7
C	Fall 2009	Final	19 ± 19	5.8×10^6
C	Spring 2010	Final	9.2 ± 9.7	2.8×10^6

Table 4-2. Summary of Methane Abatement Efficiency from the Landfill Sites

Site	Campaign	Total Cell Fugitive Methane Emission Rate (grams/day)	Methane Flow Rate in Gas Collection System (grams/day)	Methane Abatement Efficiency* (% value with lower and upper error bounds shown in parenthesis)
A	Fall 2009	5.6×10^6	13×10^6	70 (64,74)
A	Spring 2010	2.3×10^6	7.6×10^6	77 (67,84)
B	Summer 2010	52×10^6	32×10^6	38 (31, 46)
C	Fall 2009	5.8×10^6	16×10^6	73 (51,88)
C	Spring 2010	2.8×10^6	20×10^6	88 (72,95)

* Calculated as CH_4 Collected / (CH_4 Collected + CH_4 Emissions). This is different than conventional collection efficiency used in AP 42 and other documents which include soil oxidation in the denominator.

Measurements were conducted at the new cell at Landfill B where waste had been accepted for about 3 months prior to sampling. The approximate area of the new cell was 6 acres and because the cell is new, the gas collection system had not yet been installed. The average methane emission factor for the summer 2010 measurement campaign of the new cell at Site B was 24 ± 8.6 g/day/m^2. As shown in Figure 3-4, the calculated methane emission factors from the survey did not show a large amount of variability over the two days that data were collected. The estimated surface area of the new cell is 25,650 m^2. Multiplying this value by 24 g/day/m^2 yields a total cell methane emission rate of 6.3×10^5 grams/day. This conclusion is considered important in that most models assume no methane generation for at least 6 months from initial waste placement. The data clearly show that at least for this site, that is an incorrect assumption.

In addition to optical remote sensing measurements, serpentine methane gas sampling was performed along the surface of each landfill using a Thermo TVA-1000 FID portable analyzer according to specifications by the State of California for conducting surface scans. The data were collected to compare to the US EPA Other Test Method-10 (OTM-10) measurements. For site A, a FLIR camera was used to identify VOC leaks from the landfill surface and wellheads.

Trace constituent gas data will be used in updates to EPA's AP-42 providing emission factors for municipal solid waste landfills. Although the data are provided in this report, the focus is on the methane abatement efficiency to compare to existing values being used. For mercury, both total and elemental mercury measurements were conducted at each landfill. For one of the sites, speciated mercury samples were collected and analyzed in the fall of 2009.

Table 4-3 presents a summary of the results of the total mercury measurements at the three landfill sites. The table presents the average and range of total mercury concentrations from gas header pipes at each site. For the mercury measurements, there was little variation in the concentration between the fall and spring measurements. The concentration of total mercury varied between the three sites from 2.9 to 9.0 μg/m^3. Speciated measurements for mercury made at Site B during the fall 2009 campaign had an average of 1.2% oxidized mercury and 98.8% elemental mercury.

Table 4-3. Summary of Total Mercury Measurements from the Landfill Sites

Site	Campaign	Range of Total Mercury Concentration (μg/m^3)	Average Total Mercury Concentration (μg/m^3)

A	Fall 2009	3.4 to 3.7	3.5
A	Spring 2010	2.9 to 3.4	3.1
B	Fall 2009	8.4 to 8.9	8.7
B	Spring 2010	8.0 to 8.4	8.2
C	Fall 2010	8.8 to 9.0	8.9
C	Spring 2010	8.4 to 9.0	8.8

Next steps include developing more specific guidance for OTM-10 measurements at landfills working with U.S. EPA's Office of Air Quality Planning and Standards. Landfills are dynamic and constantly in flux so that attempting to quantify methane abatement efficiency is more difficult than other area sources. Regardless, based on the statistical analysis of the results and the relatively good agreement between the different measurement campaigns suggests promise with the use of OTM-10 for quantifying whole landfill emissions. Guidance is being developed to incorporate findings from this work for the future use of OTM-10 at landfills. The data provided in this report is considered the best available data to date to evaluate methane abatement efficiency by measuring emissions across the surface and side slopes using a scanning GasFinder 2.0 methane Open-Path Tunable Diode Laser (OP-TDL) instrument (Boreal, Inc). Each of the landfills met applicable regulatory requirements and volunteered to participate in this research. Ideally we would like to get additional data for multiple landfills at different time periods in the life of the landfill and different design and operating parameters.

The methane abatement efficiency was found to range from 38 to 88%. The site that was found to have 38% efficiency upgraded the gas collection system just a few months after the field measurements were conducted. It would be helpful to re-test to see what level of reduction occurred as a result of improvements in the gas collection system. The data collected does not support the use of collection efficiency values of 90% or greater as has been published in other studies.. We suspect that the use of flux boxes will lead to higher gas collection efficiencies because cracks and leaks across surface and side slopes were not accounted for. As additional data are gathered through either OTM-10 or other technologies that consider landfill emissions across the entire surface and side slopes, more accurate estimates can be made regarding carbon emissions from landfills and collection efficiencies.

Chapter 5
Quality Assurance/Quality Control

5.1 Equipment Calibration

All project instrumentation is calibrated annually or cal-checked as part of standard operating procedures. Certificates of calibration are kept on file. Maintenance records are kept for any equipment adjustments or repairs in bound project notebooks that include the data and description of maintenance performed. Instrument calibration procedures and frequency are listed in Table 5-1 and further described in the text.

Table 5-1. Instrumentation Calibration Frequency and Description

Instrument	Measurement	Calibration Date	Calibration Detail
Boreal Methane GasFinder 2.0 OP-TDLAS	Methane PIC	Pre-deployment and in-field checks	Reference cell calibration
R.M. Young Meteorological Head	Wind Speed in meters per second	6 May 2009	Calibrated by manufacturer during routine maintenance
R.M. Young Meteorological Head	Wind direction in degrees from North	6 May 2009	Calibrated by manufacturer during routine maintenance
Lumex 915+ Mercury Analyzer	Elemental Mercury Concentration	Pre-deployment and in-field checks	Insertion of test cell
Topcon Model GTS-211D Theodolite	Distance Measurement	11 November 2009	Calibration of distance measurement. Actual distance #1 =12.32 m #1 Measured distance= 12.39 m Actual distance #2= 10.13 #2 Measured distance= 10.17 m Actual distance #3= 8.99 #3 Measured distance= 8.93 m
Topcon Model GTS-211D Theodolite	Angle Measurement	11 November 2009	Calibration of angle measurement. Actual angle= 360º #1 Measured angle= 359º57'05" #2 Measured angle= 359º58'58" #3 Measure angle= 359º59'33"

As part of the preparation for this project, a Category III Quality Assurance Project Plan (QAPP) was prepared and approved for the field campaigns. In addition, standard operating procedures were in place during the field campaigns.

5.2 Assessment of DQI Goals

The critical measurements associated with this project and the established data quality indicator (DQI) goals in terms of accuracy, precision, and completeness are listed in Table 5-2.

Table 5-2. DQI Goals for Instrumentation

Measurement Parameter	Analysis Method	Accuracy	Precision	Acceptance Criterion (%Bias/Recovery)	Completeness
Methane PIC	OP-TDLAS	±20%	±20%	Not applicable	90%
Ambient Wind Speed	R.M. Young Met heads post-deployment calibration in EPA Metrology Lab	±1 m/s	±1 m/s	Not applicable	90%
Ambient Wind Direction	R.M. Young Met heads post-deployment calibration in EPA Metrology Lab	±10º	±10º	Not applicable	90%
Distance Measurement	Theodolite- Topcon	±1m	±1m	Not applicable	100%
Beam angle	Theodolite- Topcon	±0.1º	±0.1º	Not applicable	100%
Mercury concentrations	Lumex Mercury Analyzer	±25%	±25%	Not applicable	90%
Total Mercury	Thermal Decomposition / 30B	Not applicable	±20%	50-150% recovery	90%
VOCs	EPA Method TO-15	Not applicable	±20%	50-150% recovery	90%

* The accuracy acceptance criterion of ±25% is for pathlengths of less than 50m, ±15% is for pathlengths between 50 and 100m, and ±10% is for pathlengths greater than 100m.

5.2.1 DQI Check for Methane PIC Measurement with OP-TDLAS

The Boreal *GasFinder* 2.0 OP-TDLAS provides an R^2 value for each concentration measurement. The R^2 value is calculated by the internal software of the instrument, and is an indication of the similarity between the waveform of the sample gas and the reference cell gas. When the instrument detector receives the returning laser signal after it has passed through the sample beam path, it converts the signal to the shape of a specific waveform (sample waveform). The instrument also receives a similar laser signal after the laser has passed through the reference cell in the instrument (reference waveform). The two waveforms are then digitized and compared as two numeric arrays. The instrument software then performs a Linear Least Squares Regression for each measurement, to evaluate the similarity (R^2) between the sample and reference waveforms.

The R^2 value was used to assess the accuracy of each concentration measurement from this project. Table 5-3, taken from the Boreal Laser, Inc. *GasFinder 2.0 Operation Manual,* presents a range of R^2 values, and the corresponding accuracy of the measurement.

Table 5-3. Accuracy of Concentration Measurements for Different R^2 Value

R^2	Measurement Accuracy
> 0.95	± 2%
0.9	± 5%
0.7	± 10%
0.5	± 15%
0.4	± 20%
0.3	± 25%
0.15	± 50%
0.1	± 70%
< 0.05	± 100%

The R^2 value of each data point (measured methane concentration) was analyzed to assess whether or not it met the DQI criterion for accuracy of ±20%, which corresponds to an R^2 value of greater than 0.4. A total of 96,987 data points were analyzed, and 93,271 met the DQI criteria for accuracy, for a total completeness of 96%. This value met the project DQI criteria of 90% completeness.

The precision of the OP-TDLAS methane concentration measurements was assessed by analyzing methane concentration values measured along the same beam path during the August 9 background survey at Site B. Data were collected along the measurement path for 45 minutes. Based on the DQI criterion set forth for precision of ±20%, the data were found to be acceptable for a completeness of 100%. The calculated relative standard deviationof the data from this survey were 0.1311 ppmv, which represents 7.7% RSD.

5.2.2 DQI Checks for Ambient Wind Speed and Wind Direction Measurements

The meteorological heads are checked annually as part of the standard calibration procedure. Before deployment to the field, the team verified the calibration date of the instrument by referencing the calibration sticker. The meteorological heads used for the current campaign were calibrated on May 6, 2009 by the instrument manufacturer (R.M. Young) during routine servicing. Additionally, a reasonableness check was performed in the field on the measured wind direction data. While data collection was occurring, the field team leader compared the wind direction measured with the heads to the forecasted wind direction for that particular day

5.2.3 DQI Check for Precision and Accuracy of Theodolite Measurements

Calibration checks are not performed before each field campaign; however, the user should verify the calibration date of the instrument by referencing the calibration sticker. If the date indicates the instrument is in need of calibration, it should be returned to the manufacturer before use in the field. Before field deployment, ensure the battery packs are charged for this equipment. The following additional checks were made on November 11, 2009. The calibration of distance measurement was done in the field at Site A using a tape measure. Three separate calibration experiments were performed. The actual distances for experiments #1, #2, and #3 were 12.32, 10.13, and 8.99 meters, respectively. The distances measured with the theodolite were 12.39, 10.17, and 8.93 meters, respectively. The results indicate accuracy fell well within the DQI goal. The calibration of angle measurement was also performed. The actual angle was 360°. The angles measured with the theodolite were 359°57’05”, 359°58’58”, and 359°59’33”. The results indicate accuracy and precision fall well within the DQI goals, and completeness was 100%.

Additionally, there are several internal checks in the theodolite software that prevent data collection from occurring if the instrument is not properly aligned on the object being measured, or if the instrument has not been balanced correctly. When this occurs, it is necessary to re-initialize the instrument to collect data.

5.2.4 DQI Check for Lumex Elemental Mercury Analyzer and Total Mercury Samples

The Lumex Mercury Analyzer DQIs of accuracy and precision are checked by the insertion of a test cell, containing gas from the calibration standard. The cell is built into the instrument, and is accessed by setting the instrument to the “test” mode, and collecting measurements. If the measured value of the mercury vapor concentration in the test cell is within ±25% from that of the tabulated value and the standard deviation of the measurements is within ±25%, the accuracy and precision of the instrument are deemed acceptable. For the real-time elemental mercury analysis, the Lumex mercury analyzer was zeroed using the internal carbon filter sample conditioner. Yearly calibrations are performed on this analyzer by factory personnel at Ohio Lumex.

The total and speciated mercury traps were analyzed using the Lumex analyzer and a combustion furnace to decompose the mercury on the carbon tubes to elemental mercury for detection. The precision criteria of ±25 % established in the QAPP was met for samples collected at Site A (5.3 % RSD), Site B (3.3 % RSD), and Site C (1.0 % RSD) during DQI Check of total mercury samples during the Fall 2009 sampling campaign. The precision of the total mercury sampling during the Spring 2010 sampling was 10%, 3%, and 4% for Sites A, B, and C respectively.

Laboratory control spike recovery for the total mercury sampling was performed using a NIST traceable standard prepared by SCP Science (100.3 mg/kg mercury in water) reference standard. Three spike recoveries were performed with 60%, 94%, and 98% recovery for an average of 93.8%. Analytical spikes were performed on at Site B during the Fall 2009 sampling had recoveries of 93.9% and 97.9% with an average recovery of 95.9%. Continuous calibration verification standards during the Fall 2009 sampling had recoveries of 102% and 94%. Continuous calibration verification standards during the Spring 2010 sampling had recoveries of 97% and 102%. Recovery goals established in the QAPP of 50 to 150% were met.

During the Fall 2009 sampling campaign, analytical replicates were performed on Site B with 10 values ranging from 5.5 to 6.1 ng/m^{3}for an average of 5.9 ng/m^3 and a relative percent difference of 4.6%. Blank values were less than 0.07 ng per trap with an average of 0.02 ng per trap. The analyzer has a MDL of 0.21 ng per trap.

The precision assessment was performed using data from duplicate or replicate samples and spikes (when available). Precision was expressed as %RPD for samples that were done in duplicate and as %RSD for samples performed in triplicate. Table 5-4 represents precision values calculated for total mercury of samples at each site. Precision goals established in the QAPP of <20%for total mercury were met for all samples for a completeness of 100%.

Table 5-4. Precision Ranges for Total Mercury Measurements at Sites A, B, and C

Location	Fall 2009 RSD (%)	Spring 2010 RSD (%)
Site A	5.3	9.7
Site B	4.6	2.7
Site C	1.0	4.1

5.2.5 DQI Check of VOC Samples with SUMMA® Canisters

Summa canister samples of the landfill gas were analyzed for the TO-15 list of volatile organic compounds. Triplicate gas samples were collected at each site, one nitrogen sampling system blank, and one ambient sample were also collected. The reported method detection limits for the TO-15 target list was 0.5 ppbv. The recovery goals for accuracy for this project were met by the laboratory, but the precision between replicates and completeness goals were not met during the spring 2010 field campaign possibly due to leaks on the Summa cans or dilution errors. The completeness for the VOCs by TO-15 for the fall 2009 campaign was 100% and for the spring 2010 campaign was 67%

A set of Summa can samples was analyzed for NMOC by Method 25-C. The results from the Methods 25-C have good reproducibility for Site A and C, but Site B had a higher relative standard deviation of results. Tables 5-5, 5-6 and 5-7 present the precision values of the Method, 25-C and landfill gas monitoring datasets respectively. While no goals were set for these measurements in the QAPP, one sample from Site C during the spring 2010 campaign had leaked during sampling resulting in an overall 94% completeness for these measurements. Completeness for the NMOC measurements by Method-25 for the fall 2009 campaign was 100% and for the spring 2010 campaign was 89%.

Table 5-5. Precision Ranges for NMOC Measurements at Sites A, B, and C

Location	Fall 2009 RSD (%)	Spring 2010 RSD (%)
Site A	1.3	0.0
Site B	61.3	47
Site C	4.3	25

Table 5-6. Precision Ranges for GC/FID/TCD Measurements at Sites A, B and C for Fall 2009

RSD (%)	Methane	Oxygen	Nitrogen	Carbon Dioxide
Site A	6.1	13.1	11.4	7.2
Site B	NA	NA	NA	NA
Site C	NA	NA	NA	NA

NA = only single measurements taken

Table 5-7. Precision Ranges for GC/FID/TCD Measurements at Sites A, B and C for Spring 2010

RSD (%)	Methane	Oxygen	Nitrogen	Carbon Dioxide	Hydrogen Sulfide	Carbon Monoxide
Site A	0.4	0	0	1.1	0	90
Site B	2.1	0	0	1.8	0	8.8
Site C	0.9	0	0	1.1	6.0	41

NA = only single measurements taken

Chapter 6
References

Hashmonay, R.A., and M.G. Yost, Innovative approach for estimating fugitive gaseous fluxes using computed tomography and remote optical sensing techniques, *J. Air Waste Manage. Assoc*., 49, 966-972, 1999.

Hashmonay, R.A., D.F. Natschke, K.Wagoner, D.B. Harris, E.L.Thompson, and M.G. Yost, Field evaluation of a method for estimating gaseous fluxes from area sources using open-path Fourier transform infrared, *Environ. Sci. Technol*., 35, 2309-2313, 2001.

Hashmonay, R.A., M.G. Yost, D.B. Harris, and E.L. Thompson, Simulation study for gaseous fluxes from an area source using computed tomography and optical remote sensing, presented at SPIE Conference on Environmental Monitoring and Remediation Technologies, Boston, MA, Nov., 1998, in SPIE Vol. 3534, 405-410.

Hashmonay, R.A., R.M. Varma, M.T. Modrak, R.H. Kagann, R.R. Segall, and P.D. Sullivan, Radial Plume Mapping: A US EPA Test Method for Area and Fugitive Source Emission Monitoring Using Optical Remote Sensing, *Advanced Environmental Monitoring*, 21-36, edited by Y.J. Kim and U. Platt, Springer, 2008.

Thoma, E.D., Shores, R.C, Thompson, E.L., Harris, D.B., Thorneloe, S.A., Varma, R.V., Hashmonay, R.A.., Modrak, M.T., Natschke, D.F., and Gamble, H. A., Open path tunable diode laser absorption spectroscopy for acquisition of fugitive emission flux data, J. Air & Waste Manage Assoc., 55, 658-668, 2005.

Thoma, E. D., R. B. Green, G. R. Hater, C. D. Goldsmith, N. D. Swan, M. J. Chase, and R. A. Hashmonay. Development of EPA OTM 10 for Landfill Applications. *Journal of Environmental Engineering.* American Society of Civil Engineers (ASCE), Reston, VA, Vol 136, No. 8, pp. 769-776, 2010.

U.S. Environmental Protection Agency (2004) *Measurement of Fugitive Emissions at Region I Landfill* (EPA-600/R-04-001,January 2004). Available at: http://www.epa.gov/appcdwww/apb/EPA-600-R-04-001.pdf

U.S. Environmental Protection Agency (2005a) *Guidance for Evaluating Landfill Gas Emissions from Closed or Abandoned Facilities* (EPA-600/R-05/123a). Available at: http://www.epa.gov/ORD/NRMRL/pubs/600r05123/600r05123.pdf

U.S. Environmental Protection Agency (2005b) *Guidance for Evaluating Landfill Gas Emissions from Closed or Abandoned Facilities*: Appendix C - *Quality Assurance Project Plan* (EPA-600/R-05/123b), available at: http://www.epa.gov/ORD/NRMRL/pubs/600r05123/600r05123b.pdf

U.S. Environmental Protection Agency (2005c) *Evaluation of Former Landfill Site in Fort Collins, Colorado Using Ground-Based Optical Remote Sensing Technology* (EPA-600/R-05/-42, April 2005). Available at: http://www.epa.gov/ORD/NRMRL/pubs/600r05042/600r05042.pdf

U.S. Environmental Protection Agency (2005d) *Evaluation of Former Landfill Site in Colorado Springs, Colorado Using Ground-Based Optical Remote Sensing Technology* (EPA-600/R-05/-41, April 2005). Available at: http://www.epa.gov/ORD/NRMRL/pubs/600r05041/600r05041.pdf

U.S. Environmental Protection Agency, *Other Test Method 10, Optical Remote Sensing for Emission Characterization from Non-point Sources*, June 2006, available at: http://www.epa.gov/ttn/emc/prelim/otm10.pdf.

U.S. Environmental Protection Agency, *Evaluation of Fugitive Emissions Using Ground-Based Optical Remote Sensing Technology* (EPA/600/R-07/032), Feb 2007; available at: http://www.epa.gov/nrmrl/pubs/600r07032/600r07032.pdf].

U.S. Environmental Protection Agency, *background Information Document for Updating AP42 Section 2.4 for Estimating Emissions from Municipal Solid Waste Landfills (valuation of Fugitive Emissions Using Ground-Based Optical Remote Sensing Technology* (EPA/600/R-08/116), Sept 2008; available at: http://www.epa.gov/nrmrl/pubs/600r08116/600r08116.htm

U.S. Environmental Protection Agency, *Investigation of Fugitive Emissions from Petrochemical Transport Barges Using Optical Remote Sensing* (EPA/600/R-07/032), Sept 2009; available at: http://www.epa.gov/nrmrl/pubs/600r09136/600r09136.pdf

APPENDIX A
Vertical Radial Plume Mapping Method

The VRPM method is generally discussed in EPA OTM 10, *Optical remote sensing for emission characterization from non-point sources,* which describes direct measurement of pollutant mass emission flux from area sources using ground-based optical remote sensing (ORS). The technique utilizes scanning open-path spectroscopic instrumentation to obtain path-integrated pollutant concentration information along multiple plane-configured optical paths, which are defined as the distance between the ORS instrument and a mirror placed in the field. The multi-path pollutant concentration data along with wind vector information are processed with a plane-integrating computer algorithm to yield a mass emission flux for the source. Figure 3-3 shows a schematic of a general VRPM measurement configuration.

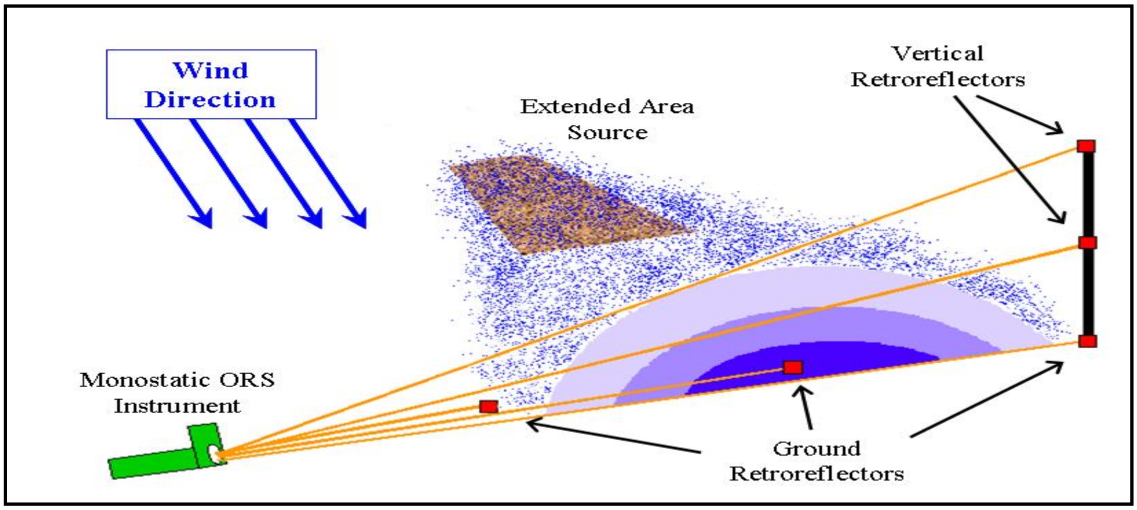

Figure 3-3. General OTM 10 VRPM Measurement Configuration

The VRPM computer algorithm uses a smooth basis function minimization (SBFM) routine of a bivarate Gaussian function to generate mass emission flux information from species concentration and wind data. In the two-phase SBFM approach, a one-dimensional SBFM reconstruction procedure is first applied in order to reconstruct the smoothed ground level and crosswind concentration profile. The reconstructed parameters are then substituted into the bivariate Gaussian function when applying a two-dimensional SBFM procedure.

A one-dimensional SBFM reconstruction is applied to the ground level segmented beam paths of the same beam geometry to find the cross wind concentration profile. A univariate Gaussian function is fitted to measured PIC ground-level values.

The error function for the minimization procedure is the Sum of Squared Errors (SSE) function and is defined in the one-dimensional SBFM approach as follows:

$$SSE(B_j, m_{y\,j}, \sigma_{y\,j}) = \sum_i \left(PIC_i - \sum_j \frac{B_j}{\sqrt{2\pi}\sigma_{y\,j}} \int_0^{r_i} \exp\left[-\frac{1}{2}\left(\frac{m_{y\,j} - r}{\sigma_{y\,j}} \right)^2 \right] dr \right)^2 \qquad (1)$$

Where:

- B = equal to the area under the one-dimensional Gaussian distribution (integrated concentration);
- r_i = the path length of the i^{th} beam;
- m_y = the mean (peak location);
- σ_y = the standard deviation of the j^{th} Gaussian function; and
- PIC_i = the measured PIC value of the i^{th} path

The SSE function is minimized using the Simplex minimization procedure to solve for the unknown parameters. When there are more than three beams at the ground level, two Gaussian functions are fitted to retrieve skewed and sometimes bi-modal concentration profiles. This is the reason for the index *j* in Equation 1.

Once the one-dimensional phase is completed, the two-dimensional phase of the two-phase process is applied. To derive the bivariate Gaussian function used in the second phase, it is convenient to express the generic bivariate function *G* in polar coordinates *r* and *θ*:

$$G(r,\theta) = \frac{A}{2\pi\sigma_y\sigma_z\sqrt{1-\rho_{12}^2}} \exp\left\{ -\frac{1}{2\left(1-\rho_{12}^2\right)} \left[\frac{(r\cdot\cos\theta - m_y)^2}{\sigma_y^2} - \frac{2\rho_{12}\left(r\cdot\cos\theta - m_y\right)\left(r\cdot\sin\theta - m_z\right)}{\sigma_y\sigma_z} + \frac{\left(r\cdot\sin\theta - m_z\right)^2}{\sigma_z^2} \right] \right\} \qquad (2)$$

The bivariate Gaussian has six unknown independent parameters:

- A = normalizing coefficient which adjusts for the peak value of the bivariate surface;
- ρ_{12} = correlation coefficient which defines the direction of the distribution-independent variations in relation to the Cartesian directions *y* and *z* (ρ_{12}=0 means that the distribution variations overlap the Cartesian coordinates);
- m_y and m_z = peak locations in Cartesian coordinates; and
- σ_y and σ_z = standard deviations in Cartesian coordinates.

Six independent beam paths are sufficient to determine one bivariate Gaussian that has six independent unknown parameters. Some reasonable assumptions are made when applying the VRPM methodology to this problem, to reduce the number of unknown parameters. The first is setting the correlation parameter ρ_{12} equal to zero. This assumes that the reconstructed bivariate Gaussian is limited only to changes in the vertical and crosswind directions. Secondly, when ground level emissions are known to exist, the ground level PIC is expected to be the largest of the vertical beams. Therefore, the peak location in the vertical direction can be fixed to the ground level. In the above ground-level scenario, Equation 2 reduces into Equation 3:

$$G(r,\theta) = \frac{A}{2\pi\sigma_y\sigma_z} \exp\left\{ -\frac{1}{2}\left[\frac{(r\cdot\cos\theta - m_y)^2}{\sigma_y^2} + \frac{\left(r\cdot\sin\theta\right)^2}{\sigma_z^2} \right] \right\} \qquad (3)$$

The standard deviation and peak location retrieved in the one-dimensional SBFM procedure are substituted in Equation 3 to yield:

$$G(A,\sigma_z)=\frac{A}{2\pi\sigma_{y-1D}\sigma_z}\exp\left\{-\frac{1}{2}\left[\frac{(r\cdot\cos\theta-m_{y-1D})^2}{\sigma_{y-1D}^2}+\frac{(r\cdot\sin\theta)^2}{\sigma_z^2}\right]\right\} \quad (4)$$

Where:

σ_{y-1D} = standard deviation along the crosswind direction (found in the one-dimensional SBFM procedure);

m_{y-1D} = peak location along the crosswind direction (found in the one-dimensional SBFM procedure);

A and σ_z are the unknown parameters to be retrieved in the second phase of the fitting procedure. An error function (SSE) for minimization is defined for this phase in a similar manner. The SSE function for the second phase is defined as:

$$SSE(A,\sigma_z)=\sum_i\left(PIC_i-\int_0^{r_i}G(r_i,\theta_i,A,\sigma_z)dr\right)^2 \quad (5)$$

Where *PIC* is the measured PIC value for the i^{th} beam. The SSE function is minimized using the Simplex method to solve for the two unknown parameters.

Further information on the VRPM method for fugitive source emission measurements in general can be found in (Hashmonay and Yost 1999, Thoma et al., 2005, U.S. EPA 2007) with specific details of this deployment in EPA OTM-10.

The Concordance Correlation Factor (CCF) is used to represent the level of fit for the reconstruction in the path-integrated domain (predicted versus measured PIC). CCF is defined as the product of two components:

$$CCF = rA \quad (6)$$

Where:

r = *the Pearson correlation coefficient*

A = *a correction factor for the shift in population and location*

This shift is a function of the relationship between the averages and standard deviations of the measured and predicted PIC vectors:

$$A=\left[\frac{1}{2}\left(\frac{\sigma_{PIC_P}}{\sigma_{PIC_M}}+\frac{\sigma_{PIC_M}}{\sigma_{PIC_P}}+\left(\frac{\overline{PIC_P}-\overline{PIC_M}}{\sqrt{\sigma_{PIC_P}\sigma_{PIC_M}}}\right)^2\right)\right]^{-1} \quad (7)$$

Where:

σ_{PIC_P} = *standard deviation of the predicted PIC vector*

σ_{PIC_M} = *standard deviation of the measured PIC vector*

$\overline{PIC_P}$ = *the mean of the predicted PIC vector*

$\overline{PIC_M}$ = *the mean of the measured PIC vector*

The Pearson correlation coefficient is a good indicator of the quality of fit to the Gaussian mathematical function. In this procedure, typically an *r* close to 1 will be followed by an *A* very close to 1. This means that the averages and standard deviations in the two concentration vectors are very similar and the mass is conserved (good flux value). However, when a poor CCF is reported (CCF<0.80) at the end of the fitting procedure it does not directly mean that the mass is not conserved. It could be a case where only a poor fit to the Gaussian function occurred and the average of the measured PIC is still very similar to the predicted PIC. In the case of very low CCF value the mass in the measurement plane is conserved but the plume may not be extrapolated beyond the top mirror height.

APPENDIX B
Open Path Instrument Mirror Coordinates

Table B-1. Distance, and Horizontal and Vertical Coordinates of Mirrors Used During the 11/17 AM Survey at Site A.

Mirror Number	Distance (meters)	Horizontal Angle from North (deg)	Vertical Angle* (deg)
1	40.7	307° 10’	0° 00’
2	84.7	304° 58’	0° 00’
3	127.9	304° 03’	0° 00’
4	128.4	304° 01’	2° 39’
5	128.5	304° 1653’	4° 44’

*Vertical angle shown is the angle from horizontal (positive values indicate elevation from the horizontal, negative values indicate descent from the horizontal).

Table B-2. Distance, and Horizontal and Vertical Coordinates of Mirrors Used During the 11/17 PM Survey at Site A.

Mirror Number	Distance (meters)	Horizontal Angle from North (deg)	Vertical Angle* (deg)
1	38.0	326° 42’	0° 00’
2	75.8	329° 11’	0° 00’
3	114.5	327° 11’	0° 00’
4	115.2	327° 07’	1° 51’
5	115.5	328° 25’	5°03’

*Vertical angle shown is the angle from horizontal (positive values indicate elevation from the horizontal, negative values indicate descent from the horizontal).

Table B-3. Distance, and Horizontal and Vertical Coordinates of Mirrors Used During the 11/18 Survey at Site A.

Mirror Number	Distance (meters)	Horizontal Angle from North (deg)	Vertical Angle* (deg)
1	45.0	325° 13’	0° 00’
2	90.0	322° 43’	0° 00’
3	136.3	323° 34’	0° 00’
4	136.6	323° 41’	2° 20’
5	136.7	324° 01’	4° 18’

*Vertical angle shown is the angle from horizontal (positive values indicate elevation from the horizontal, negative values indicate descent from the horizontal).

Table B-4. Distance, and Horizontal and Vertical Coordinates of Mirrors Used During the 11/20 Survey at Site A.

Mirror Number	Distance (meters)	Horizontal Angle from North (deg)	Vertical Angle* (deg)
1	85.5	309° 59’	0° 00’
2	171.4	307° 03’	0° 00’
3	257.9	307° 24’	0° 00’
4	258.8	307° 20’	1° 17’
5	259.0	307° 34’	2°49’

*Vertical angle shown is the angle from horizontal (positive values indicate elevation from the horizontal, negative values indicate descent from the horizontal).

Table B-5. Distance, and Horizontal and Vertical Coordinates of Mirrors Used During the 11/24 Survey at Site A.

Mirror Number	Distance (meters)	Horizontal Angle from North (deg)	Vertical Angle* (deg)
1	77.3	316° 41’	0° 00’
2	155.5	313° 29’	0° 00’
3	232.6	315° 25’	0° 00’
4	233.7	315° 20’	1° 10’
5	233.7	315° 27’	2° 51’

*Vertical angle shown is the angle from horizontal (positive values indicate elevation from the horizontal, negative values indicate descent from the horizontal).

Table B-6. Distance, and Horizontal and Vertical Coordinates of Mirrors Used During the 12/1 AM and 12/1 PM Surveys at Site A.

Mirror Number	Distance (meters)	Horizontal Angle from North (deg)	Vertical Angle* (deg)
1	46.6	325° 23’	0° 00’
2	93.5	327° 29’	0° 00’
3	141.3	326° 04’	0° 00’
4	141.7	325° 59’	2° 42’
5	141.8	326° 20’	4° 34’

*Vertical angle shown is the angle from horizontal (positive values indicate elevation from the horizontal, negative values indicate descent from the horizontal).

Table B-7. Distance, and Horizontal and Vertical Coordinates of Mirrors Used During the 5/14 Survey at Site A.

Mirror Number	Distance (meters)	Horizontal Angle from North (deg)	Vertical Angle* (deg)
1	80.1	97° 59’	0° 00’
2	136.0	97° 22’	0° 00’
3	204.6	97° 35’	0° 00’
4	205.4	97° 01’	1° 27’
5	205.2	97° 08’	2° 44’

*Vertical angle shown is the angle from horizontal (positive values indicate elevation from the horizontal, negative values indicate descent from the horizontal).

Table B-8. Distance, and Horizontal and Vertical Coordinates of Mirrors Used During the 5/20 Survey at Site A.

Mirror Number	Distance (meters)	Horizontal Angle from North (deg)	Vertical Angle* (deg)
1	75.5	79° 39’	0° 00’
2	136.1	77° 29’	0° 00’
3	209.5	78° 53’	0° 00’
4	210.2	78° 21’	1° 34’
5	209.8	78° 25’	2° 48’

*Vertical angle shown is the angle from horizontal (positive values indicate elevation from the horizontal, negative values indicate descent from the horizontal).

Table B-9. Distance, and Horizontal and Vertical Coordinates of Mirrors Used During the 5/21 Survey at Site A.

Mirror Number	Distance (meters)	Horizontal Angle from North (deg)	Vertical Angle* (deg)
1	76.0	97° 15’	0° 00’
2	136.6	95° 31’	0° 00’
3	210.0	97° 57’	0° 00’
4	210.7	96° 25’	1° 33’
5	210.3	98° 46’	2° 40’

*Vertical angle shown is the angle from horizontal (positive values indicate elevation from the horizontal, negative values indicate descent from the horizontal).

Table B-10. Distance, and Horizontal and Vertical Coordinates of Mirrors Used During the 5/26 and 5/27 Surveys at Site A.

Mirror Number	Distance (meters)	Horizontal Angle from North (deg)	Vertical Angle* (deg)
1	69.7	112° 43’	0° 00’
2	133.6	113° 37’	0° 00’
3	191.3	114° 22’	0° 00’
4	191.9	114° 40’	1° 48’
5	191.4	114° 15’	3° 07’

*Vertical angle shown is the angle from horizontal (positive values indicate elevation from the horizontal, negative values indicate descent from the horizontal).

Table B-11. Distance, and Horizontal and Vertical Coordinates of Mirrors Used During the 6/3 and 6/4 Surveys at Site A.

Mirror Number	Distance (meters)	Horizontal Angle from North (deg)	Vertical Angle* (deg)
1	72.2	99° 53’	0° 00’
2	120.2	99° 13’	0° 00’
3	188.5	98° 47’	0° 00’
4	189.2	99° 19’	1° 48’
5	188.7	99° 00’	3° 10’

*Vertical angle shown is the angle from horizontal (positive values indicate elevation from the horizontal, negative values indicate descent from the horizontal).

Table B-12. Distance, and Horizontal and Vertical Coordinates of Mirrors Used During the 6/28 Survey at Site B.

Mirror Number	Distance (meters)	Horizontal Angle from North (deg)	Vertical Angle* (deg)
1	43.7	334° 23’	0° 00’
2	83.6	335° 25’	0° 00’
3	130.2	336° 55’	0° 00’
4	131.5	336° 27’	1° 82’
5	130.9	336° 46’	2° 95’

*Vertical angle shown is the angle from horizontal (positive values indicate elevation from the horizontal, negative values indicate descent from the horizontal).

Table B-13. Distance, and Horizontal and Vertical Coordinates of Mirrors Used During the 6/30 Survey at Site B.

Mirror Number	Distance (meters)	Horizontal Angle from North (deg)	Vertical Angle* (deg)
1	95.6	327° 59’	0° 00’
2	190.4	328° 22’	0° 00’
3	289.6	329° 32’	0° 00’
4	289.5	330° 05’	0° 56’
5	288.9	330° 15’	2° 24’

*Vertical angle shown is the angle from horizontal (positive values indicate elevation from the horizontal, negative values indicate descent from the horizontal)

Table B-14. Distance, and Horizontal and Vertical Coordinates of Mirrors Used During the 7/1 Survey at Site B.

Mirror Number	Distance (meters)	Horizontal Angle from North (deg)	Vertical Angle* (deg)
1	94.2	336° 17’	0° 00’
2	189.1	336° 35’	0° 00’
3	288.3	337° 40’	0° 00’
4	288.2	338° 12’	1° 01’
5	287.6	338° 20’	2° 17’

*Vertical angle shown is the angle from horizontal (positive values indicate elevation from the horizontal, negative values indicate descent from the horizontal).

Table B-15. Distance, and Horizontal and Vertical Coordinates of Mirrors Used During the 8/2 Survey at Site B.

Mirror Number	Distance (meters)	Horizontal Angle from North (deg)	Vertical Angle* (deg)
1	93.8	331° 41’	0° 00’
2	187.0	332° 31’	0° 00’
3	280.6	331° 38’	0° 00’
4	281.5	331° 25’	0° 59’
5	281.1	331° 30’	2° 07’

*Vertical angle shown is the angle from horizontal (positive values indicate elevation from the horizontal, negative values indicate descent from the horizontal).

Table B-16. Distance, and Horizontal and Vertical Coordinates of Mirrors Used During the 8/3 Survey at Site B.

Mirror Number	Distance (meters)	Horizontal Angle from North (deg)	Vertical Angle* (deg)
1	99.9	342° 31’	0° 00’
2	194.7	341° 26’	0° 00’
3	275.3	343° 03’	0° 00’
4	276.4	342° 46’	1° 25’
5	275.9	343° 00’	2° 33’

*Vertical angle shown is the angle from horizontal (positive values indicate elevation from the horizontal, negative values indicate descent from the horizontal).

Table B-17. Distance, and Horizontal and Vertical Coordinates of Mirrors Used During the 8/4 Survey at Site B.

Mirror Number	Distance (meters)	Horizontal Angle from North (deg)	Vertical Angle* (deg)
1	113.0	303° 08’	0° 00’
2	228.5	303° 06’	0° 00’
3	329.5	302° 12’	0° 00’
4	330.5	301° 54’	0° 47’
5	330.1	302° 02’	1° 23’

*Vertical angle shown is the angle from horizontal (positive values indicate elevation from the horizontal, negative values indicate descent from the horizontal).

Table B-18. Distance, and Horizontal and Vertical Coordinates of Mirrors Used During the 8/5 Survey at Site B.

Mirror Number	Distance (meters)	Horizontal Angle from North (deg)	Vertical Angle* (deg)
1	94.8	334° 03’	0° 00’
2	187.7	334° 42’	0° 00’
3	278.3	338° 31’	0° 00’
4	279.5	338° 15’	1° 13’
5	278.9	338° 24’	2° 28’

*Vertical angle shown is the angle from horizontal (positive values indicate elevation from the horizontal, negative values indicate descent from the horizontal).

Table B-19. Distance, and Horizontal and Vertical Coordinates of Mirrors Used During the 8/10 and 8/11 Surveys at Site B.

Mirror Number	Distance (meters)	Horizontal Angle from North (deg)	Vertical Angle* (deg)
1	44.6	139° 23’	0° 00’
2	85.1	140° 16’	0° 00’
3	129.7	140° 47’	0° 00’
4	130.3	140° 15’	2° 36’
5	130.0	140° 36’	4° 15’

*Vertical angle shown is the angle from horizontal (positive values indicate elevation from the horizontal, negative values indicate descent from the horizontal).

Table B-20. Distance, and Horizontal and Vertical Coordinates of Mirrors Used During the 12/7 Survey at Site C.

Mirror Number	Distance (meters)	Horizontal Angle from North (deg)	Vertical Angle* (deg)
1	43.4	167° 01’	0° 00’
2	83.4	167° 34’	0° 00’
3	130.2	168° 11’	0° 00’
4	130.7	168° 07’	4° 36’
5	131.0	168° 25’	6° 37’

*Vertical angle shown is the angle from horizontal (positive values indicate elevation from the horizontal, negative values indicate descent from the horizontal).

Table B-21. Distance, and Horizontal and Vertical Coordinates of Mirrors Used During the 12/8 Survey at Site C.

Mirror Number	Distance (meters)	Horizontal Angle from North (deg)	Vertical Angle* (deg)
1	43.3	167° 19’	0° 00’
2	87.2	167° 51’	0° 00’
3	130.0	168° 28’	0° 00’
4	130.5	168° 28’	4° 20’
5	130.8	168° 48’	6° 44’

*Vertical angle shown is the angle from horizontal (positive values indicate elevation from the horizontal, negative values indicate descent from the horizontal).

Table B-22. Distance, and Horizontal and Vertical Coordinates of Mirrors Used During the 4/22 and 4/23 Surveys at Site C.

Mirror Number	Distance (meters)	Horizontal Angle from North (deg)	Vertical Angle* (deg)
1	96.2	16° 42’	0° 00’
2	137.6	15° 56’	0° 00’
3	306.3	15° 32’	0° 00’
4	306.6	15° 26’	1° 47’
5	306.2	15° 25’	2° 30’

*Vertical angle shown is the angle from horizontal (positive values indicate elevation from the horizontal, negative values indicate descent from the horizontal).

Table B-23. Distance, and Horizontal and Vertical Coordinates of Mirrors Used During the 4/28 and 4/30 Surveys at Site C.

Mirror Number	Distance (meters)	Horizontal Angle from North (deg)	Vertical Angle* (deg)
1	109.4	34° 03’	0° 00’
2	174.8	34° 34’	0° 00’
3	328.5	34° 28’	0° 00’
4	328.4	34° 32’	1° 39’
5	328.0	34° 20’	2° 25’

*Vertical angle shown is the angle from horizontal (positive values indicate elevation from the horizontal, negative values indicate descent from the horizontal)

Table B-24. Distance, and Horizontal and Vertical Coordinates of Mirrors Used During the 5/5 Survey at Site C.

Mirror Number	Distance (meters)	Horizontal Angle from North (deg)	Vertical Angle* (deg)
1	82.6	332° 28’	0° 00’
2	176.4	329° 00’	0° 00’
3	265.4	327° 32’	0° 00’
4	265.2	327° 16’	1° 12’
5	264.8	327° 03’	2° 08’

*Vertical angle shown is the angle from horizontal (positive values indicate elevation from the horizontal, negative values indicate descent from the horizontal)

Table B-25. Distance, and Horizontal and Vertical Coordinates of Mirrors Used During the 5/6 Survey at Site C.

Mirror Number	Distance (meters)	Horizontal Angle from North (deg)	Vertical Angle* (deg)
1	57.1	357° 23’	0° 00’
2	106.6	1° 10’	0° 00’
3	168.0	3° 37’	0° 00’
4	168.0	3° 37’	1° 37’
5	167.5	3° 37’	3° 07’

*Vertical angle shown is the angle from horizontal (positive values indicate elevation from the horizontal, negative values indicate descent from the horizontal)

Table B-26. Distance, and Horizontal and Vertical Coordinates of Mirrors Used During the 5/7 Survey at Site C.

Mirror Number	Distance (meters)	Horizontal Angle from North (deg)	Vertical Angle* (deg)
1	100.2	57° 15’	0° 00’
2	206.9	58° 21’	0° 00’
3	300.0	59° 43’	0° 00’
4	300.1	59° 22’	0° 23’
5	299.9	59° 07’	1° 14’

*Vertical angle shown is the angle from horizontal (positive values indicate elevation from the horizontal, negative values indicate descent from the horizontal)

This page intentionally left blank.

APPENDIX C
Daily OTM-10 Results

Table C-1. Calculated Methane Flux and Prevailing Wind Speed and Direction, and ACF Measured During the 11/17 Morning OTM-10 Survey at Site A

Time	Methane Flux (g/s)	Prevailing Wind Direction (degrees from North)	Prevailing Wind Speed (m/s)	ACF (m^2)
11:21:51	6.2	74	2.9	20806
11:39:48	8.5	74	3.3	21649
12:21:30	5.9	74	2.5	19964
12:24:02	6.3	74	2.7	20385
12:26:38	9.0	70	2.7	20385
Average	***7.2***		***2.8***	
Std Dev	***1.44***			

Table C-2. Calculated Methane Flux and Prevailing Wind Speed and Direction, and ACF Measured During the 11/17 Afternoon OTM-10 Survey at Site A

Time	Methane Flux (g/s)	Prevailing Wind Direction (degrees from North)	Prevailing Wind Speed (m/s)	ACF (m^2)
13:47:24	7.1	69	2.2	17369
13:52:45	8.0	79	2.1	17180
13:55:19	13	75	2.1	17180
13:57:54	12	71	2.1	17180
14:03:16	11	61	2.2	17369
14:05:51	8.4	71	2.2	17369
14:08:24	7.5	73	2.1	17180
14:10:55	8.5	78	2.3	17558
14:13:29	8.9	77	2.4	17747
14:16:01	8.4	79	2.7	18315
14:18:37	8.3	78	2.7	18315
14:21:09	7.5	79	2.7	18315
14:23:40	8.8	77	2.6	18125
14:26:15	11	69	2.7	18315
14:28:46	13	67	2.9	18693
14:31:21	12	67	2.9	18693
14:33:55	13	69	2.9	18693
14:36:24	13	71	2.8	18504
14:38:59	12	70	2.9	18693
14:41:31	12	69	2.8	18504
14:44:06	12	64	2.6	18125
14:46:39	11	68	2.3	17558
14:49:09	8.5	82	2.2	17369
14:51:44	9.5	86	2.2	17369
14:54:16	9.5	81	2.4	17747
14:56:52	12	71	2.7	18315
14:59:24	10	72	3.1	19071
15:01:54	11	73	3.4	19639
15:04:28	9.6	76	3.0	18882
15:07:01	9.2	78	2.8	18504
15:09:37	9.4	80	2.9	18693
15:12:09	11	77	3.2	19261
15:14:39	11	75	3.4	19639
15:17:14	12	71	3.2	19261
15:19:45	11	71	3.1	19071
15:22:21	11	72	2.7	18315

Time	Methane Flux (g/s)	Prevailing Wind Direction (degrees from North)	Prevailing Wind Speed (m/s)	ACF (m^2)
15:24:54	10	71	2.6	18125
15:27:27	9.3	69	2.7	18315
15:29:58	9.4	69	2.6	18125
15:32:33	14	70	2.5	17936
15:35:08	14	73	2.4	17747
15:37:39	12	76	2.6	18125
15:40:09	10	80	2.7	18315
15:42:45	11	79	2.9	18693
15:45:18	8.6	81	2.9	18693
15:47:53	8.8	79	2.9	18693
15:50:24	12	73	2.8	18504
15:52:57	14	68	2.5	17936
15:55:30	13	63	2.5	17936
15:58:03	14	60	2.7	18315
16:00:38	16	57	2.9	18693
16:03:07	18	58	3.1	19071
16:05:42	14	59	2.9	18693
16:08:13	9.7	67	2.6	18125
16:10:48	10	66	2.2	17369
16:13:22	9.1	64	2.4	17747
16:15:54	13	61	2.6	18125
16:18:27	12	63	3.0	18882
16:21:00	12	66	3.2	19261
16:23:33	10	67	3.3	19450
16:26:06	11	68	3.1	19071
16:28:39	10	69	3.1	19071
16:31:12	11	70	3.1	19071
16:33:45	9.3	70	2.8	18504
16:36:18	10	71	2.4	17747
16:38:51	9.8	72	2.4	17747
16:41:24	10	73	2.7	18315
16:43:57	9.7	73	2.8	18504
16:47:47	11	71	2.9	18693
16:50:18	9.6	72	2.7	18315
16:52:52	10	72	2.7	18315
16:56:42	10	73	2.4	17747
16:59:15	11	70	2.4	17747

Time	Methane Flux (g/s)	Prevailing Wind Direction (degrees from North)	Prevailing Wind Speed (m/s)	ACF (m^2)
17:01:48	10	70	2.3	17558
17:04:21	8.3	70	2.4	17747
17:06:56	9.3	71	2.6	18125
17:09:27	9.6	71	2.9	18693
17:12:12	10	72	3.1	19071
17:14:33	11	71	3.1	19071
17:17:06	12	69	3.1	19071
Average	***11***		***2.7***	
Std Dev	***1.94***			

Table C-3. Calculated Methane Flux and Prevailing Wind Speed and Direction, and ACF Measured During the 11/18 OTM-10 Survey at Site A

Time	Methane Flux (g/s)	Prevailing Wind Direction (degrees from North)	Prevailing Wind Speed (m/s)	ACF (m^2)
9:51:38	7.7	57	3.6	23847
9:54:20	9.1	52	3.8	24298
9:56:53	8.4	52	3.9	24523
9:59:27	9.8	52	3.7	24072
10:02:02	8.4	56	3.4	23396
10:04:35	9.7	55	3.4	23396
10:07:05	8.6	53	3.7	24072
10:09:43	10	51	3.9	24523
10:12:19	10	53	3.9	24523
10:14:51	9.6	55	3.8	24298
10:17:25	10	56	3.7	24072
10:20:00	8.1	56	3.8	24298
10:22:37	7.5	57	3.7	24072
10:25:08	6.8	61	3.6	23847
10:27:40	7.2	62	3.5	23621
10:30:16	7.7	58	3.3	23171
10:32:52	10	52	3.4	23396
10:35:22	9.0	50	3.4	23396
10:37:57	9.9	51	3.4	23396
10:40:32	11	53	3.5	23621
10:43:05	10	55	3.4	23396
10:45:43	11	57	3.5	23621
10:48:15	9.2	63	3.5	23621
10:50:49	8.7	64	3.5	23621
10:53:21	10	61	3.1	22720
10:55:54	9.6	56	2.9	22269
10:58:29	12	50	3.2	22945
11:01:05	12	51	3.4	23396
11:03:36	12	51	3.5	23621
11:06:11	9.1	57	3.3	23171
11:08:45	9.6	59	2.9	22269
11:11:19	9.6	60	2.7	21818
11:13:57	8.3	62	2.4	21142
11:16:27	6.4	65	2.1	20466
11:19:03	6.4	68	1.9	20015
11:21:36	6.5	64	1.8	19790

Time	Methane Flux (g/s)	Prevailing Wind Direction (degrees from North)	Prevailing Wind Speed (m/s)	ACF (m^2)
11:24:13	8.9	57	2.3	20917
11:26:46	8.7	57	2.9	22269
11:29:20	9.7	58	3.1	22720
11:31:54	9.4	59	3.3	23171
11:34:26	10	55	3.1	22720
11:37:00	11	53	3.0	22495
11:39:34	9.9	50	3.0	22495
11:42:07	9.9	52	3.1	22720
11:44:43	10	54	3.1	22720
11:47:15	9.1	59	3.0	22495
11:49:48	9.9	61	3.1	22720
11:52:23	8.8	62	3.0	22495
11:55:00	8.1	62	2.7	21818
11:57:26	8.0	59	2.4	21142
12:00:06	9.9	59	2.4	21142
12:02:41	10	56	2.4	21142
12:05:11	11	56	2.5	21368
12:07:49	10	59	2.7	21818
12:10:24	10	62	2.9	22269
12:12:57	8.9	66	3.1	22720
12:15:31	10	63	3.0	22495
12:18:05	9.9	61	3.2	22945
12:20:38	13	55	2.9	22269
12:23:10	12	53	3.2	22945
12:25:44	11	52	3.3	23171
12:28:18	12	52	3.9	24523
12:30:55	13	52	3.8	24298
12:33:24	12	49	3.5	23621
12:36:23	9.6	47	3.0	22495
12:38:57	11	48	3.2	22945
12:41:53	13	50	3.6	23847
12:44:29	13	51	3.9	24523
12:47:03	12	53	3.9	24523
12:49:34	12	57	4.0	24748
12:52:09	13	56	4.1	24974
12:54:43	13	56	3.9	24523
12:57:24	12	55	3.9	24523

Time	Methane Flux (g/s)	Prevailing Wind Direction (degrees from North)	Prevailing Wind Speed (m/s)	ACF (m^2)
12:59:51	11	56	3.7	24072
13:02:23	12	55	3.8	24298
13:05:02	10	60	3.5	23621
13:07:33	9.9	63	3.6	23847
13:10:09	9.0	66	3.3	23171
13:12:45	9.5	63	3.2	22945
13:15:14	8.9	62	3.1	22720
13:17:49	11	60	3.3	23171
13:20:24	10	58	3.4	23396
13:22:59	8.3	59	3.4	23396
13:25:29	8.4	62	2.9	22269
13:28:05	12	57	2.9	22269
13:30:41	13	54	3.1	22720
13:33:15	15	55	3.6	23847
13:35:48	13	56	3.6	23847
13:38:21	12	57	3.3	23171
13:40:55	11	54	3.0	22495
13:43:29	10	55	2.8	22044
13:46:03	10	51	2.6	21593
13:48:39	12	50	2.6	21593
13:51:11	13	50	2.8	22044
13:53:45	13	52	2.7	21818
13:56:19	12	50	2.7	21818
13:58:55	11	48	2.4	21142
14:01:27	9.4	45	2.4	21142
14:05:15	11	46	2.5	21368
14:07:46	12	45	2.6	21593
14:11:35	14	46	2.7	21818
14:14:44	15	47	2.5	21368
14:17:17	16	48	2.8	22044
14:19:50	15	48	2.8	22044
14:23:03	15	43	3.2	22945
14:25:37	12	42	2.9	22269
14:28:10	13	44	2.9	22269
14:30:43	13	50	2.6	21593
14:33:15	14	48	2.6	21593
14:35:48	15	45	2.7	21818

Time	Methane Flux (g/s)	Prevailing Wind Direction (degrees from North)	Prevailing Wind Speed (m/s)	ACF (m^2)
14:38:21	18	41	3.0	22495
14:40:54	18	44	3.1	22720
14:43:25	15	46	3.0	22495
14:45:59	13	48	2.9	22269
14:48:36	13	49	3.1	22720
14:51:05	10	50	3.1	22720
14:53:39	13	49	2.9	22269
14:56:15	13	49	2.8	22044
14:58:44	15	51	2.7	21818
15:01:19	13	54	2.8	22044
15:03:52	12	52	2.6	21593
15:06:24	12	50	2.6	21593
15:08:56	10	50	2.7	21818
15:11:30	12	54	3.0	22495
15:14:04	9.5	57	3.0	22495
15:16:36	9.6	57	2.8	22044
15:19:09	7.1	57	2.4	21142
15:21:42	7.2	57	2.3	20917
15:24:15	9.1	59	2.5	21368
15:26:47	10	58	2.8	22044
15:29:20	11	54	2.8	22044
15:31:51	12	50	2.7	21818
15:34:25	15	45	2.7	21818
15:37:01	14	46	2.8	22044
15:39:37	15	47	3.0	22495
15:42:03	13	50	3.0	22495
15:44:35	14	51	3.1	22720
15:47:12	13	51	2.9	22269
15:49:48	13	50	3.0	22495
15:52:18	9.7	50	2.8	22044
15:54:54	10	49	2.8	22044
15:57:24	11	49	2.7	21818
Average	***11***		***3.1***	
Std Dev	***2.27***			

Table C-4. Calculated Methane Flux and Prevailing Wind Speed and Direction, and ACF Measured During the 11/20 OTM-10 Survey at Site A

Time	Methane Flux (g/s)	Prevailing Wind Direction (degrees from North)	Prevailing Wind Speed (m/s)	ACF (m^2)
9:34:49	18	30	3.4	40786
9:37:21	19	39	3.1	39692
9:39:53	18	48	3.4	40786
9:42:24	15	51	3.5	41151
9:44:57	13	49	3.6	41516
9:47:28	13	48	3.8	42246
9:50:01	17	47	4.0	42975
9:52:32	19	44	4.2	43705
9:55:04	17	44	4.1	43340
9:57:37	15	42	4.3	44070
10:00:10	14	44	3.9	42611
10:02:42	12	41	3.3	40421
10:05:13	16	42	2.7	38232
10:07:44	19	45	3.3	40421
10:10:18	13	50	3.7	41881
10:12:50	16	52	4.3	44070
10:15:20	14	49	4.2	43705
10:17:53	14	39	4.2	43705
10:20:26	14	39	3.7	41881
10:22:58	15	40	3.6	41516
10:25:30	16	52	4.3	44070
10:28:54	18	54	4.6	45164
10:31:24	18	52	4.4	44435
10:34:45	15	47	3.7	41881
10:37:18	14	45	3.8	42246
10:39:49	14	48	3.8	42246
10:42:21	12	46	4.1	43340
10:44:53	12	45	4.7	45529
10:47:26	15	42	4.4	44435
10:49:57	17	40	4.2	43705
10:52:29	19	41	4.1	43340
10:55:01	18	40	4.0	42975
10:57:33	13	28	3.4	40786
11:00:05	14	7	3.1	39692
11:02:38	14	12	3.3	40421
11:05:09	13	15	3.0	39327
11:07:41	15	34	3.4	40786
11:10:14	18	37	3.6	41516
11:12:45	19	39	4.5	44800
11:15:17	18	39	4.8	45894
11:17:49	13	38	4.8	45894

Time	Methane Flux (g/s)	Prevailing Wind Direction (degrees from North)	Prevailing Wind Speed (m/s)	ACF (m^2)
11:20:21	11	39	4.4	44435
11:22:53	11	32	3.9	42611
11:25:25	11	30	4.2	43705
11:27:57	15	31	4.5	44800
11:30:29	16	35	4.7	45529
11:33:00	18	37	4.4	44435
11:35:33	14	31	4.3	44070
11:38:04	17	27	4.3	44070
11:40:37	12	27	3.8	42246
11:43:09	15	25	3.3	40421
11:45:41	14	28	2.6	37868
11:48:13	11	36	2.9	38962
11:50:44	13	46	3.4	40786
11:53:17	16	46	3.8	42246
11:55:49	12	43	3.8	42246
11:58:21	14	44	3.8	42246
12:00:54	13	42	3.3	40421
12:03:25	17	43	3.2	40057
12:05:58	17	46	2.7	38232
12:08:29	14	52	2.8	38597
12:11:01	19	49	2.9	38962
12:13:33	14	29	2.9	38962
12:16:05	12	18	3.1	39692
12:18:38	10	13	2.7	38232
12:21:10	10	23	2.5	37503
12:23:42	13	17	2.5	37503
12:26:14	14	3	2.7	38232
12:28:45	12	357	3.0	39327
12:35:09	10	14	2.3	36773
12:37:42	8.8	12	1.9	35314
12:40:14	10	8	2.4	37138
12:59:18	9.5	357	2.5	37138
13:01:48	7.5	2	2.4	38962
13:04:23	14	21	2.9	40057
13:06:55	13	23	3.2	41881
13:09:27	10	31	3.7	41151
13:11:58	11	37	3.5	41516
13:14:30	11	43	3.6	40786
13:17:03	13	40	3.4	39327
13:19:35	13	31	3.0	38597
13:22:05	12	25	2.8	38962
13:24:38	13	26	2.9	40786
13:27:10	13	37	3.4	40421

Time	Methane Flux (g/s)	Prevailing Wind Direction (degrees from North)	Prevailing Wind Speed (m/s)	ACF (m^2)
13:29:42	14	36	3.3	38962
13:32:15	12	32	2.9	37868
13:34:46	12	6	2.6	38597
13:39:51	12	359	2.8	37138
13:42:23	10	23	2.4	36408
13:44:54	10	56	2.2	34949
13:47:24	8.6	64	1.8	33124
13:49:58	14	34	1.3	33854
13:52:31	12	21	1.5	35314
13:55:03	18	15	1.9	36773
13:57:34	14	35	2.3	38232
14:00:06	17	44	2.7	40057
14:02:39	19	54	3.2	38232
14:05:11	13	54	2.7	36773
14:07:42	11	54	2.3	34584
14:10:15	12	59	1.7	34219
14:12:47	14	56	1.6	35678
14:15:20	15	39	2.0	38232
14:17:49	19	33	2.7	41151
14:20:22	14	40	3.5	40421
14:22:54	13	50	3.3	39692
14:25:26	14	53	3.1	37138
14:27:59	15	35	2.4	36408
14:30:30	18	8	2.2	33124
14:35:35	16	23	1.3	34219
14:38:07	15	60	1.6	35314
14:40:41	17	70	1.9	36408
14:43:12	11	76	2.2	34949
14:48:15	12	77	1.8	34949
14:58:23	16	74	1.8	36408
15:00:55	24	50	2.2	36773
15:03:25	23	30	2.3	37868
15:05:58	18	28	2.6	36043
15:08:30	16	24	2.1	35678
15:11:01	23	32	2.0	35314
15:13:35	23	38	1.9	34219
15:16:07	14	39	1.6	33124
15:18:38	16	44	1.3	33124
15:21:11	18	45	1.3	33489
15:23:41	11	58	1.4	33854
15:26:15	14	63	1.5	33854
15:28:48	15	65	1.5	34949
15:31:18	24	60	1.8	36043

Time	Methane Flux (g/s)	Prevailing Wind Direction (degrees from North)	Prevailing Wind Speed (m/s)	ACF (m^2)
15:33:51	29	53	2.1	35678
15:36:23	28	48	2.0	35314
15:38:54	15	41	1.9	34219
15:41:26	14	31	1.6	34949
15:43:59	28	38	1.8	35314
15:46:33	29	52	1.9	36408
15:49:03	28	65	2.2	36043
15:51:34	25	72	2.1	36408
15:54:06	26	71	2.2	36043
15:56:39	23	72	2.1	36408
15:59:11	28	69	2.2	36043
16:01:44	23	74	2.1	35314
16:04:14	24	76	1.9	33854
16:21:59	16	77	1.5	33124
16:24:30	13	74	1.3	32760
16:27:02	16	73	1.2	32760
16:29:35	16	74	1.2	32760
16:32:06	16	72	1.2	32760
16:34:38	17	71	1.2	32760
16:37:10	18	70	1.2	40786
Average	***16***		***2.9***	
Std Dev	***4.37***			

Table C-5. Calculated Methane Flux and Prevailing Wind Speed and Direction, and ACF Measured During the 11/24 OTM-10 Survey at Site A

Time	Methane Flux (g/s)	Prevailing Wind Direction (degrees from North)	Prevailing Wind Speed (m/s)	ACF (m^2)
11:44:05	19	359	3.0	38257
11:46:38	17	353	2.9	37874
11:49:14	15	353	2.8	37490
11:51:46	13	348	2.4	35957
11:54:21	15	350	2.4	35957
11:56:57	16	355	2.6	36724
11:59:29	13	5	2.8	37490
12:02:03	11	11	2.6	36724
12:04:36	14	13	2.4	35957
12:07:10	18	22	2.6	36724
12:09:45	22	27	3.3	39407
12:12:20	17	28	3.5	40174
12:14:53	18	26	3.3	39407
12:17:56	14	21	2.9	37874
12:20:30	12	28	2.4	35957
12:24:21	12	20	2.8	37490
12:27:25	15	13	2.8	37490
12:31:14	17	6	3.2	39024
12:33:47	19	15	3.1	38640
12:36:20	15	33	2.9	37874
12:46:37	16	32	2.2	35191
12:49:11	20	19	2.5	36340
12:51:43	21	22	2.7	37107
12:54:20	23	22	2.2	35191
12:56:52	18	33	1.7	33274
12:59:26	14	17	1.7	33274
13:02:01	11	19	1.8	33657
13:04:36	13	14	2.0	34424
13:07:09	11	31	2.2	35191
13:09:44	12	41	2.5	36340
13:12:18	16	42	2.2	35191
13:27:42	14	41	2.3	35574
13:30:17	13	24	1.8	33657
13:32:48	15	22	1.5	32507
13:35:23	13	33	1.8	33657
13:37:57	13	42	2.0	34424

Time	Methane Flux (g/s)	Prevailing Wind Direction (degrees from North)	Prevailing Wind Speed (m/s)	ACF (m^2)
13:40:31	8.5	39	1.9	34041
13:55:54	9.2	38	2.5	36340
13:58:29	15	29	2.4	35957
14:01:02	15	23	2.1	34807
14:03:37	16	17	1.7	33274
14:06:11	9.4	31	1.5	32507
14:31:51	16	33	2.3	35574
14:34:25	17	34	2.4	35957
14:36:59	14	41	2.4	35957
Average	***15***		***2.4***	
Std Dev	***3.20***			

Table C-6. Calculated Methane Flux and Prevailing Wind Speed and Direction, and ACF Measured During the 12/1 Morning OTM-10 Survey at Site A

Time	Methane Flux (g/s)	Prevailing Wind Direction (degrees from North)	Prevailing Wind Speed (m/s)	ACF (m^2)
10:17:43	13	234	2.9	21361
10:20:15	11	229	3.3	22162
10:22:54	10	237	3.2	21962
10:25:25	6.8	240	2.8	21161
10:27:56	6.5	247	2.4	20361
10:30:33	8.7	250	2.2	19961
10:33:06	12	259	2.4	20361
10:35:41	13	259	2.5	20561
10:38:15	12	263	2.6	20761
10:40:48	8.7	264	2.5	20561
10:43:22	9.3	258	2.6	20761
10:45:57	8.3	245	2.7	20961
10:48:33	9.2	249	2.5	20561
10:51:04	10	254	2.2	19961
10:53:39	9.4	259	1.9	19361
10:56:15	11	247	1.9	19361
10:58:45	7.5	259	2.0	19561
11:01:16	7.9	272	1.7	18961
11:16:58	7.0	270	1.7	18961
11:19:32	6.1	252	2.2	19961
11:22:08	7.3	250	2.2	19961
11:24:42	9.3	261	1.8	19161
11:32:23	10	270	1.9	19361
11:34:57	12	242	2.0	19561
11:37:31	12	239	1.9	19361
11:40:04	14	242	1.9	19361
11:42:39	15	254	1.9	19361
11:45:12	15	256	2.0	19561
11:47:44	13	271	1.9	19361
11:50:20	13	261	2.0	19561
11:52:54	14	250	1.9	19361
11:55:30	13	235	2.0	19561
11:58:03	13	230	1.8	19161
12:00:35	11	231	1.8	19161
12:03:10	13	247	1.6	18761
12:05:44	12	259	1.7	18961

Time	Methane Flux (g/s)	Prevailing Wind Direction (degrees from North)	Prevailing Wind Speed (m/s)	ACF (m^2)
12:08:20	13	249	1.9	19361
12:10:53	13	240	2.3	20161
12:13:26	17	230	2.4	20361
12:18:01	19	237	2.2	19961
12:20:33	18	244	1.8	19161
12:23:09	14	262	1.6	18761
12:35:24	8.4	271	2.2	19961
12:37:59	7.9	263	2.4	20361
12:40:35	7.9	256	2.0	19561
12:43:07	7.3	249	1.8	19161
12:45:40	7.0	247	1.3	18161
13:39:35	2.5	178	1.3	17961
13:42:08	4.4	209	1.2	17561
13:54:57	4.7	269	1.0	17761
13:57:32	4.6	259	1.1	18561
14:00:06	8.0	246	1.5	18961
14:02:40	10	234	1.7	19161
14:05:14	11	221	1.8	18761
14:07:49	10	217	1.6	18361
14:10:23	8.7	223	1.4	17561
14:12:54	6.3	224	1.0	18561
14:25:46	10	259	1.5	19561
14:28:19	12	255	2.0	19961
14:30:55	13	240	2.2	19761
14:33:28	11	225	2.1	21361
Average	***10***		***2.0***	
Std Dev	***3.19***			

Table C-7. Calculated Methane Flux and Prevailing Wind Speed and Direction, and ACF Measured During the 12/1 Afternoon OTM-10 Survey at Site A

Time	Methane Flux (g/s)	Prevailing Wind Direction (degrees from North)	Prevailing Wind Speed (m/s)	ACF (m^2)
14:36:02	8.7	205	1.9	19361
14:38:36	8.6	200	1.8	19161
14:43:44	8.3	205	1.3	18161
14:46:17	8.4	210	1.3	18161
14:48:52	12	231	1.4	18361
14:51:26	13	226	1.6	18761
14:53:59	10	215	1.4	18361
14:56:33	8.6	200	1.7	18961
14:59:08	7.8	202	1.7	18961
15:01:41	10	203	1.9	19361
15:24:48	18	230	1.0	17561
15:27:23	15	212	1.1	17761
15:29:58	8.2	204	1.2	17961
15:42:47	16	198	1.6	18761
15:45:20	24	207	1.8	19161
15:47:53	17	204	1.5	18561
15:50:28	19	205	1.5	18561
15:53:02	18	200	1.5	18561
15:55:35	21	203	1.6	18761
15:58:08	23	206	1.7	18961
16:00:44	26	215	1.7	18961
16:03:19	23	206	1.6	18761
16:05:50	18	197	1.4	18361
Average	***15***		***1.5***	
Std Dev	***5.97***			

Table C-8. Calculated Methane Flux and Prevailing Wind Speed and Direction, and ACF Measured During the 5/14 OTM-10 Survey at Site A

Time	Methane Flux (g/s)	Prevailing Wind Direction (degrees from North)	Prevailing Wind Speed (m/s)	ACF (m^2)
13:32:05	2.6	211	1.8	25430
13:34:37	2.3	206	1.8	25430
13:37:08	2.4	195	1.5	24561
13:39:39	3.2	209	1.7	25140
13:42:10	3.5	220	2	26009
14:22:26	4.3	227	1.7	25140
14:24:57	4.1	200	1.9	25719
14:27:28	3.6	214	2	26009
14:47:37	5.2	227	1.9	25719
14:50:07	7.6	213	1.5	24561
14:52:39	8.8	220	1.7	25140
15:05:12	5.2	206	2	26009
15:07:44	5.5	196	2.2	26588
15:10:15	4.8	194	2.3	26878
15:12:47	5.9	215	2.3	26878
15:15:17	5.9	225	2.3	26878
15:17:48	6.5	225	2.4	27168
15:20:19	5.4	228	2.3	26878
15:22:50	4.9	218	2.3	26878
15:25:21	3.6	202	2.2	26588
15:27:52	3.2	191	2.8	28326
15:30:23	3.3	192	2.8	28326
15:32:54	4.0	206	3	28905
15:35:25	4.7	213	3	28905
13:32:05	2.6	211	1.8	25430
13:34:37	2.3	206	1.8	25430
13:37:08	2.4	195	1.5	24561
13:39:39	3.2	209	1.7	25140
13:42:10	3.5	220	2	26009
14:22:26	4.3	227	1.7	25140
14:24:57	4.1	200	1.9	25719
14:27:28	3.6	214	2	26009
14:47:37	5.2	227	1.9	25719
14:50:07	7.6	213	1.5	24561
14:52:39	8.8	220	1.7	25140
15:05:12	5.2	206	2	26009

Time	Methane Flux (g/s)	Prevailing Wind Direction (degrees from North)	Prevailing Wind Speed (m/s)	ACF (m^2)
15:07:44	5.5	196	2.2	26588
15:10:15	4.8	194	2.3	26878
15:12:47	5.9	215	2.3	26878
15:15:17	5.9	225	2.3	26878
15:17:48	6.5	225	2.4	27168
15:20:19	5.4	228	2.3	26878
15:22:50	4.9	218	2.3	26878
15:25:21	3.6	202	2.2	26588
15:27:52	3.2	191	2.8	28326
15:30:23	3.3	192	2.8	28326
15:32:54	4.0	206	3	28905
15:35:25	4.7	213	3	28905
Average	***4.6***		***2.1***	
Std Dev	***1.61***			

Table C-9. Calculated Methane Flux and Prevailing Wind Speed and Direction, and ACF Measured During the 5/20 OTM-10 Survey at Site A

Time	Methane Flux (g/s)	Prevailing Wind Direction (degrees from North)	Prevailing Wind Speed (m/s)	ACF (m^2)
10:20:05	3.6	3	1.8	26050
10:22:36	3.9	9	1.7	25753
10:25:09	2.7	20	1.7	25753
11:05:40	1.8	28	1.4	24863
11:10:45	2.4	23	1.9	26347
11:13:17	2.5	27	2.2	27237
11:26:21	1.3	11	1.0	23677
11:28:54	2.3	7	1.5	25160
11:31:26	3.4	13	1.8	26050
11:33:57	3.2	15	1.7	25753
11:36:27	3.5	14	1.8	26050
11:39:02	4.6	355	1.8	26050
11:41:34	4.8	0	1.6	25457
11:44:04	3.6	358	1.0	23677
11:46:37	1.8	19	1.0	23677
11:56:48	2.1	21	1.0	23677
11:59:18	4.3	351	1.8	26050
12:01:48	6.5	339	1.9	26347
12:04:22	6.0	327	1.4	24863
12:06:54	3.4	322	0.80	23083
12:09:24	2.4	6	0.80	23083
12:24:41	3.4	17	1.0	23677
12:27:10	4.1	335	1.1	23973
12:34:45	5.4	337	1.5	25160
12:37:18	3.1	5	1.8	26050
12:39:50	2.2	16	1.7	25753
12:42:21	1.7	356	1.2	24270
12:44:54	3.8	347	1.8	26050
12:47:25	4.4	347	2.3	27533
12:49:59	4.1	355	2.4	27830
12:52:30	3.1	350	2.0	26643
12:55:03	2.7	348	1.5	25160
12:57:34	2.7	345	1.3	24567
13:00:05	3.1	327	1.2	24270
13:02:40	3.8	326	1.2	24270
13:05:10	2.8	358	1.1	23973

Time	Methane Flux (g/s)	Prevailing Wind Direction (degrees from North)	Prevailing Wind Speed (m/s)	ACF (m^2)
13:50:45	1.9	29	1.2	24270
13:53:18	2.8	333	1.2	24270
13:55:48	3.2	320	1.6	25457
13:58:22	1.4	316	0.90	23380
14:03:24	3.8	354	1.6	25457
14:05:57	5.1	346	1.9	26347
14:08:31	3.5	339	1.5	25160
14:11:03	2.3	358	1.0	23677
14:13:34	1.9	28	1.1	23973
14:18:38	2.2	23	1.2	24270
14:21:11	4.0	7	1.9	26347
14:23:44	5.7	3	2.4	27830
14:26:13	4.4	359	2.5	28127
14:28:46	3.4	352	2.0	26643
14:31:18	2.7	352	1.5	25160
14:33:50	2.6	352	1.0	23677
14:36:21	1.2	356	0.60	22490
Average	***3.3***		***1.5***	
Std Dev	***1.22***			

Table C-10. Calculated Methane Flux and Prevailing Wind Speed and Direction, and ACF Measured During the 5/21 OTM-10 Survey at Site A

Time	Methane Flux (g/s)	Prevailing Wind Direction (degrees from North)	Prevailing Wind Speed (m/s)	ACF (m^2)
11:37:36	3.6	158	2.5	28087
11:40:09	3.1	158	2.5	28087
11:42:41	2.9	160	2.2	27198
11:45:12	2.0	155	2.0	26606
12:35:52	1.7	155	1.3	24532
12:38:26	2.9	150	1.8	26013
12:51:05	3.4	153	2.3	27495
12:53:36	2.7	148	2.2	27198
12:56:06	2.7	147	2.3	27495
12:58:40	2.1	145	2.5	28087
13:16:24	1.8	150	1.1	23939
13:18:56	2.0	176	1.3	24532
13:21:27	2.9	169	1.6	25421
13:24:24	2.0	163	1.8	26013
14:03:50	4.1	148	2.5	28087
14:06:24	3.7	153	2.4	27791
14:08:54	3.6	171	2.2	27198
14:11:27	4.4	190	2.1	26902
14:14:00	5.3	182	1.9	26310
14:16:32	4.7	164	1.6	25421
14:19:04	3.6	154	1.8	26013
14:21:36	2.9	177	1.8	26013
14:24:08	2.8	195	2.0	26606
14:26:39	3.0	199	1.8	26013
14:29:12	3.2	195	1.8	26013
14:31:42	3.2	188	1.7	25717
14:34:15	3.6	187	2.0	26606
14:36:47	3.5	178	1.8	26013
14:39:20	2.5	173	1.5	25124
14:41:52	2.0	164	1.2	24236
14:44:24	2.0	154	1.2	24236
14:46:55	3.2	147	1.5	25124
14:49:27	5.4	147	1.6	25421
14:52:01	5.7	157	1.7	25717
14:54:30	6.4	164	1.8	26013
14:57:03	4.9	166	1.9	26310

Time	Methane Flux (g/s)	Prevailing Wind Direction (degrees from North)	Prevailing Wind Speed (m/s)	ACF (m^2)
14:59:37	4.2	171	1.5	25124
15:02:06	3.5	187	1.3	24532
15:04:40	2.9	204	1.1	23939
15:07:12	3.8	187	1.2	24236
15:09:45	5.1	165	1.8	26013
15:12:19	5.8	159	2.3	27495
15:14:52	4.3	163	2.0	26606
15:17:20	4.3	173	1.6	25421
15:19:46	4.6	176	1.6	25421
Average	***3.5***		***1.8***	
Std Dev	***1.24***			

Table C-11. Calculated Methane Flux and Prevailing Wind Speed and Direction, and ACF Measured During the 5/26 OTM-10 Survey at Site A

Time	Methane Flux (g/s)	Prevailing Wind Direction (degrees from North)	Prevailing Wind Speed (m/s)	ACF (m^2)
12:13:05	13	358	4.0	29630
12:15:32	11	7	3.4	28011
12:18:03	10	19	2.9	26661
12:20:34	12	21	3.6	28550
12:23:03	12	13	3.5	28280
12:25:36	14	12	3.8	29090
12:28:05	12	5	3.4	28011
12:30:37	14	13	3.6	28550
12:33:09	15	12	3.6	28550
12:35:35	15	24	3.2	27471
12:38:11	12	29	2.9	26661
12:40:42	10	27	2.1	24503
12:43:09	9	351	2.2	24772
12:45:42	11	354	2.9	26661
12:48:15	11	14	3.3	27741
12:50:44	12	34	3.7	28820
12:53:14	11	43	3.3	27741
12:55:48	14	32	3.3	27741
12:58:19	15	25	3.6	28550
13:00:47	15	14	3.8	29090
13:03:20	13	5	3.8	29090
13:05:52	13	359	3.9	29360
13:08:21	12	353	4.0	29630
13:10:54	14	348	3.7	28820
13:13:25	13	352	3.3	27741
13:15:56	16	1	3.5	28280
13:18:27	17	13	4.1	29899
13:20:58	18	16	4.6	31249
13:23:27	15	20	4.4	30709
13:25:59	15	20	4.0	29630
13:28:28	11	22	3.2	27471
13:31:00	12	14	2.4	25312
13:33:32	13	357	2.7	26122
13:36:04	16	354	3.7	28820
13:38:35	14	354	4.4	30709
13:41:06	14	357	4.5	30979

Time	Methane Flux (g/s)	Prevailing Wind Direction (degrees from North)	Prevailing Wind Speed (m/s)	ACF (m^2)
13:43:37	15	356	4.6	31249
13:46:09	15	357	4.6	31249
13:48:39	16	4	4.8	31788
13:51:10	14	15	4.5	30979
13:53:40	14	24	4.6	31249
13:56:12	15	30	4.6	31249
13:58:44	18	31	4.9	32058
14:01:13	19	31	4.9	32058
14:03:46	13	27	3.8	29090
14:06:16	11	5	3.3	27741
14:08:47	12	348	4.2	30169
14:13:48	13	348	4.7	31519
14:16:20	14	359	4.6	31249
14:18:51	16	9	4.7	31519
14:21:20	18	16	4.6	31249
14:23:54	18	11	4.6	31249
14:26:24	17	5	5.2	32868
14:28:56	16	3	5.6	33947
14:31:26	16	10	4.5	30979
14:33:57	15	19	4.1	29899
14:36:29	16	26	4.2	30169
14:39:39	16	31	4.6	31249
14:41:29	17	28	4.7	31519
14:44:01	14	19	4.3	30439
14:46:32	16	12	4.8	31788
14:49:01	16	15	4.7	31519
14:51:33	17	17	4.9	32058
14:54:09	17	16	5.1	32598
14:56:36	16	17	5.2	32868
14:59:07	15	23	5.3	33138
15:01:39	16	29	5.2	32868
15:04:09	16	35	5.0	32328
15:06:38	17	36	4.2	30169
15:09:11	15	34	3.8	29090
15:11:42	16	20	4.0	29630
15:14:13	16	16	4.5	30979
15:16:44	16	22	4.5	30979

Time	Methane Flux (g/s)	Prevailing Wind Direction (degrees from North)	Prevailing Wind Speed (m/s)	ACF (m^2)
15:19:15	15	29	4.7	31519
15:21:46	16	26	4.3	30439
15:24:19	16	31	4.5	30979
15:26:45	18	33	4.7	31519
15:29:19	17	36	5.4	33407
15:31:50	17	26	5.3	33138
15:34:19	15	13	4.7	31519
15:36:53	16	359	4.5	30979
15:39:21	16	360	4.5	30979
15:41:54	19	7	5.0	32328
15:44:26	18	13	5.3	33138
15:46:54	20	16	5.0	32328
Average	***15***		***4.2***	
Std Dev	***2.29***			

Table C-12. Calculated Methane Flux and Prevailing Wind Speed and Direction, and ACF Measured During the 5/27 OTM-10 Survey at Site A

Time	Methane Flux (g/s)	Prevailing Wind Direction (degrees from North)	Prevailing Wind Speed (m/s)	ACF (m^2)
9:32:22	4.0	13	1.4	22582
9:34:53	4.5	15	1.8	23660
9:37:24	4.9	21	2.2	24738
9:39:55	4.4	13	2.1	24468
9:42:24	5.2	18	2.1	24468
9:44:57	4.3	24	2.2	24738
9:47:29	4.3	35	2.6	25815
9:49:57	4.0	37	2.6	25815
9:52:31	4.1	31	2.6	25815
9:55:00	3.8	28	2.2	24738
9:57:30	3.7	29	2.0	24199
10:00:03	4.5	41	2.0	24199
10:02:33	4.9	47	2.5	25546
10:05:06	5.8	50	2.8	26354
10:07:36	5.3	49	2.9	26624
10:10:07	6.6	45	3.1	27163
10:12:37	5.7	42	3.1	27163
10:15:08	6.0	36	3.0	26893
10:17:38	5.9	32	2.5	25546
10:20:09	5.8	27	2.5	25546
10:22:40	5.2	26	2.6	25815
10:25:10	5.1	31	2.8	26354
10:27:44	3.6	36	2.6	25815
10:30:18	3.4	42	2.6	25815
10:32:42	3.1	44	2.6	25815
10:35:18	5.3	34	2.6	25815
10:37:48	4.9	25	2.6	25815
10:40:19	4.7	14	2.4	25276
10:42:50	3.5	19	2.1	24468
10:45:21	2.7	17	1.8	23660
10:47:53	2.7	21	1.8	23660
10:50:23	2.9	23	1.8	23660
10:52:57	2.7	28	1.7	23390
10:55:27	1.5	34	1.1	21773
11:02:59	2.1	34	1.2	22043
11:05:29	2.1	21	1.3	22312
11:07:59	2.3	33	1.6	23121
11:10:31	2.8	42	1.9	23929
11:13:04	3.3	42	2.2	24738
11:15:33	2.7	33	2.0	24199
11:18:04	3.3	32	2.1	24468

Time	Methane Flux (g/s)	Prevailing Wind Direction (degrees from North)	Prevailing Wind Speed (m/s)	ACF (m^2)
11:20:35	3.2	35	2.3	25007
11:23:06	3.0	40	2.2	24738
11:25:37	2.7	30	2.0	24199
11:28:09	3.0	31	2.1	24468
11:30:39	4.2	41	2.5	25546
11:33:10	5.4	30	2.8	26354
11:35:41	4.9	22	2.5	25546
11:38:12	4.4	14	2.7	26085
11:40:43	4.1	26	2.7	26085
11:43:14	4.8	22	3.1	27163
11:45:45	5.3	14	3.2	27432
11:48:16	6.6	6	3.6	28510
11:50:47	7.6	6	3.9	29318
11:53:18	7.6	4	4.2	30127
11:55:49	5.9	2	3.9	29318
11:58:21	5.2	5	3.1	27163
12:00:51	4.9	9	2.6	25815
12:03:22	5.0	3	2.4	25276
12:05:53	5.8	354	2.7	26085
12:08:24	5.9	355	2.7	26085
12:10:56	5.7	4	2.7	26085
12:13:26	5.2	1	2.5	25546
12:15:59	4.5	354	2.4	25276
12:18:29	4.1	347	2.3	25007
12:20:59	3.9	353	2.3	25007
12:23:31	4.7	1	2.1	24468
12:26:01	4.3	16	2.1	24468
12:28:32	4.7	19	2.1	24468
12:31:03	5.2	17	2.5	25546
12:33:34	4.5	12	2.6	25815
12:36:05	3.6	16	2.5	25546
12:38:37	3.3	9	2.5	25546
12:41:07	4.6	7	2.6	25815
12:43:38	6.8	15	3.0	26893
12:46:09	8.0	31	3.2	27432
12:48:40	8.1	39	4.0	29588
12:51:12	5.9	37	3.7	28779
12:53:42	4.8	35	3.4	27971
12:56:13	4.8	33	3.2	27432
12:58:44	5.1	35	3.2	27432
13:01:15	5.9	35	3.3	27702
13:03:47	5.3	24	2.8	26354
13:06:17	6.0	7	2.5	25546

Time	Methane Flux (g/s)	Prevailing Wind Direction (degrees from North)	Prevailing Wind Speed (m/s)	ACF (m^2)
13:08:48	5.7	353	2.6	25815
13:11:19	6.2	360	2.9	26624
13:13:50	6.2	10	3.3	27702
13:16:21	6.4	17	3.7	28779
13:18:52	6.8	16	3.5	28241
13:21:23	6.0	10	3.3	27702
13:23:54	6.2	11	3.1	27163
13:26:25	6.2	14	3.5	28241
13:28:56	7.1	20	3.6	28510
13:31:27	7.2	22	3.5	28241
13:33:58	6.7	27	3.1	27163
13:36:29	6.5	35	2.8	26354
13:39:00	6.2	39	2.8	26354
13:41:31	6.1	44	2.9	26624
13:44:02	4.2	42	2.9	26624
13:46:33	4.2	44	2.7	26085
13:49:04	3.3	47	2.4	25276
13:51:37	3.5	47	2.0	24199
13:54:06	3.1	32	1.6	23121
13:56:37	3.9	5	1.6	23121
13:59:09	2.9	351	1.6	23121
14:01:39	2.5	346	1.4	22582
14:31:52	4.1	359	1.4	22582
14:34:22	6.1	351	2.7	26085
14:36:53	8.9	351	4.0	29588
14:45:39	7.8	6	3.6	28510
Average	***4.8***		***2.6***	
Std Dev	***1.56***			

Table C-13. Calculated Methane Flux and Prevailing Wind Speed and Direction, and ACF Measured During the 6/3 OTM-10 Survey at Site A

Time	Methane Flux (g/s)	Prevailing Wind Direction (degrees from North)	Prevailing Wind Speed (m/s)	ACF (m^2)
12:53:52	4.4	228	1.7	23145
12:56:21	5.4	223	1.8	23412
12:58:54	5.4	230	1.5	22612
13:09:02	4.3	219	1.5	22612
13:11:35	5.3	217	1.7	23145
13:14:07	4.6	215	1.5	22612
13:16:39	3.4	222	1.4	22345
13:29:18	3.3	224	1.3	22079
13:31:50	5.0	204	1.1	21545
13:34:23	5.4	208	1.5	22612
13:36:54	5.5	221	2.0	23945
13:39:27	3.3	228	1.9	23679
14:02:15	5.5	228	1.7	23145
14:04:46	9.2	209	2.3	24745
14:07:18	7.8	197	2.4	25012
14:09:50	6.8	191	2.4	25012
14:12:23	8.0	193	2.4	25012
14:14:55	8.3	201	2.7	25812
14:17:27	8.2	202	3.1	26878
14:19:59	7.7	204	3.0	26612
14:22:30	8.0	205	3.1	26878
14:25:03	8.3	200	3.0	26612
14:27:34	9.4	195	2.9	26345
14:30:06	9.2	194	2.8	26078
14:32:39	7.0	203	2.6	25545
14:35:09	6.2	220	2.6	25545
14:40:14	6.3	221	2.7	25812
14:42:47	8.8	204	2.7	25812
14:45:19	8.5	198	3.1	26878
14:47:51	7.8	201	2.8	26078
14:50:22	7.6	203	2.9	26345
14:52:54	8.9	195	2.7	25812
14:55:27	8.4	196	2.7	25812
14:57:59	8.2	195	2.7	25812
15:00:30	8.5	197	2.9	26345
15:03:00	8.8	196	2.9	26345

Time	Methane Flux (g/s)	Prevailing Wind Direction (degrees from North)	Prevailing Wind Speed (m/s)	ACF (m^2)
15:05:34	9.8	194	2.8	26078
15:08:07	8.9	196	2.7	25812
15:10:39	9.5	204	2.6	25545
15:13:10	6.9	215	2.7	25812
15:15:42	5.5	222	2.6	25545
15:18:14	6.1	208	2.7	25812
15:20:47	7.7	189	2.3	24745
15:23:18	9.9	184	2.5	25278
15:25:50	8.8	182	2.4	25012
15:28:23	8.4	187	2.5	25278
15:30:54	7.7	187	2.3	24745
15:33:26	7.8	188	2.3	24745
15:35:58	9.1	190	2.5	25278
15:38:30	8.7	191	2.7	25812
15:41:02	7.4	194	2.5	25278
15:43:35	7.2	192	2.3	24745
15:46:06	10.5	185	2.3	24745
15:48:38	11.3	181	2.5	25278
15:51:11	10.5	188	2.8	26078
15:53:44	6.7	197	2.6	25545
15:56:15	7.7	193	2.6	25545
15:58:46	9.2	186	2.7	25812
16:01:18	10.7	179	2.9	26345
16:03:51	8.3	179	2.5	25278
16:06:24	7.6	174	2.3	24745
16:08:54	7.0	176	2.4	25012
16:11:26	7.6	177	2.7	25812
16:13:58	7.6	172	2.5	25278
16:16:31	7.4	164	2.2	24479
16:19:04	7.3	169	2.0	23945
16:21:34	7.9	180	2.1	24212
16:24:06	8.6	177	2.2	24479
16:26:38	7.9	166	2.4	25012
16:29:11	7.4	162	2.5	25278
Average	***7.5***		***2.4***	
Std Dev	***1.82***			

Table C-14. Calculated Methane Flux and Prevailing Wind Speed and Direction, and ACF Measured During the 6/4 OTM-10 Survey at Site A

Time	Methane Flux (g/s)	Prevailing Wind Direction (degrees from North)	Prevailing Wind Speed (m/s)	ACF (m^2)
9:43:01	3.9	232	1.5	22644
9:45:33	4.2	230	1.5	22644
9:48:05	6.2	219	1.7	23178
9:50:36	7.0	209	1.5	22644
9:53:07	5.3	220	1.4	22377
10:05:49	4.7	225	2.3	24780
10:10:50	4.7	224	1.9	23712
10:13:21	4.6	226	2.0	23979
11:06:37	4.4	227	2.5	25314
11:26:52	5.9	227	1.6	22911
11:29:25	6.7	223	1.9	23712
11:31:57	5.9	222	2.4	25047
11:34:28	4.7	223	2.7	25848
11:37:04	4.9	223	2.6	25581
11:39:33	5.3	219	2.5	25314
11:42:05	5.6	218	2.3	24780
11:44:36	5.4	216	2.4	25047
11:47:08	4.9	224	2.5	25314
11:49:41	4.8	226	2.9	26382
11:52:13	4.6	228	2.9	26382
11:54:45	5.2	225	2.8	26115
11:57:16	5.8	220	2.5	25314
11:59:48	5.8	217	2.5	25314
12:02:21	6.1	215	2.2	24513
12:04:53	4.8	222	1.9	23712
12:07:23	4.3	228	1.8	23445
12:09:56	4.6	224	2.2	24513
12:12:29	6.0	212	2.3	24780
12:15:15	6.9	209	2.7	25848
12:17:32	6.8	211	2.7	25848
12:20:07	5.4	220	3.0	26649
12:22:36	6.2	218	2.7	25848
12:25:07	6.7	219	2.3	24780
12:27:39	5.6	227	2.1	24246
12:42:53	6.4	217	1.8	23445
12:45:24	8.3	209	2.2	24513

Time	Methane Flux (g/s)	Prevailing Wind Direction (degrees from North)	Prevailing Wind Speed (m/s)	ACF (m^2)
12:47:57	6.0	219	2.3	24780
12:50:28	4.6	225	2.0	23979
13:13:17	5.3	230	2.3	24780
13:15:48	5.4	226	2.2	24513
13:18:20	4.7	230	2.7	25848
13:20:52	5.5	225	2.6	25581
13:23:24	5.5	218	2.5	25314
13:25:57	5.8	210	2.4	25047
13:28:28	6.4	209	2.4	25047
13:31:00	6.5	212	2.5	25314
13:33:33	6.5	214	2.4	25047
13:36:03	5.2	219	2.4	25047
13:38:36	5.4	216	1.9	23712
13:41:08	6.1	206	1.5	22644
13:43:40	5.4	201	1.4	22377
13:46:12	5.8	206	1.7	23178
13:48:44	5.9	214	1.9	23712
13:51:16	5.1	219	1.9	23712
13:53:48	4.4	229	1.9	23712
14:01:24	6.5	217	2.2	24513
14:03:57	5.4	220	2.8	26115
14:06:28	6.6	217	2.9	26382
14:09:00	7.0	210	3.1	26916
14:11:34	8.6	196	3.0	26649
14:14:04	9.0	188	3.1	26916
14:16:36	8.7	191	2.7	25848
14:19:09	7.5	199	2.7	25848
14:21:40	7.0	210	2.7	25848
14:24:12	6.4	220	2.7	25848
14:26:44	6.3	220	2.2	24513
14:29:16	6.9	209	2.6	25581
14:31:49	8.5	202	2.9	26382
14:34:20	7.9	201	3.3	27450
14:36:53	7.9	203	2.9	26382
14:39:24	7.1	204	2.9	26382
14:41:57	6.3	207	2.6	25581
14:44:29	7.0	207	2.8	26115

Time	Methane Flux (g/s)	Prevailing Wind Direction (degrees from North)	Prevailing Wind Speed (m/s)	ACF (m^2)
14:47:00	6.9	208	2.9	26382
14:49:32	8.6	204	3.0	26649
14:52:04	9.5	199	3.3	27450
14:54:36	11	198	3.1	26916
Average	***6.1***		***2.4***	
Std Dev	***1.43***			

Table C-15. Calculated Methane Flux and Prevailing Wind Speed and Direction, and ACF Measured During the 6/28 OTM-10 Survey at Site B

Time	Methane Flux (g/s)	Prevailing Wind Direction (degrees from North)	Prevailing Wind Speed (m/s)	ACF (m^2)
14:26:26	17	303	4.6	21432
14:28:59	19	296	4.8	21802
14:33:33	21	281	4.6	21432
14:35:31	18	279	4.9	21988
14:38:04	20	279	4.7	21617
14:42:05	24	281	4.6	21432
14:44:35	28	272	4.7	21617
14:47:11	37	264	5.2	22543
14:49:44	39	254	5.5	23098
Average	***25***		***4.8***	
Std Dev	***8.35***			

Table C-16. Calculated Methane Flux and Prevailing Wind Speed and Direction, and ACF Measured During the 6/30 OTM-10 Survey at Site B

Time	Methane Flux (g/s)	Prevailing Wind Direction (degrees from North)	Prevailing Wind Speed (m/s)	ACF (m^2)
11:35:03	44	59	0.9	32175
11:47:48	38	17	1.3	33808
11:50:18	72	15	1.6	35033
11:52:47	84	14	1.4	34217
11:55:19	89	12	1.7	35442
11:57:51	82	7	1.9	36258
12:00:20	36	3	1.8	35850
12:04:12	28	5	1.1	32992
12:09:19	54	10	1.1	32992
12:34:31	43	355	2.1	37075
12:37:14	48	353	2.1	37075
12:39:47	72	354	2.1	37075
12:42:18	61	355	1.9	36258
12:44:47	70	357	1.9	36258
12:47:20	69	358	1.8	35850
12:49:49	74	352	1.9	36258
12:52:23	58	350	2.0	36666
12:54:52	66	352	2.3	37891
12:57:22	57	359	2.6	39116
12:59:54	43	1	2.8	39933
13:02:26	52	2	2.9	40341
13:04:57	47	359	2.8	39933
13:07:28	68	358	2.6	39116
13:09:59	66	358	2.6	39116
13:12:29	89	359	2.8	39933
13:15:01	68	1	3.1	41158
13:17:31	63	1	3.3	41974
13:20:03	72	0	3.3	41974
13:22:34	61	355	3.3	41974
13:25:05	71	355	3.0	40749
13:27:36	70	354	2.9	40341
13:30:08	96	355	3.0	40749
13:32:38	82	352	3.2	41566
13:35:09	85	350	3.2	41566
13:37:40	111	351	3.0	40749
13:40:11	123	354	2.9	40341

Time	Methane Flux (g/s)	Prevailing Wind Direction (degrees from North)	Prevailing Wind Speed (m/s)	ACF (m^2)
13:42:42	162	356	3.1	41158
13:45:13	138	354	3.0	40749
13:47:45	100	350	2.8	39933
13:50:16	71	346	2.5	38708
13:52:46	68	346	2.4	38300
13:55:18	75	347	2.4	38300
13:57:47	61	344	2.4	38300
14:00:19	26	339	2.4	38300
14:02:50	34	339	2.3	37891
14:05:21	42	343	2.3	37891
14:07:51	57	348	2.2	37483
14:10:23	55	347	2.1	37075
14:12:54	47	343	2.0	36666
14:15:24	45	342	2.0	36666
14:17:57	53	343	2.0	36666
14:20:26	55	346	1.9	36258
14:22:58	50	344	1.9	36258
14:25:28	41	342	1.9	36258
14:28:01	37	340	1.9	36258
14:30:30	34	340	1.9	36258
14:33:02	63	343	1.9	36258
14:35:33	59	347	2.0	36666
14:38:06	79	350	2.2	37483
14:40:36	63	353	2.4	38300
14:43:06	58	358	2.5	38708
14:45:37	55	2	2.6	39116
14:48:07	57	8	2.7	39524
14:50:40	56	9	2.7	39524
14:53:10	61	9	3.0	40749
14:55:41	59	4	2.9	40341
14:58:15	64	1	2.8	39933
15:00:42	67	355	2.4	38300
15:03:14	63	351	2.3	37891
15:05:44	67	345	2.3	37891
15:08:16	70	343	2.5	38708
15:10:49	64	339	2.7	39524
15:13:18	106	341	2.9	40341

Time	Methane Flux (g/s)	Prevailing Wind Direction (degrees from North)	Prevailing Wind Speed (m/s)	ACF (m^2)
15:15:50	59	347	3.2	41566
15:18:20	70	352	3.2	41566
15:46:36	73	14	3.5	42791
15:49:12	58	13	3.2	41566
15:51:39	58	14	3.1	41158
15:54:11	49	13	3.0	40749
15:56:42	53	13	3.0	40749
15:59:15	46	12	2.9	40341
16:01:44	49	13	2.9	40341
16:04:19	51	12	2.6	39116
16:06:48	61	10	2.9	40341
16:09:18	64	11	3.2	41566
16:11:49	70	16	3.8	44016
16:14:21	64	17	3.8	44016
16:16:51	65	15	3.4	42383
16:19:23	59	10	3.0	40749
16:21:53	51	8	2.8	39933
16:24:27	43	8	2.8	39933
16:26:55	34	5	2.6	39116
16:29:26	34	0	2.6	39116
16:31:55	55	359	2.6	39116
16:34:31	46	360	2.7	39524
16:36:57	55	3	2.9	40341
16:39:30	62	6	3.0	40749
16:42:42	56	9	3.1	41158
16:44:31	61	11	3.1	41158
16:47:02	72	10	3.1	41158
16:49:35	52	8	3.1	41158
16:52:04	44	4	3.2	41566
16:54:34	41	3	3.2	41566
Average	***62***		***2.6***	
Std Dev	***21.1***			

Table C-17. Calculated Methane Flux and Prevailing Wind Speed and Direction, and ACF Measured During the 7/1 OTM-10 Survey at Site B

Time	Methane Flux (g/s)	Prevailing Wind Direction (degrees from North)	Prevailing Wind Speed (m/s)	ACF (m^2)
9:29:13	98	60	3.7	43456
9:31:38	96	56	3.3	41829
9:34:09	92	59	3.1	41015
9:36:39	85	57	3.0	40608
9:39:10	107	55	3.7	43456
9:41:40	112	49	4.0	44677
9:44:13	129	43	4.4	46305
9:46:44	127	42	4.4	46305
9:49:15	117	41	4.4	46305
9:51:44	103	40	4.3	45898
9:54:15	106	38	4.6	47118
9:56:47	105	42	4.5	46712
9:59:18	109	47	4.5	46712
10:01:50	81	51	4.0	44677
10:04:20	86	52	4.0	44677
10:06:51	86	56	4.0	44677
10:09:21	103	60	3.8	43863
10:17:42	100	51	3.7	43456
10:20:12	116	51	3.6	43050
10:22:44	114	52	3.6	43050
10:31:06	119	67	3.6	43050
10:33:33	105	63	3.6	43050
10:36:06	113	56	4.0	44677
10:38:36	104	46	4.1	45084
10:41:07	115	46	4.4	46305
10:43:37	118	50	4.4	46305
11:08:21	118	48	3.8	43863
11:12:12	126	50	4.2	45491
11:14:32	125	55	4.6	47118
11:17:00	118	64	4.3	45898
11:19:32	101	70	4.1	45084
11:22:05	106	70	4.2	45491
11:24:33	103	66	4.1	45084
11:27:03	116	67	4.0	44677
11:29:38	110	70	3.8	43863
11:42:33	121	69	3.7	43456

Time	Methane Flux (g/s)	Prevailing Wind Direction (degrees from North)	Prevailing Wind Speed (m/s)	ACF (m^2)
11:45:03	122	60	4.0	44677
11:47:35	126	67	4.5	46712
11:50:04	114	72	4.6	47118
11:52:39	119	76	4.3	45898
11:55:06	118	73	3.9	44270
12:04:12	98	62	3.2	41422
12:31:09	93	57	2.5	38574
12:33:25	95	47	2.3	37760
12:37:14	88	31	2.7	39388
12:39:47	102	30	3.2	41422
12:43:31	102	40	3.3	41829
12:46:00	126	45	2.7	39388
12:48:30	120	69	2.4	38167
12:51:01	106	92	2.7	39388
12:53:33	101	97	3.3	41829
12:56:04	75	78	2.6	38981
12:58:35	94	60	2.8	39795
13:01:06	84	54	2.8	39795
13:03:36	80	61	2.5	38574
13:06:07	62	56	2.0	36540
13:08:39	78	40	2.2	37353
13:11:12	96	44	2.5	38574
13:13:41	93	75	2.4	38167
13:16:12	81	86	2.6	38981
13:18:43	84	83	3.1	41015
13:21:13	92	65	3.3	41829
13:32:59	112	54	3.6	43050
13:35:21	105	63	3.5	42643
13:37:53	120	68	4.0	44677
13:40:23	131	81	4.5	46712
13:42:56	132	83	4.6	47118
13:45:25	131	83	4.9	48339
13:47:57	148	77	4.5	46712
13:50:27	143	71	4.0	44677
13:52:59	162	58	4.0	44677
13:55:28	128	59	4.2	45491
13:58:01	126	67	4.6	47118

Time	Methane Flux (g/s)	Prevailing Wind Direction (degrees from North)	Prevailing Wind Speed (m/s)	ACF (m^2)
14:00:32	112	74	4.4	46305
14:03:04	108	77	4.1	45084
14:05:34	96	67	3.4	42236
14:08:06	99	57	3.2	41422
14:10:34	98	65	3.2	41422
14:13:08	105	84	3.5	42643
14:15:38	92	97	3.1	41015
14:18:09	98	73	2.5	38574
14:20:39	122	57	3.3	41829
14:23:12	120	54	4.1	45084
14:25:41	105	60	4.0	44677
14:28:12	112	54	3.5	42643
14:30:45	109	51	3.0	40608
14:33:15	128	56	3.3	41829
14:35:47	85	67	3.2	41422
14:38:17	149	75	3.9	44270
14:40:46	134	72	3.7	43456
14:43:18	142	66	4.0	44677
14:45:50	128	59	3.9	44270
14:48:22	113	65	3.6	43050
14:50:52	98	73	3.3	41829
14:53:24	107	74	2.8	39795
14:55:55	104	78	2.6	38981
14:58:23	123	75	2.8	39795
15:00:56	116	74	3.2	41422
15:03:27	126	67	3.6	43050
15:05:57	113	71	3.3	41829
15:08:29	84	79	2.5	38574
15:11:01	84	85	2.1	36946
15:13:30	90	87	2.6	38981
15:16:01	106	80	2.9	40201
15:18:33	102	66	3.1	41015
15:21:06	98	50	2.8	39795
15:23:35	87	52	2.5	38574
15:26:07	80	67	2.4	38167
15:28:37	82	77	2.4	38167
15:31:09	84	81	2.4	38167

Time	Methane Flux (g/s)	Prevailing Wind Direction (degrees from North)	Prevailing Wind Speed (m/s)	ACF (m^2)
15:33:38	85	82	2.1	36946
15:36:10	84	84	2.1	36946
15:38:40	99	86	2.2	37353
15:41:12	101	86	2.1	36946
15:43:41	109	81	1.7	35319
15:46:14	84	69	1.4	34098
15:48:45	83	45	1.5	34505
15:51:15	71	43	1.8	35726
15:53:47	86	53	1.8	35726
15:56:17	85	70	1.7	35319
15:58:48	86	82	1.7	35319
16:01:20	80	88	1.9	36133
16:03:51	89	78	2.2	37353
16:06:21	104	64	2.5	38574
16:08:55	113	51	2.9	40201
16:12:47	110	59	2.8	39795
16:15:12	111	59	2.9	40201
16:17:43	112	61	2.9	40201
16:21:30	95	58	2.8	39795
16:24:01	88	62	2.7	39388
16:26:31	95	53	2.9	40201
16:39:23	92	66	2.1	36946
16:42:10	85	58	2.4	38167
16:44:40	83	59	2.3	37760
16:47:02	79	65	2.3	37760
16:50:09	88	56	2.3	37760
16:52:44	92	48	2.4	38167
16:55:32	98	39	2.8	39795
16:58:02	91	35	3.2	41422
17:00:37	99	38	3.6	43050
17:03:06	104	40	3.6	43050
Average	***104***		***3.3***	
Std Dev	***17.6***			

Table C-18. Calculated Methane Flux and Prevailing Wind Speed and Direction, and ACF Measured During the 8/2 OTM-10 Survey at Site B

Time	Methane Flux (g/s)	Prevailing Wind Direction (degrees from North)	Prevailing Wind Speed (m/s)	ACF (m^2)
13:02:47	45	76	1.6	34015
13:05:18	25	100	1.3	32826
13:07:49	28	104	1.3	32826
13:10:19	14	126	1.3	32826
13:12:51	8	140	1.4	33223
13:15:24	1	157	1.4	33223
13:22:54	48	15	1.4	33223
13:25:27	126	24	1.8	34808
13:27:57	96	26	1.6	34015
13:30:29	64	18	1.6	34015
13:32:59	49	13	1.4	33223
13:35:29	22	7	1.4	33223
13:37:58	11	357	1.2	32430
13:40:31	25	9	1.6	34015
13:43:05	111	32	1.9	35205
13:45:34	70	55	1.7	34412
13:48:06	49	77	1.4	33223
13:50:36	46	108	1.1	32033
13:53:06	65	86	0.8	30844
13:55:37	66	33	0.9	31240
13:58:09	34	3	1.6	34015
14:00:40	59	13	2.0	35601
14:03:11	36	9	1.6	34015
14:05:42	51	14	1.5	33619
14:08:12	29	16	1.4	33223
14:10:43	22	30	1.2	32430
14:15:45	18	55	1.0	31637
14:18:19	48	47	1.5	33619
14:20:48	73	41	2.2	36394
14:23:18	42	37	1.6	34015
14:25:49	32	35	1.4	33223
14:38:26	10	348	1.7	34412
14:40:58	35	354	2.0	35601
14:43:30	47	355	1.6	34015
15:03:37	35	32	1.2	32430
15:06:05	65	36	2.1	35998

Time	Methane Flux (g/s)	Prevailing Wind Direction (degrees from North)	Prevailing Wind Speed (m/s)	ACF (m^2)
15:08:36	89	28	2.6	37980
15:11:08	59	21	2.7	38376
15:13:39	48	14	2.4	37187
15:16:10	30	17	1.8	34808
15:18:41	18	28	1.1	32033
15:21:09	24	54	1.0	31637
15:23:42	35	62	1.0	31637
15:26:14	29	70	0.9	31240
15:31:16	13	6	1.0	31637
15:33:47	8	3	1.1	32033
15:38:51	34	22	1.3	32826
15:41:20	46	21	1.9	35205
15:43:51	57	26	2.2	36394
15:46:22	34	20	2.1	35998
15:48:53	22	356	2.1	35998
15:51:23	2	336	2.2	36394
15:53:55	2	338	2.3	36790
15:56:27	35	357	2.5	37583
15:58:57	76	7	3.4	41151
16:01:28	117	9	3.5	41548
16:03:59	61	14	3.2	40358
16:06:29	62	25	2.7	38376
16:09:01	67	37	2.7	38376
16:11:32	70	40	2.6	37980
16:14:03	70	34	2.8	38773
16:16:34	74	29	2.9	39169
16:19:05	77	27	3.0	39565
13:02:47	45	76	1.6	34015
13:05:18	25	100	1.3	32826
13:07:49	28	104	1.3	32826
13:10:19	14	126	1.3	32826
13:12:51	8.2	140	1.4	33223
13:15:24	1.0	157	1.4	33223
13:22:54	48	15	1.4	33223
13:25:27	126	24	1.8	34808
13:27:57	96	26	1.6	34015
13:30:29	64	18	1.6	34015

Time	Methane Flux (g/s)	Prevailing Wind Direction (degrees from North)	Prevailing Wind Speed (m/s)	ACF (m^2)
13:32:59	49	13	1.4	33223
13:35:29	22	7	1.4	33223
13:37:58	11	357	1.2	32430
13:40:31	25	9	1.6	34015
13:43:05	111	32	1.9	35205
13:45:34	70	55	1.7	34412
13:48:06	49	77	1.4	33223
13:50:36	46	108	1.1	32033
13:53:06	65	86	0.8	30844
13:55:37	66	33	0.9	31240
13:58:09	34	3	1.6	34015
14:00:40	59	13	2.0	35601
14:03:11	36	9	1.6	34015
14:05:42	51	14	1.5	33619
14:08:12	29	16	1.4	33223
14:10:43	22	30	1.2	32430
14:15:45	18	55	1.0	31637
14:18:19	48	47	1.5	33619
14:20:48	73	41	2.2	36394
14:23:18	42	37	1.6	34015
14:25:49	32	35	1.4	33223
14:38:26	10	348	1.7	34412
14:40:58	35	354	2.0	35601
14:43:30	47	355	1.6	34015
15:03:37	35	32	1.2	32430
15:06:05	65	36	2.1	35998
15:08:36	89	28	2.6	37980
15:11:08	59	21	2.7	38376
15:13:39	48	14	2.4	37187
15:16:10	30	17	1.8	34808
15:18:41	18	28	1.1	32033
15:21:09	24	54	1.0	31637
15:23:42	35	62	1.0	31637
15:26:14	29	70	0.9	31240
15:31:16	13	6	1.0	31637
15:33:47	8	3	1.1	32033
15:38:51	34	22	1.3	32826

Time	Methane Flux (g/s)	Prevailing Wind Direction (degrees from North)	Prevailing Wind Speed (m/s)	ACF (m^2)
15:41:20	46	21	1.9	35205
15:43:51	57	26	2.2	36394
15:46:22	34	20	2.1	35998
15:48:53	22	356	2.1	35998
15:51:23	2.4	336	2.2	36394
15:53:55	2.6	338	2.3	36790
15:56:27	35	357	2.5	37583
15:58:57	76	7	3.4	41151
16:01:28	117	9	3.5	41548
16:03:59	61	14	3.2	40358
16:06:29	62	25	2.7	38376
16:09:01	67	37	2.7	38376
16:11:32	70	40	2.6	37980
16:14:03	70	34	2.8	38773
16:16:34	74	29	2.9	39169
16:19:05	77	27	3.0	39565
Average	***45***		***1.8***	
Std Dev	***27.9***			

Table C-19. Calculated Methane Flux and Prevailing Wind Speed and Direction, and ACF Measured During the 8/3 OTM-10 Survey at Site B

Time	Methane Flux (g/s)	Prevailing Wind Direction (degrees from North)	Prevailing Wind Speed (m/s)	ACF (m^2)
12:09:45	95	74	2.2	35797
12:12:18	76	80	1.9	34627
12:14:50	70	95	2.0	35017
12:17:20	53	114	2.2	35797
12:19:52	71	109	2.2	35797
12:22:24	62	115	2.2	35797
12:24:58	68	100	2.0	35017
12:27:30	38	109	1.4	32677
12:30:05	36	89	1.2	31898
12:32:34	49	68	1.3	32288
12:35:03	91	50	2.1	35407
12:37:40	92	37	2.2	35797
12:40:09	82	37	2.1	35407
12:42:40	62	37	1.5	33067
12:45:12	47	45	1.0	31118
12:50:18	37	58	1.1	31508
12:52:48	53	48	1.5	33067
12:55:19	74	40	1.5	33067
12:57:52	74	38	1.6	33457
13:00:26	37	48	1.1	31508
13:08:02	36	23	1.3	32288
13:10:30	30	15	1.5	33067
13:13:04	19	6	1.8	34237
13:15:37	9	2	1.2	31898
13:18:07	18	6	1.4	32677
13:20:40	23	8	1.5	33067
13:23:13	37	15	1.9	34627
13:25:45	25	17	1.5	33067
13:28:18	33	20	1.2	31898
13:30:47	46	26	1.5	33067
13:33:23	64	41	1.8	34237
13:35:54	59	42	1.6	33457
13:38:26	42	41	1.2	31898
13:40:58	41	28	1.3	32288
13:56:08	33	63	1.1	31508
13:58:42	70	55	1.6	33457

Time	Methane Flux (g/s)	Prevailing Wind Direction (degrees from North)	Prevailing Wind Speed (m/s)	ACF (m^2)
14:01:12	77	44	1.8	34237
14:03:45	54	32	1.9	34627
14:06:18	62	38	1.8	34237
14:08:50	57	43	1.7	33847
14:11:22	58	52	1.9	34627
14:13:54	31	44	1.5	33067
14:16:24	38	60	1.5	33067
14:18:56	43	83	1.3	32288
14:21:28	63	100	1.8	34237
14:24:02	68	118	1.4	32677
14:26:33	96	99	1.2	31898
14:29:00	114	75	1.5	33067
14:31:36	136	60	2.3	36187
14:34:10	126	54	2.5	36967
14:36:42	117	58	2.4	36577
14:39:10	132	64	2.5	36967
14:41:46	124	88	2.9	38526
14:44:17	134	99	3.2	39696
14:46:49	95	110	3.2	39696
14:49:21	96	113	2.9	38526
14:51:53	102	116	2.5	36967
14:54:24	129	108	2.4	36577
14:56:57	125	80	2.2	35797
14:59:26	91	51	2.2	35797
15:02:00	84	27	2.8	38136
15:04:28	117	41	3.1	39306
15:07:04	142	59	3.8	42036
15:09:37	138	74	4.3	43985
15:12:06	122	78	4.1	43206
15:14:41	107	79	3.6	41256
15:17:12	91	82	3.5	40866
15:19:46	89	81	3.0	38916
15:22:19	82	87	2.6	37357
15:24:49	67	67	2.0	35017
15:27:24	79	67	2.1	35407
15:29:53	105	62	2.7	37747
15:32:25	115	72	3.0	38916

Time	Methane Flux (g/s)	Prevailing Wind Direction (degrees from North)	Prevailing Wind Speed (m/s)	ACF (m^2)
15:34:58	90	80	2.6	37357
15:37:30	75	81	2.1	35407
15:40:01	75	86	2.0	35017
15:42:33	77	88	2.0	35017
15:45:05	73	104	2.0	35017
15:47:36	68	103	2.3	36187
15:50:09	56	95	2.2	35797
15:52:42	69	81	2.6	37357
15:55:13	69	81	2.7	37747
15:57:45	92	83	2.5	36967
16:00:15	98	87	2.4	36577
16:02:48	91	83	2.0	35017
Average	***74***		***2.1***	
Std Dev	***32.4***			

Table C-20. Calculated Methane Flux and Prevailing Wind Speed and Direction, and ACF Measured During the 8/4 OTM-10 Survey at Site B

Time	Methane Flux (g/s)	Prevailing Wind Direction (degrees from North)	Prevailing Wind Speed (m/s)	ACF (m^2)
14:04:48	66	218	4.5	53524
14:07:21	65	223	4.6	53990
14:09:51	62	234	4.4	53057
14:12:20	57	246	4.4	53057
14:14:52	56	244	4.3	52591
14:17:24	53	240	4.3	52591
14:19:54	56	230	4.1	51659
14:22:26	58	229	3.7	49794
14:24:56	48	230	3.2	47463
14:27:28	51	230	3.1	46997
14:29:58	55	243	3.0	46530
14:32:28	49	244	3.3	47929
14:42:12	43	257	3.7	49794
14:44:44	45	253	3.7	49794
14:47:15	58	251	3.7	49794
14:56:58	108	231	3.8	50260
14:59:30	109	236	4.2	52125
15:02:02	106	239	4.3	52591
15:04:34	105	241	4.3	52591
15:07:08	104	239	4.1	51659
15:09:37	91	236	4.0	51193
15:12:07	88	228	4.0	51193
15:14:40	93	229	3.7	49794
15:17:12	98	230	3.8	50260
15:19:45	96	237	3.6	49328
15:22:18	89	236	3.6	49328
15:24:51	79	235	3.3	47929
15:27:22	82	231	3.2	47463
15:29:53	81	236	3.2	47463
15:32:26	94	240	3.3	47929
15:34:59	81	244	3.4	48395
15:37:28	95	250	3.5	48861
15:40:03	109	253	3.6	49328
15:42:37	110	251	3.7	49794
15:45:07	87	237	3.6	49328
15:47:39	94	226	4.0	51193

Time	Methane Flux (g/s)	Prevailing Wind Direction (degrees from North)	Prevailing Wind Speed (m/s)	ACF (m^2)
15:50:11	101	222	4.2	52125
15:52:43	102	225	4.2	52125
15:55:14	109	231	4.2	52125
15:57:47	123	235	4.4	53057
16:00:19	145	236	4.6	53990
16:02:51	125	234	4.6	53990
16:05:23	133	226	4.7	54456
16:07:55	134	219	5.0	55855
16:10:27	144	219	4.8	54922
16:13:01	107	226	4.5	53524
16:15:29	111	231	4.4	53057
16:18:04	97	230	4.5	53524
16:20:36	113	226	4.6	53990
16:23:07	90	232	4.2	52125
16:25:40	80	237	3.8	50260
16:28:12	78	242	3.4	48395
16:30:43	95	237	3.6	49328
16:33:15	104	228	4.2	52125
16:35:48	103	223	4.8	54922
16:38:17	108	221	5.0	55855
16:40:50	105	228	4.4	53057
16:43:26	103	230	3.9	50726
16:45:56	105	224	3.9	50726
16:48:27	131	219	4.3	52591
16:51:01	137	216	4.7	54456
16:53:30	145	216	5.0	55855
17:05:30	93	223	4.7	54456
17:08:03	107	226	4.5	53524
17:10:35	115	229	4.3	52591
17:13:08	127	230	3.9	50726
17:15:39	144	221	4.0	51193
17:18:10	126	219	3.8	50260
17:20:44	128	219	3.8	50260
17:23:15	118	233	3.8	50260
17:25:47	112	235	4.2	52125
17:28:19	104	237	4.4	53057
17:30:52	121	227	4.5	53524

Time	Methane Flux (g/s)	Prevailing Wind Direction (degrees from North)	Prevailing Wind Speed (m/s)	ACF (m^2)
17:33:24	140	221	5.0	55855
17:35:55	146	219	5.2	56787
17:38:29	142	220	5.1	56321
17:41:00	150	222	4.4	53057
17:43:32	125	223	3.8	50260
17:46:03	112	219	3.9	50726
17:48:37	120	223	4.3	52591
17:51:09	129	220	4.9	55389
17:53:40	137	221	5.0	55855
Average	***101***		***4.1***	
Std Dev	***28.1***			

Table C-21. Calculated Methane Flux and Prevailing Wind Speed and Direction, and ACF Measured During the 8/5 OTM-10 Survey at Site B

Time	Methane Flux (g/s)	Prevailing Wind Direction (degrees from North)	Prevailing Wind Speed (m/s)	ACF (m^2)
10:49:48	207	216	6.4	52741
10:52:23	194	218	6.2	51953
10:54:52	199	213	6.5	53135
10:57:23	95	212	6.4	52741
10:59:56	117	209	6.0	51164
11:02:29	167	210	5.5	49193
11:05:00	162	209	5.6	49588
11:07:32	160	211	5.4	48799
11:10:04	136	213	5.7	49982
11:12:36	149	214	5.8	50376
11:15:06	169	207	6.2	51953
11:17:40	116	206	6.4	52741
11:20:11	173	205	6.2	51953
11:22:45	147	205	6.0	51164
11:25:17	133	199	5.8	50376
11:27:46	159	196	5.7	49982
11:30:20	182	195	5.6	49588
11:32:53	129	195	6.2	51953
11:35:21	162	197	6.1	51558
11:37:57	181	202	5.9	50770
11:40:25	164	200	5.4	48799
11:42:59	76	193	5.2	48011
11:45:33	132	196	5.1	47617
11:48:00	146	206	5.0	47223
11:50:36	160	216	4.8	46434
11:53:09	119	209	4.7	46040
11:55:39	151	208	5.0	47223
11:58:12	245	212	5.3	48405
12:00:43	196	217	5.7	49982
12:03:16	258	219	5.4	48799
12:05:48	82	213	5.1	47617
12:08:21	170	215	4.6	45646
12:10:53	165	212	4.7	46040
12:13:24	184	208	5.2	48011
12:15:56	133	200	6.0	51164
12:18:28	171	202	5.6	49588

Time	Methane Flux (g/s)	Prevailing Wind Direction (degrees from North)	Prevailing Wind Speed (m/s)	ACF (m^2)
12:21:00	176	203	5.6	49588
12:23:33	171	204	5.5	49193
12:26:05	196	203	6.3	52347
12:28:37	171	206	5.9	50770
12:31:08	143	207	6.1	51558
12:33:38	101	207	5.9	50770
12:36:13	96	209	6.0	51164
12:38:45	106	214	6.2	51953
12:41:15	119	217	6.5	53135
12:43:48	110	218	6.6	53529
12:46:17	142	217	6.0	51164
12:48:51	196	206	5.7	49982
12:51:24	219	202	5.8	50376
12:53:57	241	206	5.6	49588
12:56:24	210	217	5.6	49588
12:59:00	149	222	5.8	50376
13:01:32	70	217	5.9	50770
13:04:03	100	218	5.9	50770
13:06:34	229	223	5.6	49588
13:09:09	249	224	5.9	50770
13:11:41	225	216	5.7	49982
13:14:12	131	201	6.1	51558
13:16:44	134	199	6.6	53529
13:19:15	134	205	6.6	53529
13:21:49	136	211	7.1	55500
13:24:20	127	210	6.9	54712
13:26:51	173	206	7.0	55106
13:29:24	169	211	6.6	53529
13:31:55	138	216	6.6	53529
13:34:29	175	219	6.5	53135
13:37:04	149	212	6.2	51953
13:39:33	186	208	5.6	49588
13:42:04	139	213	5.4	48799
13:44:36	149	223	6.2	51953
13:47:08	135	223	6.9	54712
13:49:40	114	222	6.8	54318
13:52:12	142	222	6.1	51558

Time	Methane Flux (g/s)	Prevailing Wind Direction (degrees from North)	Prevailing Wind Speed (m/s)	ACF (m^2)
13:54:45	141	226	6.4	52741
13:57:16	158	224	7.2	55894
13:59:48	120	219	7.9	58653
14:02:21	116	217	7.9	58653
14:04:51	160	220	7.0	55106
14:07:26	190	225	6.3	52347
14:09:56	196	216	5.8	50376
14:12:28	148	202	6.3	52347
14:15:00	106	199	6.6	53529
14:17:29	92	208	6.7	53923
14:20:04	100	220	6.4	52741
14:22:39	121	224	6.2	51953
14:25:09	181	223	6.4	52741
14:27:40	163	218	6.6	53529
14:30:12	189	222	6.3	52347
14:32:44	158	219	6.1	51558
14:35:16	139	216	6.0	51164
14:37:49	99	208	6.9	54712
14:40:21	91	206	6.9	54712
14:42:52	94	205	7.0	55106
14:45:21	109	203	7.2	55894
14:47:54	86	202	7.2	55894
14:50:26	80	203	7.3	56288
14:53:01	112	201	6.7	53923
14:55:33	141	203	6.5	53135
14:58:03	165	199	6.1	51558
15:00:34	177	206	6.0	51164
15:03:07	141	205	6.2	51953
15:05:39	119	209	6.5	53135
15:08:13	90	204	7.0	55106
15:10:45	111	208	7.1	55500
15:13:13	134	208	6.9	54712
15:15:47	115	208	6.0	51164
15:18:19	99	203	5.9	50770
15:20:52	102	201	5.8	50376
15:23:24	103	201	6.0	51164
15:25:54	81	197	6.1	51558

Time	Methane Flux (g/s)	Prevailing Wind Direction (degrees from North)	Prevailing Wind Speed (m/s)	ACF (m^2)
15:28:28	96	193	6.5	53135
15:31:01	114	201	6.4	52741
15:33:31	159	214	6.1	51558
15:36:04	151	220	5.9	50770
15:38:35	198	212	6.3	52347
15:41:09	180	203	7.4	56683
15:43:39	195	202	7.8	58259
15:46:10	149	201	7.3	56288
15:48:43	168	200	6.7	53923
15:51:15	154	198	6.6	53529
15:53:51	118	197	6.6	53529
15:56:20	116	197	6.4	52741
15:58:50	88	195	6.0	51164
16:01:24	111	195	6.1	51558
16:03:56	123	195	6.4	52741
16:06:25	148	201	6.8	54318
16:09:01	129	204	7.0	55106
16:11:31	142	208	6.4	52741
16:14:04	140	209	6.8	54318
16:16:36	172	210	6.8	54318
16:19:08	130	208	6.8	54318
16:21:39	98	198	5.8	50376
16:24:11	134	195	5.4	48799
16:26:45	131	195	6.1	51558
16:29:15	188	200	6.8	54318
16:31:48	133	200	7.1	55500
16:34:19	136	202	7.3	56288
16:36:51	150	201	7.8	58259
16:41:56	248	198	7.8	58259
16:44:28	134	195	7.3	56288
16:47:01	174	198	6.6	53529
16:49:30	156	201	6.3	52347
16:52:04	177	211	6.2	51953
16:54:34	202	214	6.3	52347
16:57:09	180	214	6.1	51558
16:59:39	136	205	5.7	49982
17:02:12	118	196	6.0	51164

Time	Methane Flux (g/s)	Prevailing Wind Direction (degrees from North)	Prevailing Wind Speed (m/s)	ACF (m^2)
17:04:44	91	193	6.2	51953
17:07:14	117	200	6.3	52347
17:09:48	109	211	6.4	52741
17:12:21	110	217	6.7	53923
17:14:51	128	213	6.3	52347
17:17:25	112	203	6.1	51558
17:19:55	150	195	5.9	50770
17:22:27	139	196	6.4	52741
17:25:00	162	205	6.4	52741
17:27:33	169	213	6.4	52741
17:30:04	171	213	5.7	49982
17:32:35	175	210	5.7	49982
17:35:08	173	209	5.8	50376
Average	***147***		***6.2***	
Std Dev	***38.29***			

Table C-22. Calculated Methane Flux and Prevailing Wind Speed and Direction, and ACF Measured During the 8/10 OTM-10 Survey at Site B

Time	Methane Flux (g/s)	Prevailing Wind Direction (degrees from North)	Prevailing Wind Speed (m/s)	ACF (m^2)
12:11:46	8.2	193	2.4	17228
12:14:17	10.0	193	2.3	17045
12:16:50	12.0	181	2.4	17228
12:19:24	5.1	199	1.6	15759
12:21:57	4.4	219	1.6	15759
12:24:33	3.7	254	2.1	16677
12:27:06	3.8	252	1.7	15943
12:29:40	2.7	258	1.4	15392
12:32:16	3.0	238	1.2	15024
12:34:49	3.2	242	1.4	15392
12:37:23	3.5	225	1.2	15024
12:39:58	2.7	218	1.3	15208
12:42:32	5.2	213	1.5	15575
12:45:04	3.9	215	2.2	16861
12:47:39	9.3	204	2.2	16861
12:50:15	11.0	192	2.1	16677
12:52:42	6.6	191	1.5	15575
12:55:21	2.9	213	1.3	15208
12:57:55	2.1	241	1.1	14841
13:00:27	2.2	243	1.0	14657
13:03:04	4.8	190	1.2	15024
13:05:36	6.2	171	1.7	15943
13:08:13	6.0	164	1.9	16310
13:10:45	2.9	181	1.3	15208
13:13:17	3.5	214	1.4	15392
13:15:55	3.0	245	1.6	15759
13:18:27	2.8	264	1.3	15208
13:21:01	1.7	287	1.2	15024
13:23:35	2.9	284	1.3	15208
13:26:08	3.3	242	1.3	15208
13:28:42	4.5	218	1.6	15759
13:31:15	3.9	192	2.3	17045
13:33:51	3.9	196	2.4	17228
13:36:25	3.3	192	2.6	17596
13:38:58	2.0	193	2.0	16494
13:41:33	3.4	176	1.4	15392

Time	Methane Flux (g/s)	Prevailing Wind Direction (degrees from North)	Prevailing Wind Speed (m/s)	ACF (m^2)
13:44:07	3.8	160	1.5	15575
13:46:41	6.7	166	1.9	16310
13:49:14	4.5	173	1.9	16310
13:51:47	4.1	173	2.1	16677
13:54:23	8.2	163	2.8	17963
13:56:57	10.0	169	3.2	18697
13:59:30	13.0	173	3.2	18697
14:02:06	7.1	183	3.1	18514
14:04:41	6.0	184	2.5	17412
14:07:13	5.6	193	2.0	16494
14:09:47	5.8	187	2.0	16494
14:12:20	7.4	182	2.3	17045
14:14:51	7.4	176	2.7	17779
14:27:36	9.2	172	2.9	18146
14:30:07	7.2	172	2.6	17596
14:32:42	5.6	170	1.8	16126
14:35:15	3.2	171	1.5	15575
14:37:50	4.1	157	1.5	15575
14:40:26	4.5	179	1.9	16310
14:42:57	6.9	205	2.2	16861
14:45:32	5.0	218	2.7	17779
14:48:06	7.5	215	2.3	17045
14:50:39	7.9	210	1.8	16126
14:53:13	8.8	199	1.8	16126
14:55:48	9.9	206	2.3	17045
14:58:22	6.9	202	2.3	17045
15:00:56	6.0	202	2.5	17412
15:03:29	8.4	195	2.7	17779
15:06:03	9.4	194	3.0	18330
15:08:37	7.3	197	3.1	18514
15:11:13	5.1	214	2.3	17045
15:13:46	5.0	232	1.9	16310
15:16:19	3.7	258	1.9	16310
15:18:52	3.2	259	2.0	16494
15:21:28	4.3	245	1.8	16126
15:24:02	6.1	232	2.3	17045
15:26:35	6.4	224	2.6	17596

Time	Methane Flux (g/s)	Prevailing Wind Direction (degrees from North)	Prevailing Wind Speed (m/s)	ACF (m^2)
15:29:09	5.1	237	2.9	18146
15:31:44	6.8	239	2.4	17228
15:34:18	6.1	243	2.3	17045
15:36:51	4.9	234	1.9	16310
15:39:25	3.7	227	1.9	16310
15:42:00	4.6	208	1.9	16310
15:44:34	4.6	200	2.0	16494
15:47:08	6.7	183	2.5	17412
15:49:41	6.8	178	2.8	17963
15:52:15	11.0	171	3.4	19065
15:54:50	9.7	172	3.6	19432
15:57:24	9.0	176	3.3	18881
15:59:59	6.2	187	3.1	18514
16:02:33	5.5	195	2.8	17963
16:05:04	5.0	190	2.8	17963
16:07:40	7.6	180	2.9	18146
16:10:13	13.0	173	3.1	18514
16:12:45	13.0	177	3.2	18697
16:15:21	8.2	192	2.7	17779
16:17:56	4.5	205	2.6	17596
16:20:29	4.8	202	2.6	17596
16:23:04	4.0	192	2.5	17412
16:25:38	4.1	188	2.4	17228
16:28:13	4.5	185	2.7	17779
16:30:43	5.3	184	3.1	18514
16:33:20	5.8	177	3.3	18881
16:35:54	5.2	180	3.2	18697
16:38:27	5.0	180	3.1	18514
16:41:00	5.3	185	3.0	18330
16:43:39	9.4	179	2.9	18146
16:46:08	12.0	178	2.8	17963
16:48:41	9.3	184	2.7	17779
16:51:16	5.1	193	2.8	17963
Average	***5.9***		***2.2***	
Std Dev	***2.64***			

Table C-23. Calculated Methane Flux and Prevailing Wind Speed and Direction, and ACF Measured During the 8/11 OTM-10 Survey at Site B

Time	Methane Flux (g/s)	Prevailing Wind Direction (degrees from North)	Prevailing Wind Speed (m/s)	ACF (m^2)
8:57:15	5.0	241	2.8	17963
8:59:48	6.4	238	2.9	18146
9:02:22	6.3	237	2.9	18146
9:04:54	7.4	230	2.7	17779
9:07:27	7.4	227	2.6	17596
9:10:00	6.9	239	2.7	17779
9:12:32	5.4	246	2.7	17779
9:15:05	5.2	249	2.6	17596
9:17:40	5.5	238	2.3	17045
9:20:12	5.9	236	2.4	17228
9:22:46	4.8	246	2.8	17963
9:25:18	5.3	258	3.0	18330
9:27:51	5.1	263	2.8	17963
9:30:24	5.1	251	2.5	17412
9:32:57	4.6	247	2.4	17228
9:35:29	4.0	253	2.7	17779
9:38:03	4.6	260	3.1	18514
9:40:36	5.0	253	3.1	18514
9:43:09	6.0	246	2.9	18146
9:45:42	7.1	235	2.7	17779
9:48:16	5.5	239	2.4	17228
9:50:49	4.4	243	2.3	17045
9:53:21	4.7	248	2.3	17045
9:55:55	6.6	244	2.5	17412
9:58:28	7.9	225	2.8	17963
10:01:00	6.5	219	2.5	17412
10:03:33	5.0	218	2.4	17228
10:06:06	4.3	226	2.3	17045
10:08:38	4.0	222	2.7	17779
10:11:12	4.0	228	2.9	18146
10:13:45	4.2	227	2.9	18146
10:16:18	4.6	236	2.9	18146
10:18:54	4.6	233	2.7	17779
10:21:24	4.2	236	2.6	17596
10:23:57	3.8	238	2.3	17045
10:26:32	4.7	229	2.4	17228

Time	Methane Flux (g/s)	Prevailing Wind Direction (degrees from North)	Prevailing Wind Speed (m/s)	ACF (m^2)
10:29:03	4.3	234	2.3	17045
10:31:37	4.3	243	2.3	17045
10:34:10	4.4	251	2.4	17228
10:36:41	4.3	262	2.5	17412
10:39:16	4.2	261	2.7	17779
10:41:48	4.9	251	2.8	17963
10:44:21	5.9	240	2.9	18146
10:46:54	7.0	234	2.9	18146
10:49:27	6.1	237	2.8	17963
10:52:00	6.4	229	2.7	17779
10:54:33	5.4	234	2.7	17779
10:57:03	4.4	242	2.5	17412
10:59:39	4.6	254	2.7	17779
11:02:12	5.1	252	2.8	17963
11:04:45	4.8	249	2.7	17779
11:07:18	4.0	230	2.5	17412
11:09:51	4.3	209	2.5	17412
11:12:24	5.2	201	3.0	18330
11:14:56	6.2	202	3.3	18881
11:17:30	5.2	205	3.3	18881
11:20:03	4.9	208	3.1	18514
11:22:36	4.3	215	3.1	18514
11:25:09	4.5	222	3.1	18514
11:27:42	4.2	219	3.0	18330
11:30:15	4.5	214	2.9	18146
11:32:48	5.6	217	2.8	17963
11:35:22	5.8	220	3.0	18330
11:37:54	5.6	227	2.8	17963
11:40:27	4.5	236	2.7	17779
11:43:00	2.9	252	2.5	17412
11:45:33	3.5	251	2.2	16861
11:48:07	2.8	241	2.0	16494
11:50:40	5.5	246	2.0	16494
11:53:13	4.2	243	2.0	16494
11:55:46	4.6	232	2.0	16494
11:58:19	4.8	215	2.6	17596
12:00:52	4.5	221	2.4	17228

Time	Methane Flux (g/s)	Prevailing Wind Direction (degrees from North)	Prevailing Wind Speed (m/s)	ACF (m^2)
12:03:23	3.8	241	2.2	16861
12:05:58	3.8	263	2.4	17228
12:08:34	3.6	270	2.7	17779
12:11:04	3.9	253	2.9	18146
12:13:37	3.5	232	2.8	17963
12:16:10	4.1	218	3.2	18697
12:18:43	4.4	220	3.0	18330
12:21:16	5.2	231	3.2	18697
12:23:49	5.4	232	3.3	18881
12:26:22	5.1	226	3.3	18881
12:28:55	4.3	217	3.2	18697
12:31:28	4.3	223	3.0	18330
12:34:01	4.7	234	2.8	17963
12:36:34	6.1	237	2.8	17963
12:39:07	5.5	228	2.4	17228
12:41:36	5.3	233	2.1	16677
12:44:13	4.5	221	1.9	16310
12:46:46	6.4	216	1.9	16310
12:49:18	6.3	206	2.3	17045
12:51:51	6.7	216	2.6	17596
12:54:25	4.7	231	2.7	17779
12:56:58	5.5	230	2.9	18146
12:59:31	7.4	219	2.7	17779
13:02:06	12	197	3.1	18514
13:04:37	13	198	2.8	17963
13:07:05	9.8	219	2.5	17412
13:09:43	6.6	242	2.6	17596
13:12:14	5.3	243	2.6	17596
13:14:50	6.7	231	2.2	16861
13:17:20	5.9	214	2.2	16861
13:19:55	6.0	215	2.5	17412
13:22:28	5.3	212	2.9	18146
13:25:01	6.0	216	3.0	18330
13:39:51	5.7	218	2.3	17045
13:42:24	3.9	226	2.1	16677
13:44:56	4.6	222	2.5	17412
13:47:27	4.7	228	2.7	17779

Time	Methane Flux (g/s)	Prevailing Wind Direction (degrees from North)	Prevailing Wind Speed (m/s)	ACF (m^2)
13:49:59	4.6	234	2.5	17412
13:52:32	4.5	240	2.2	16861
13:55:04	4.0	260	2.4	17228
13:57:36	4.5	260	2.7	17779
14:00:07	4.8	263	2.5	17412
14:02:40	6.2	243	2.1	16677
14:05:14	5.2	236	2.0	16494
14:07:44	4.4	240	2.4	17228
14:10:17	4.0	243	2.6	17596
14:12:47	5.4	229	2.6	17596
14:15:22	5.3	211	2.6	17596
14:17:52	10	198	2.7	17779
14:20:24	9.9	199	2.7	17779
14:22:57	12	196	3.0	18330
14:25:29	7.6	204	2.9	18146
14:28:00	5.4	216	2.6	17596
14:30:33	4.5	239	2.2	16861
14:33:03	3.7	254	2.1	16677
14:35:37	4.4	253	1.8	16126
14:38:10	5.6	253	2.2	16861
14:40:38	6.0	241	2.5	17412
14:43:12	4.9	243	2.7	17779
14:45:42	5.1	231	2.8	17963
14:48:14	5.4	234	2.6	17596
14:50:49	5.8	228	2.8	17963
14:53:18	5.4	224	2.7	17779
14:55:50	5.0	219	2.9	18146
14:58:24	4.4	226	2.6	17596
15:00:56	4.1	239	2.5	17412
15:03:28	4.2	249	2.6	17596
15:06:00	4.8	251	2.8	17963
15:08:32	5.5	242	3.1	18514
15:11:04	5.6	246	3.0	18330
15:13:36	5.2	257	3.1	18514
15:16:09	5.5	254	2.8	17963
Average	***5.3***		***2.6***	
Std Dev	***1.56***			

Table C-24. Calculated Methane Flux and Prevailing Wind Speed and Direction, and ACF Measured During the 12/7 OTM-10 Survey at Site C

Time	Methane Flux (g/s)	Prevailing Wind Direction (degrees from North)	Prevailing Wind Speed (m/s)	ACF (m^2)
12:46:51	2.8	230	2.2	16991
12:49:23	2.3	222	2.5	17546
12:51:56	2.7	223	2.5	17546
13:20:00	2.8	221	2.3	17176
13:22:40	3.7	229	2.6	17731
13:25:08	5.6	237	2.7	17916
13:27:39	5.1	242	2.6	17731
13:30:14	6.0	243	2.2	16991
13:32:44	6.7	231	2.1	16805
13:35:17	7.1	221	2.4	17361
13:37:51	7.1	228	2.7	17916
13:40:24	5.4	242	2.7	17916
13:44:02	5.3	250	2.5	17546
13:46:37	4.8	251	2.5	17546
13:50:13	5.0	253	2.6	17731
13:52:48	5.1	255	2.6	17731
13:55:15	6.1	253	2.4	17361
13:57:51	5.7	244	2.4	17361
14:00:22	6.4	242	2.5	17546
14:02:54	4.2	241	2.4	17361
14:05:27	4.3	239	2.2	16991
14:07:59	4.7	229	2.1	16805
14:10:30	5.2	223	2.4	17361
14:13:03	6.9	226	2.7	17916
14:15:36	5.9	240	2.8	18101
14:18:09	6.7	251	2.7	17916
14:20:40	8.9	255	2.8	18101
14:23:12	6.5	250	2.8	18101
14:25:41	5.4	250	3.0	18471
14:28:16	6.7	255	3.1	18656
14:30:48	4.4	263	2.8	18101
14:33:21	4.2	266	2.9	18286
14:35:52	3.5	261	2.6	17731
14:38:23	3.5	261	2.4	17361
14:40:59	3.9	254	2.3	17176
14:43:27	4.3	242	2.4	17361
14:47:36	4.5	235	2.8	18101
14:50:57	3.5	235	2.7	17916
14:53:27	2.5	238	2.7	17916
14:58:27	2.4	236	2.8	18101
15:00:59	3.3	244	2.9	18286

Time	Methane Flux (g/s)	Prevailing Wind Direction (degrees from North)	Prevailing Wind Speed (m/s)	ACF (m^2)
15:04:18	3.0	253	2.7	17916
15:06:52	3.3	261	2.5	17546
15:09:24	2.5	264	2.4	17361
15:12:42	2.0	267	2.7	17916
15:15:12	2.5	263	3.0	18471
15:17:45	3.5	256	3.0	18471
15:20:17	3.9	248	3.1	18656
15:22:50	3.8	247	3.0	18471
15:25:27	3.5	247	2.9	18286
15:28:01	4.9	240	3.1	18656
15:30:30	6.2	238	3.4	19211
15:33:04	5.8	240	3.7	19767
15:35:36	5.6	247	3.7	19767
15:38:12	5.9	252	3.5	19397
15:40:42	6.1	253	3.3	19026
15:43:16	4.5	254	3.3	19026
15:45:47	3.9	256	3.8	19952
15:48:22	4.9	253	4.0	20322
15:50:57	5.4	252	3.9	20137
15:53:26	5.5	247	3.3	19026
15:55:59	4.7	253	3.0	18471
15:58:34	6.7	251	3.0	18471
16:01:09	5.8	252	3.2	18841
16:03:42	6.4	248	3.0	18471
16:06:12	8.3	249	3.0	18471
16:08:46	7.9	247	2.5	17546
16:11:18	5.6	250	2.0	16620
16:13:51	4.0	265	1.7	16065
16:16:27	2.4	274	1.8	16250
16:18:57	2.6	275	2.0	16620
16:21:32	2.2	273	1.8	16250
16:24:06	2.5	278	1.6	15880
16:26:37	2.0	291	1.3	15325
16:29:09	2.4	297	1.5	15695
Average	***4.7***		***2.7***	
Std Dev	***1.64***			

Table C-25. Calculated Methane Flux and Prevailing Wind Speed and Direction, and ACF Measured During the 12/8 OTM-10 Survey at Site C

Time	Methane Flux (g/s)	Prevailing Wind Direction (degrees from North)	Prevailing Wind Speed (m/s)	ACF (m^2)
8:44:39	2.9	72	2.0	16620
8:47:27	2.9	73	2.0	16620
8:50:53	3.7	78	2.1	16805
8:53:25	3.8	82	2.2	16991
8:56:24	3.7	85	2.3	17176
9:10:41	2.6	57	2.5	17546
9:13:13	3.1	56	2.5	17546
9:15:45	2.4	58	2.7	17916
9:18:17	3.9	64	2.9	18286
9:29:30	1.9	52	2.6	17731
9:33:10	1.6	42	2.6	17731
9:35:42	1.8	44	2.7	17916
9:38:14	2.0	43	2.8	18101
9:40:46	1.8	38	2.8	18101
9:48:21	2.1	38	2.9	18286
9:59:13	2.3	52	3.3	19026
10:02:28	2.1	51	3.0	18471
10:05:00	2.3	50	3.0	18471
10:07:32	2.9	53	2.9	18286
10:10:06	2.8	50	3.3	19026
10:12:37	2.4	48	3.4	19211
10:15:09	2.7	45	3.5	19397
10:17:40	3.1	48	3.5	19397
10:20:12	2.3	46	3.4	19211
10:22:44	2.7	46	3.5	19397
10:25:17	2.7	44	3.7	19767
10:29:08	3.8	46	4.1	20507
10:31:41	3.3	48	4.2	20692
10:34:13	4.3	52	4.4	21062
10:38:05	4.3	58	4.5	21247
10:40:36	4.2	58	4.5	21247
10:43:09	3.6	57	4.4	21062
10:45:40	4.0	57	4.4	21062
10:48:12	4.3	55	4.7	21617
10:50:45	3.5	48	4.5	21247
10:53:17	3.1	42	4.8	21802

Time	Methane Flux (g/s)	Prevailing Wind Direction (degrees from North)	Prevailing Wind Speed (m/s)	ACF (m^2)
10:55:49	2.9	37	4.2	20692
10:58:21	3.5	41	3.9	20137
11:00:52	3.8	47	3.5	19397
11:03:25	4.3	53	3.8	19952
11:05:55	5.8	55	3.9	20137
11:08:29	3.9	52	3.8	19952
11:11:03	5.1	53	3.6	19582
11:13:32	2.8	51	3.6	19582
11:16:05	3.1	51	3.6	19582
11:18:37	3.8	52	3.6	19582
11:21:09	4.7	54	3.7	19767
11:23:40	4.6	55	3.6	19582
11:26:12	4.3	52	3.3	19026
11:28:45	5.5	50	3.1	18656
11:31:17	6.0	50	3.3	19026
11:33:49	5.8	51	3.8	19952
11:36:20	8.0	52	4.0	20322
11:38:54	5.5	53	3.9	20137
11:41:25	5.2	55	3.4	19211
11:43:59	4.1	57	3.0	18471
11:46:29	4.2	56	2.8	18101
11:49:01	4.8	56	3.0	18471
11:51:31	4.6	58	3.0	18471
11:54:04	4.8	61	3.3	19026
11:56:35	5.1	61	3.4	19211
11:59:04	4.4	60	3.5	19397
12:01:40	3.5	61	3.6	19582
12:04:14	3.9	66	3.2	18841
12:06:45	4.9	66	3.1	18656
12:09:19	4.6	65	2.8	18101
12:11:49	5.8	58	2.9	18286
12:14:20	5.0	55	2.8	18101
12:16:53	4.2	49	2.9	18286
12:19:23	3.3	48	2.8	18101
12:21:56	4.3	50	3.0	18471
12:24:29	6.9	52	3.1	18656
12:27:00	5.8	50	3.5	19397

Time	Methane Flux (g/s)	Prevailing Wind Direction (degrees from North)	Prevailing Wind Speed (m/s)	ACF (m^2)
12:29:33	4.2	46	3.5	19397
12:32:04	5.2	46	3.9	20137
12:32:04	5.2	46	3.9	19767
12:34:37	4.9	50	3.7	19767
12:37:09	5.3	50	3.7	19397
12:39:41	5.0	49	3.5	19582
12:42:13	4.2	46	3.6	19767
12:44:44	4.8	50	3.7	19767
12:47:17	4.9	51	3.7	19952
12:49:48	5.0	49	3.8	20137
12:52:20	4.3	46	3.9	20137
12:54:51	3.4	43	3.9	19952
12:57:24	5.3	47	3.8	20507
12:59:57	6.0	48	4.1	21247
13:02:29	7.9	49	4.5	22173
13:05:01	6.9	48	5.0	22728
13:07:31	7.0	48	5.3	22728
13:10:05	4.3	47	5.3	22543
13:12:37	5.1	50	5.2	21432
13:15:08	7.3	54	4.6	20507
13:17:41	6.1	54	4.1	19397
13:20:13	4.7	53	3.5	19211
13:22:46	3.8	50	3.4	19582
13:25:18	3.4	49	3.6	19952
13:27:49	4.1	50	3.8	19582
13:30:21	5.1	54	3.6	19767
13:32:53	7.9	62	3.7	20877
13:35:26	8.0	61	4.3	21988
13:37:56	10.0	58	4.9	21247
13:40:30	7.1	56	4.5	19767
13:43:01	8.2	54	3.7	19582
13:45:32	7.3	54	3.6	20322
13:48:06	9.3	52	4.0	20877
13:50:36	8.9	53	4.3	20137
13:53:08	6.3	54	3.9	19397
13:55:41	4.8	55	3.5	19211
13:58:13	5.6	56	3.4	19952

Time	Methane Flux (g/s)	Prevailing Wind Direction (degrees from North)	Prevailing Wind Speed (m/s)	ACF (m^2)
14:00:45	4.3	52	3.8	20322
14:03:17	5.1	51	4.0	19582
14:05:48	3.0	46	3.6	17916
14:08:20	2.3	44	2.7	17731
14:21:49	2.2	38	2.6	18101
14:25:09	2.1	38	2.8	18286
14:27:39	2.0	39	2.9	18286
14:32:46	2.4	39	2.9	18101
14:35:19	2.5	39	2.8	18656
14:37:50	4.4	44	3.1	19026
14:40:23	4.3	42	3.3	19397
14:42:53	4.3	45	3.5	19026
14:45:26	2.5	44	3.3	19026
14:48:48	2.5	42	3.3	18286
14:50:30	2.9	40	2.9	17731
14:53:03	2.4	40	2.6	17546
14:55:33	3.0	44	2.5	17176
14:58:06	3.6	48	2.3	17176
15:00:36	3.9	55	2.3	16991
15:03:10	5.1	62	2.2	17916
15:05:44	5.9	58	2.7	17916
15:08:13	4.2	51	2.7	18101
15:10:44	2.5	44	2.8	17546
15:13:18	1.9	39	2.5	16991
15:15:50	1.7	37	2.2	16620
15:18:29	2.1	41	2.0	16435
15:21:02	3.8	50	1.9	16435
15:23:33	5.4	57	1.9	16805
15:26:13	6.3	61	2.1	17176
15:28:45	6.4	58	2.3	17731
15:31:16	5.8	56	2.6	18101
15:33:48	5.0	52	2.8	18101
15:36:20	3.4	48	2.8	18841
15:38:51	2.5	42	3.2	18841
15:41:25	2.2	38	3.2	18286
15:43:58	3.6	39	2.9	17546
15:46:30	3.0	41	2.5	17731

Time	Methane Flux (g/s)	Prevailing Wind Direction (degrees from North)	Prevailing Wind Speed (m/s)	ACF (m^2)
15:49:00	3.2	46	2.6	18471
15:51:31	2.9	50	3.0	18101
15:54:06	4.3	54	2.8	17546
15:56:36	3.7	54	2.5	16991
15:59:08	2.9	48	2.2	17176
16:01:41	2.0	45	2.3	17361
16:04:14	2.5	45	2.4	17731
16:06:46	3.5	45	2.6	18101
16:09:18	4.1	45	2.8	18101
16:11:48	3.0	43	2.8	17916
16:14:22	2.1	41	2.7	16620
Average	***4.2***		***3.3***	
Std Dev	***1.67***			

Table C-26. Calculated Methane Flux and Prevailing Wind Speed and Direction, and ACF Measured During the 4/22 OTM-10 Survey at Site C

Time	Methane Flux (g/s)	Prevailing Wind Direction (degrees from North)	Prevailing Wind Speed (m/s)	ACF (m^2)
15:48:19	2.1	262	1.1	34932
15:50:51	3.5	299	1.2	35365
15:53:23	3.2	305	1.3	35797
15:55:54	1.6	311	1.0	34500
16:16:13	4.6	276	1.5	36662
16:18:45	3.3	314	2.3	40120
16:21:17	2.5	322	2.9	42714
16:23:48	1.2	315	2.5	40985
16:26:21	1.6	322	2.0	38823
Average	***2.6***		***1.8***	
Std Dev	***1.11***			

Table C-27. Calculated Methane Flux and Prevailing Wind Speed and Direction, and ACF Measured During the 4/23 OTM-10 Survey at Site C

Time	Methane Flux (g/s)	Prevailing Wind Direction (degrees from North)	Prevailing Wind Speed (m/s)	ACF (m^2)
10:20:07	6.4	245	1.0	34500
10:22:39	6.6	245	1.0	34500
10:25:10	7.8	252	1.1	34932
10:27:42	8.3	256	1.0	34500
10:30:15	7.4	260	1.0	34500
10:32:47	6.1	259	1.0	34500
11:15:51	7.9	256	1.3	35797
11:18:23	13	291	1.4	36229
11:20:56	8.5	311	1.6	37094
11:23:27	7.7	316	1.6	37094
11:25:59	6.4	318	1.5	36662
11:28:32	5.0	324	1.4	36229
11:43:45	4.4	321	1.1	34932
11:46:17	5.2	291	1.0	34500
11:48:48	5.9	283	1.1	34932
11:51:20	6.2	258	1.2	35365
11:53:53	6.5	250	1.2	35365
11:56:25	6.6	247	1.1	34932
12:01:28	6.9	249	1.2	35365
12:04:00	6.7	246	1.2	35365
12:06:33	5.6	252	1.0	34500
12:14:08	8.3	247	1.6	37094
12:16:41	10	258	1.9	38391
12:19:13	11	263	1.9	38391
12:21:46	13	274	1.9	38391
12:24:16	14	283	1.8	37959
12:26:48	14	289	1.9	38391
12:29:21	18	291	1.8	37959
12:31:53	18	288	1.8	37959
12:34:25	14	282	1.6	37094
12:36:56	12	282	1.4	36229
12:39:29	9.2	287	1.0	34500
12:42:01	6.8	302	1.0	34500
12:44:33	10	314	1.0	34500
12:47:05	6.1	325	1.1	34932
13:14:57	5.5	321	1.1	34932

Time	Methane Flux (g/s)	Prevailing Wind Direction (degrees from North)	Prevailing Wind Speed (m/s)	ACF (m^2)
13:17:31	7.8	305	1.0	34500
13:20:02	5.0	260	1.0	34500
13:55:30	6.4	247	1.0	34500
13:58:01	8.2	251	1.0	34500
14:00:34	11	253	1.0	34500
14:03:06	10	256	1.0	34500
14:05:38	12	261	1.0	34500
14:08:09	5.8	258	1.0	34500
14:10:41	6.6	258	1.0	34500
14:13:14	9.3	255	1.1	34932
14:15:46	8.1	256	1.2	35365
14:18:18	7.5	266	1.1	34932
14:20:49	8.5	285	1.0	34500
14:23:21	6.8	310	1.0	34500
14:25:54	7.0	315	1.0	34500
14:28:26	5.4	317	1.1	34932
14:30:57	4.2	313	1.0	34500
14:38:34	5.0	277	1.0	34500
14:41:06	5.5	282	1.0	34500
14:43:37	4.6	304	1.0	34500
14:51:14	4.8	297	1.0	34500
14:53:46	6.4	269	1.2	35365
14:56:17	6.4	263	1.3	35797
14:58:50	5.3	278	1.1	34932
15:01:22	4.0	306	1.0	34500
Average	***8.0***		***1.2***	
Std Dev	***3.18***			

Table C-28. Calculated Methane Flux and Prevailing Wind Speed and Direction, and ACF Measured During the 4/28 OTM-10 Survey at Site C

Time	Methane Flux (g/s)	Prevailing Wind Direction (degrees from North)	Prevailing Wind Speed (m/s)	ACF (m^2)
11:25:05	3.5	329	5.6	58297
11:29:21	2.8	335	5.6	58297
11:31:51	3.3	332	5.9	59687
11:34:19	3.1	334	5.4	57370
11:36:52	3.5	330	5.7	58760
11:39:21	4.8	326	6.0	60150
11:41:52	5.2	319	7.1	65247
11:44:21	5.2	318	6.8	63857
11:46:51	4.4	320	6.9	64321
11:49:23	5.3	320	6.4	62004
11:51:51	4.7	319	6.3	61540
11:54:24	4.4	317	6.1	60614
11:56:52	3.9	324	6.1	60614
11:59:21	3.6	330	5.9	59687
12:01:53	3.9	334	6.3	61540
12:04:22	4.4	324	6.0	60150
12:06:51	4.8	322	6.5	62467
12:09:21	4.3	318	6.1	60614
12:11:52	4.4	324	6.3	61540
12:14:21	4.2	320	5.7	58760
12:16:53	4.0	318	5.1	55980
12:19:22	3.9	314	5.1	55980
12:21:52	3.7	307	4.9	55053
12:24:21	3.0	304	4.8	54589
12:26:52	1.8	304	3.4	48102
12:29:22	2.4	307	2.9	45785
12:31:51	3.8	300	4.1	51346
12:34:22	5.1	293	5.5	57833
12:36:51	5.4	293	6.2	61077
12:39:21	4.4	297	5.3	56906
12:41:53	3.9	294	4.8	54589
12:44:21	3.8	295	4.8	54589
12:46:51	4.5	288	5.4	57370
12:49:22	5.4	297	6.1	60614
12:51:52	5.5	305	6.4	62004
12:54:21	5.5	310	6.6	62930

Time	Methane Flux (g/s)	Prevailing Wind Direction (degrees from North)	Prevailing Wind Speed (m/s)	ACF (m^2)
12:56:52	4.8	308	5.4	57370
12:59:21	4.3	297	4.9	55053
13:01:52	3.9	282	4.6	53663
13:04:21	4.4	275	5.9	59687
13:06:51	5.2	276	6.8	63857
13:09:21	5.5	282	6.6	62930
13:11:52	5.2	286	6.0	60150
13:14:21	3.9	283	4.6	53663
13:16:51	3.5	277	4.0	50882
13:19:22	2.6	275	3.2	47175
13:21:49	3.5	270	4.1	51346
13:24:23	3.1	266	4.6	53663
13:26:52	3.5	264	5.2	56443
13:29:12	4.2	273	5.4	57370
13:36:38	4.8	285	6.2	61077
13:39:08	2.7	291	6.5	62467
13:41:38	2.0	294	6.6	62930
13:48:55	3.7	313	7.0	64784
13:51:25	4.3	312	6.6	62930
13:53:57	4.3	308	6.0	60150
13:56:28	4.5	307	5.9	59687
13:58:59	4.8	310	5.7	58760
14:01:30	4.1	314	5.5	57833
14:04:00	3.2	310	4.6	53663
14:06:32	2.1	305	4.5	53199
14:09:02	2.8	305	4.7	54126
14:11:33	4.5	302	5.0	55516
14:14:04	4.4	292	4.7	54126
14:16:36	3.3	288	3.9	50419
14:19:05	0.8	289	2.4	43468
14:21:37	0.6	302	1.6	39761
14:24:07	0.4	291	1.1	37444
14:31:40	3.0	265	5.0	55516
14:34:09	3.3	280	4.6	53663
14:36:42	4.3	296	5.5	57833
14:39:12	4.2	295	5.7	58760
14:41:43	4.1	290	6.1	60614

Time	Methane Flux (g/s)	Prevailing Wind Direction (degrees from North)	Prevailing Wind Speed (m/s)	ACF (m^2)
14:44:13	3.7	282	5.4	57370
14:46:45	3.9	282	5.4	57370
14:49:17	4.0	291	5.5	57833
14:51:46	4.5	296	6.1	60614
14:54:19	5.0	292	7.2	65711
14:56:47	5.3	286	6.9	64321
14:59:18	4.8	281	6.3	61540
15:01:50	3.9	279	5.1	55980
15:04:19	3.7	283	4.8	54589
15:06:52	3.6	295	4.9	55053
15:09:21	3.3	303	4.9	55053
15:11:52	3.3	306	5.2	56443
15:14:24	3.8	302	5.4	57370
15:16:54	4.1	305	5.6	58297
15:19:25	3.3	306	5.0	55516
15:21:56	2.8	294	4.5	53199
15:28:45	3.7	271	5.6	58297
15:31:17	4.3	267	6.1	60614
15:33:48	4.7	265	6.0	60150
15:50:45	2.5	291	2.3	43005
16:44:45	5.8	297	6.3	61540
16:48:09	4.4	294	5.2	56443
16:50:39	4.2	287	4.7	54126
16:53:12	4.1	273	4.6	53663
16:55:44	4.0	276	4.5	53199
16:58:15	4.4	297	5.0	55516
Average	***3.9***		***5.3***	
Std Dev	***1.02***			

Table C-29. Calculated Methane Flux and Prevailing Wind Speed and Direction, and ACF Measured During the 4/30 OTM-10 Survey at Site C

Time	Methane Flux (g/s)	Prevailing Wind Direction (degrees from North)	Prevailing Wind Speed (m/s)	ACF (m^2)
11:26:25	21	237	4.6	53587
11:28:57	19	239	4.0	50811
11:31:28	20	239	4.1	51273
11:34:00	19	239	3.9	50348
11:36:33	21	240	4.5	53124
11:39:05	22	240	4.7	54050
11:41:36	23	239	5.1	55901
11:44:08	22	235	4.9	54975
11:46:40	22	235	4.8	54512
11:49:13	21	234	4.4	52661
11:51:45	21	237	4.5	53124
11:54:16	20	239	4.2	51736
11:56:48	19	233	4.1	51273
11:59:20	19	233	3.8	49885
12:01:53	18	230	3.7	49422
12:04:24	19	234	3.8	49885
12:06:56	20	229	4.0	50811
12:09:29	23	229	4.6	53587
12:12:00	24	233	4.7	54050
12:14:33	23	238	4.7	54050
12:17:04	18	233	4.1	51273
12:19:36	16	223	3.6	48960
12:22:09	15	213	3.4	48034
12:24:41	17	213	3.9	50348
12:27:13	19	216	4.3	52199
12:29:44	22	220	4.5	53124
12:32:18	22	228	4.1	51273
12:34:49	23	231	4.3	52199
12:37:21	21	226	4.2	51736
12:39:53	20	221	4.3	52199
12:42:25	17	215	3.9	50348
12:44:57	18	226	3.9	50348
12:47:29	18	235	3.9	50348
12:50:00	17	241	3.8	49885
12:52:32	17	227	3.9	50348
12:55:05	17	216	4.3	52199
12:57:36	18	208	4.5	53124
13:29:46	19	216	4.4	52661
13:32:15	20	217	4.4	52661
14:12:46	20	239	4.6	53587
14:23:58	20	247	4.8	54512

Time	Methane Flux (g/s)	Prevailing Wind Direction (degrees from North)	Prevailing Wind Speed (m/s)	ACF (m^2)
14:26:26	20	249	4.5	53124
14:29:02	18	249	4.1	51273
14:31:32	18	231	4.0	50811
14:34:05	18	220	4.2	51736
14:36:38	17	219	4.1	51273
14:39:10	14	217	3.3	47571
15:03:38	15	237	3.7	49422
15:06:08	18	248	4.5	53124
15:08:42	18	252	4.4	52661
15:28:32	15	213	3.5	48497
15:33:11	13	203	3.3	47571
15:35:43	14	199	3.7	49422
15:38:13	15	201	3.8	49885
15:40:46	15	202	3.7	49422
15:43:18	15	198	4.0	50811
15:45:49	17	199	4.6	53587
15:48:23	17	197	4.5	53124
15:50:54	19	206	4.6	53587
15:53:28	19	211	4.5	53124
15:55:59	19	211	4.8	54512
15:58:33	19	207	4.9	54975
16:01:03	19	206	5.0	55438
16:03:36	20	210	5.2	56363
16:06:06	18	210	4.7	54050
16:08:39	17	211	4.2	51736
16:11:09	13	206	3.5	48497
16:13:44	14	211	3.3	47571
16:16:13	14	212	3.3	47571
16:18:45	17	219	3.9	50348
16:21:16	18	219	4.3	52199
16:23:49	21	226	4.6	53587
Average	***18***		***4.2***	
Std Dev	***2.58***			

Table C-30. Calculated Methane Flux and Prevailing Wind Speed and Direction, and ACF Measured During the 5/5 OTM-10 Survey at Site C

Time	Methane Flux (g/s)	Prevailing Wind Direction (degrees from North)	Prevailing Wind Speed (m/s)	ACF (m^2)
15:54:24	0.88	252	2.9	36991
15:56:56	0.69	252	3.2	38114
15:59:28	0.64	247	2.4	35119
16:02:00	0.31	238	1.7	32498
Average	***0.63***		***2.6***	
Std Dev	***0.237***			

Table C-31. Calculated Methane Flux and Prevailing Wind Speed and Direction, and ACF Measured During the 5/6 OTM-10 Survey at Site C

Time	Methane Flux (g/s)	Prevailing Wind Direction (degrees from North)	Prevailing Wind Speed (m/s)	ACF (m^2)
9:22:13	1.9	235	1.7	20574
9:25:17	1.9	235	1.8	20811
9:44:31	2.5	233	2.1	21522
9:47:06	2.6	233	2.0	21285
9:49:39	2.5	236	2.1	21522
10:36:57	1.7	237	2.8	23181
10:39:30	1.9	240	2.8	23181
10:42:02	1.8	239	3.0	23655
10:44:36	1.6	238	3.1	23892
10:57:21	1.5	243	3.2	24129
10:59:54	1.8	247	3.0	23655
11:02:26	2.0	243	2.9	23418
11:05:00	1.0	238	3.0	23655
11:07:33	0.80	234	3.0	23655
11:15:12	0.74	245	2.9	23418
11:17:44	0.91	254	2.8	23181
11:20:18	0.87	263	2.7	22944
11:22:50	1.3	254	2.7	22944
11:25:23	0.78	241	2.9	23418
11:27:57	0.75	236	2.9	23418
11:30:30	0.93	238	3.4	24603
11:33:02	1.0	246	3.1	23892
11:35:36	0.91	249	3.2	24129
11:38:08	1.1	252	2.7	22944
11:40:42	1.2	249	3.0	23655
11:43:14	0.80	235	3.1	23892
11:50:53	1.3	239	3.1	23892
11:53:27	0.86	250	2.9	23418
11:55:59	0.56	260	2.9	23418
11:58:33	0.63	266	3.1	23892
12:01:07	0.70	268	3.1	23892
12:03:38	1.0	265	2.9	23418
12:06:12	0.62	261	2.6	22707
12:08:45	0.61	249	2.6	22707
12:11:21	0.79	249	2.8	23181
12:13:51	0.78	250	3.1	23892

Time	Methane Flux (g/s)	Prevailing Wind Direction (degrees from North)	Prevailing Wind Speed (m/s)	ACF (m^2)
12:16:22	0.78	253	3.2	24129
12:18:57	0.56	245	3.1	23892
12:21:30	0.67	239	3.4	24603
12:24:03	0.72	240	3.2	24129
12:26:36	0.75	242	2.9	23418
12:29:12	1.3	240	2.4	22233
12:36:50	1.2	235	3.4	24603
12:39:22	0.61	243	2.7	22944
12:41:54	0.36	247	2.0	21285
12:44:30	0.39	247	1.6	20337
12:47:00	0.42	257	1.5	20100
12:49:34	0.47	259	1.8	20811
12:52:06	1.1	256	2.5	22470
12:54:39	0.80	249	3.3	24366
12:57:12	0.67	254	3.6	25077
12:59:46	0.48	267	3.2	24129
13:02:18	0.41	274	2.6	22707
13:04:52	0.34	269	2.1	21522
13:07:29	0.40	251	1.9	21048
13:09:57	0.45	243	2.1	21522
13:12:30	0.42	234	2.3	21996
13:15:03	0.37	233	2.0	21285
13:17:36	0.39	247	2.1	21522
13:20:08	0.58	261	2.0	21285
13:22:43	0.49	263	2.2	21759
13:25:15	0.37	255	1.9	21048
13:27:54	0.32	256	1.5	20100
13:42:12	0.71	288	1.8	20811
13:45:00	0.31	296	2.0	21285
13:47:33	0.30	258	1.8	20811
13:55:12	1.0	237	2.6	22707
13:57:45	0.64	249	2.4	22233
14:00:18	0.42	285	1.5	20100
14:02:51	0.24	302	1.7	20574
14:05:24	0.27	303	1.6	20337
14:07:57	0.35	278	1.8	20811
14:10:30	0.51	279	2.3	21996

Time	Methane Flux (g/s)	Prevailing Wind Direction (degrees from North)	Prevailing Wind Speed (m/s)	ACF (m^2)
14:13:03	0.75	273	2.5	22470
14:15:36	0.56	284	2.2	21759
14:18:09	0.35	269	1.6	20337
14:20:42	0.57	279	1.7	20574
14:23:16	0.62	266	1.8	20811
14:25:47	0.81	284	1.6	20337
14:28:22	0.59	283	1.5	20100
14:30:52	1.1	271	2.2	21759
14:33:25	0.88	251	2.5	22470
Average	***0.87***		***2.5***	
Std Dev	***0.538***			

Table C-32. Calculated Methane Flux and Prevailing Wind Speed and Direction, and ACF Measured During the 5/7 OTM-10 Survey at Site C

Time	Methane Flux (g/s)	Prevailing Wind Direction (degrees from North)	Prevailing Wind Speed (m/s)	ACF (m^2)
11:58:45	1.1	123	1.0	33776
12:01:16	1.5	131	1.0	33776
12:36:29	1.7	114	2.3	39278
12:39:01	1.8	132	2.3	39278
12:41:32	1.3	143	1.4	35469
12:49:05	1.6	166	1.7	36739
12:51:37	2.3	166	2.5	40124
12:54:08	2.6	158	2.4	39701
12:56:38	2.3	162	2.1	38432
12:59:09	2.1	144	1.8	37162
13:01:41	2.2	144	2.3	39278
13:04:12	2.1	140	2.3	39278
13:06:41	2.0	153	2.0	38008
13:09:15	1.7	154	1.4	35469
13:11:44	2.1	142	1.9	37585
13:14:13	2.5	130	2.8	41394
13:16:46	2.4	129	3.6	44780
13:19:15	2.8	125	3.2	43087
13:21:48	2.5	121	2.7	40971
13:24:19	2.0	125	1.8	37162
13:26:53	1.9	137	1.9	37585
13:29:21	2.1	139	2.3	39278
13:31:52	2.4	137	2.4	39701
13:34:23	2.7	135	2.6	40548
13:36:54	2.4	149	2.1	38432
13:39:25	2.6	154	2.4	39701
13:41:56	2.4	157	2.6	40548
13:44:26	2.7	142	3.5	44357
13:46:58	2.0	141	3.7	45203
13:49:30	2.2	144	3.5	44357
13:52:03	2.1	158	3.2	43087
13:54:31	2.5	162	3.2	43087
13:57:00	2.5	162	3.6	44780
13:59:33	2.4	155	3.5	44357
14:02:04	2.0	149	3.4	43934
14:04:36	2.3	148	2.9	41817

Time	Methane Flux (g/s)	Prevailing Wind Direction (degrees from North)	Prevailing Wind Speed (m/s)	ACF (m^2)
14:07:04	2.3	147	2.8	41394
14:09:37	2.6	135	3.0	42241
14:12:09	2.8	133	3.6	44780
14:14:40	3.0	125	4.1	46896
14:17:08	2.7	135	3.6	44780
14:19:41	2.4	147	3.3	43510
14:22:12	2.1	160	2.9	41817
14:24:42	2.1	170	3.3	43510
14:27:15	2.2	168	3.4	43934
14:29:46	2.0	172	3.9	46050
14:32:16	2.1	168	3.9	46050
14:34:50	2.0	165	3.7	45203
14:37:15	2.8	157	3.9	46050
14:39:50	3.1	149	3.7	45203
14:42:20	2.8	167	3.6	44780
14:44:51	2.4	186	3.5	44357
14:49:53	2.9	171	3.3	43510
14:52:26	2.3	155	3.1	42664
14:54:56	2.1	154	3.1	42664
Average	***2.3***		***2.8***	
Std Dev	***0.411***			

This page intentionally left black.

APPENDIX D
Sample Calculations of Methane Emission Factors and Measurement Uncertainty

The following sections describe the method used for calculating the methane emission factors, and measurement uncertainty for all measurement campaigns during the project. The example calculations are performed using data collected during the Fall 2009 measurement campaign at Site A. Table C-1 presents a sample of the methane emission flux, wind speed, and wind direction collected during the measurements conducted on November 17, 2009.

Table D-1. Sample of Methane Flux, Wind Speed, and Wind Direction Data Collected During the November 17, 2009 OTM-10 Survey at Site A

Time	Methane Flux (g/s)	Wind Speed (m/s)	Wind Direction (deg)	Length of OTM-10 Plane (m)
13:47:24	7.1	2.2	69	115

As shown in Figure 2-1 of the document, the upwind area contributing to the measured flux (ACF) was located on the flat surface of the cell being surveyed. As discussed in Section 1.7, the first step in calculating the corresponding methane emission factor is to calculate the ACF value. The ACF is defined using the following equation:

ACF (m^2) = ½ [(Length to 0% mass capture)(length of the OTM 10 plane]* (D-1)

The Length to 0% mass capture is calculated using the following equation when the OTM 10 plane is configured to capture emissions from a flat surface area:

Length to 0% mass capture (m) = [(0.102)(WS) + 0.712]/ 0.0031* (D-2)

Where:

WS = the average prevailing wind speed (in m/s) during the measurement period.

In order to calculate a methane emission factor value that incorporates the error associated with the calculation of ACF, the standard error coefficient of 5.10 X 10^{-4} associated with the calculation of the Length to 0% mass capture (Thoma et al., 2010) is incorporated into Equation C-2 as follows:

Length to 0% mass capture (m) = [(0.102)(WS) + 0.712]/ [0.0031 ± 0.000510]* (D-3)

Using the data presented in Table D-1 and Equation D-3, the lower and upper bounds of the Length to 0% mass capture value are calculated (259.4 meters and 361.5 meters, respectively). These values are inserted into Equation D-1 to yield the lower and upper bounds of the ACF value (14,915 m^2 and 20,788 m^2, respectively).

In order to calculate the lower and upper bounds of the methane emission factor value, the measured flux (7.1 g/s) is converted to units of grams per day, and divided by the lower and upper bound ACF values, yielding lower and upper bound values of 29.5 and 41.1 grams/day/m^2, respectively.

In order to incorporate the uncertainty associated with the methane flux measurement of ± 20%, the following equations are applied to calculate the overall lower and upper bound of the emission factor values:

Overall lower bound methane emission factor (grams/day/m^2) = 29.5 – (0.2*29.5) = 23.6 grams/day/m^2

Overall upper bound methane emission factor (grams/day/m^2) = 41.1 + (0.2*41.1) = 49.4 grams/day/m^2

The average methane emission factor, incorporating error associated with the ACF calculation and uncertainty associated with the flux measurement is the average of the overall lower and upper bound methane emission factor values, which is 36.5 grams/day/m^2. The methane emission factor values calculated from data acquired each day are averaged to yield a daily average methane emission factor.

In order to calculate the uncertainty associated with the calculation of the average methane emission factor from each site, it is necessary to consider the fact that a different number of measurements were collected on each day of a campaign at a particular site. This is important in assessing the representativeness of the emission factor calculated for each site.

During the Fall 2009 campaign at Site A, the following average daily methane emission factor values (in units of g/day/m^2) were calculated:

{51, 43, 36, 37, 54}

The average methane emission factor for the site was found by averaging the five daily average methane emission factor values (44 g/day/m^2). The uncertainty in the average site methane emission factor is found by first calculating the standard error of the five daily average methane emission factor values (3.624914), and multiplying this value by the *t*-distribution critical value for a 95% confidence interval based on four degrees of freedom (2.776). The result of this calculation yields an uncertainty value of ± 10 g/day/m^2.